

การกระจายตัวของตัวรับวิตามินดีและการกระตุ้นแมพไคเนสในหนูที่ถูกเหนี่ยวนำ  
ให้เป็นโรคถุงลมโป่งพองด้วยควันบุหรี่



นายพาสิต โอกฤษ

บทคัดย่อและแฟ้มข้อมูลฉบับเต็มของวิทยานิพนธ์ตั้งแต่ปีการศึกษา 2554 ที่ให้บริการในคลังปัญญาจุฬาฯ (CUIR)  
เป็นแฟ้มข้อมูลของนิสิตเจ้าของวิทยานิพนธ์ ที่ส่งผ่านทางบัณฑิตวิทยาลัย

The abstract and full text of theses from the academic year 2011 in Chulalongkorn University Intellectual Repository (CUIR)  
are the thesis authors' files submitted through the University Graduate School.

วิทยานิพนธ์นี้เป็นส่วนหนึ่งของการศึกษาตามหลักสูตรปริญญาวิทยาศาสตรมหาบัณฑิต

สาขาวิชาวิทยาศาสตร์การแพทย์

คณะแพทยศาสตร์ จุฬาลงกรณ์มหาวิทยาลัย

ปีการศึกษา 2560

ลิขสิทธิ์ของจุฬาลงกรณ์มหาวิทยาลัย



จุฬาลงกรณ์มหาวิทยาลัย  
**CHULALONGKORN UNIVERSITY**

Vitamin D receptors distribution and MAPK activation in cigarette smoke induced  
emphysema rats



A Thesis Submitted in Partial Fulfillment of the Requirements  
for the Degree of Master of Science Program in Medical Science

Faculty of Medicine

Chulalongkorn University

Academic Year 2017

Copyright of Chulalongkorn University



จุฬาลงกรณ์มหาวิทยาลัย  
**CHULALONGKORN UNIVERSITY**

Thesis Title Vitamin D receptors distribution and MAPK activation in cigarette smoke induced emphysema rats

By Mr. Fatist Okrit

Field of Study Medical Science

Thesis Advisor Associate Professor Sompol Sanguanrungrasirikul, M.D.,M.Sc.

---

Accepted by the Faculty of Medicine, Chulalongkorn University in Partial Fulfillment of the Requirements for the Master's Degree

.....Dean of the Faculty of Medicine  
(Professor Suttipong Wacharasindhu, M.D.)

THESIS COMMITTEE

.....Chairman  
(Professor Vilai Chentanez, M.D.,Ph.D.)

.....Thesis Advisor  
(Associate Professor Sompol Sanguanrungrasirikul, M.D.,M.Sc.)

.....Examiner  
(Assistant Professor Wacharee Limpanasithikul, Ph.D.)

.....Examiner  
(Professor Juraiporn Somboonwong, M.D.,M.Sc.)

.....External Examiner  
(Associate Professor Wilai Anomasiri, Ph.D.)

ฟาภูิส โอภฤช : การกระจายตัวของตัวรับวิตามินดีและการกระตุ้นแมฟไคเนสในหนูที่ถูกเหนี่ยวนำให้เป็นโรคถุงลมโป่งพองด้วยควันบุหรี่ (Vitamin D receptors distribution and MAPK activation in cigarette smoke induced emphysema rats) อ.ที่ปรึกษาวิทยานิพนธ์หลัก: รศ. นพ. สมพล สงวนรังศิริกุล, หน้า.

จุดมุ่งหมายของการศึกษา เพื่อศึกษาผลการเปลี่ยนแปลงของตัวรับวิตามินดีและการเปลี่ยนแปลงของโปรตีนแมฟไคเนสที่ระดับเซลล์ในปอดของโมเดลหนูที่เป็นโรคถุงลมโป่งพองจากการได้รับควันบุหรี่เป็นระยะเวลา 7 วัน (ระยะเฉียบพลัน) และ 14 วัน (ระยะกึ่งเฉียบพลัน) โดยหนูสายพันธุ์ Wistar rat เพศผู้จำนวน 30 ตัว จะได้รับการสุ่มออกเป็น 3 กลุ่มในแต่ละช่วงเวลา ดังนี้ 1) กลุ่มควบคุม ได้รับอากาศปกติที่อุณหภูมิห้อง, 2) กลุ่มที่ได้รับควันบุหรี่ชนิดไม่ผ่านไส้กรอง และ 3) กลุ่มที่ได้รับควันบุหรี่ชนิดผ่านไส้กรอง (n=5 ต่อกลุ่ม) หนูแต่ละตัวจะได้รับควันบุหรี่จากบุหรี่จำนวน 6 มวน ในอัตราที่คงที่เป็นเวลา 7 และ 14 วันข้างต้น จากนั้น 24 ชั่วโมงหลังจากการรมควันบุหรี่ครั้งสุดท้าย สัตว์ทดลองจะถูกทำการุณยฆาตด้วยการฉีดยาสลบเกินขนาดทางช่องท้อง เพื่อเก็บปอดด้านซ้ายสำหรับศึกษาผลการเปลี่ยนแปลงทางพยาธิวิทยา ร่วมกับการย้อมโปรตีนที่สนใจด้วยวิธี immunohistochemistry และเก็บปอดด้านขวาเพื่อนำมาสกัดโปรตีนในการศึกษาการกระจายตัวของตัวรับวิตามินดีและวิถีแมฟไคเนส ผลการศึกษาในวันที่ 7 พบว่า มีแนวโน้มการลดลงของตัวรับวิตามินดีในไซโทพลาสซึมทั้งสองกลุ่มที่ได้รับควันบุหรี่ แต่ตัวรับวิตามินดีในนิวเคลียสมีแนวโน้มลดลงเฉพาะในกลุ่มที่ได้รับควันบุหรี่ชนิดไม่ผ่านไส้กรอง สำหรับการแสดงออกของวิถีแมฟไคเนสได้แก่ p-ERK, p-JNK และ p-p38 ในกลุ่มที่ได้รับควันบุหรี่ชนิดไม่ผ่านไส้กรองมีการเพิ่มขึ้นในขณะที่กลุ่มที่ได้รับควันบุหรี่ชนิดผ่านไส้กรองพบแค่การแสดงออกของ p-JNK ทั้งในไซโทพลาสซึมและนิวเคลียส ซึ่งสอดคล้องกับผลทางพยาธิวิทยาที่พบว่า มีการเพิ่มขึ้นของแมโครฟาจในถุงลมปอดและการเพิ่มขึ้นของอิพิทีเลียลเซลล์รอบท่อลมปอดอย่างมีนัยสำคัญทางสถิติ ( $p < 0.05$ ) ในกลุ่มที่ได้รับควันบุหรี่ชนิดไม่ผ่านไส้กรอง ส่วนการเปลี่ยนแปลงของอิพิทีเลียลเซลล์ที่หลอดเลือดและการแทรกตัวของเซลล์อักเสบในเนื้อเยื่อปอด พบแนวโน้มเพิ่มขึ้นทั้งสองกลุ่มที่ได้รับควันบุหรี่ สำหรับผลการทดลองในวันที่ 14 พบว่า ตัวรับวิตามินดีในไซโทพลาสซึมมีแนวโน้มลดลงทั้งสองกลุ่มที่ได้รับควันบุหรี่เช่นเดียวกับในระยะ 7 วัน แต่กลับพบการลดลงอย่างมีนัยสำคัญทางสถิติ ( $p < 0.05$ ) ของตัวรับวิตามินดีในนิวเคลียสเฉพาะในกลุ่มที่ได้รับควันบุหรี่ชนิดผ่านไส้กรอง นอกจากนี้พบการกระตุ้นเพิ่มขึ้นของ p-ERK และ p-JNK ภายในไซโทพลาสซึมและนิวเคลียส ของทั้งสองกลุ่มที่ได้รับควันบุหรี่ ในทางตรงกันข้าม p-p38 ในไซโทพลาสซึมมีแนวโน้มที่จะเพิ่มขึ้นเฉพาะในกลุ่มที่ได้รับควันบุหรี่ชนิดที่ผ่านไส้กรองแต่ไม่พบความแตกต่างของ p-p38 ระหว่างกลุ่มการทดลองในส่วนของนิวเคลียส ดังนั้นผลการแสดงออกของโปรตีนดังกล่าวจึงมีความสอดคล้องกับผลทางพยาธิวิทยาของทั้งสองกลุ่มที่ได้รับควันบุหรี่ในวันที่ 14 ในลักษณะที่ใกล้เคียงกัน โดยพบการเพิ่มขึ้นอย่างมีนัยสำคัญทางสถิติ ( $p < 0.05$ ) ของแมโครฟาจในถุงลม การเปลี่ยนแปลงของอิพิทีเลียลเซลล์รอบท่อลม และการเปลี่ยนแปลงของอิพิทีเลียลเซลล์รอบท่อลม ส่วนการแทรกตัวของเซลล์อักเสบในเนื้อเยื่อปอด พบแนวโน้มเพิ่มขึ้นทั้งสองกลุ่มที่ได้รับควันบุหรี่ ผลการย้อมชิ้นเนื้อด้วยวิธี immunohistochemistry แสดงให้เห็นว่ามี การลดลงของตัวรับวิตามินดีทั้งสองกลุ่มการทดลองในวันที่ 7 และจะเห็นได้ชัดในวันที่ 14 ในกลุ่มที่ได้รับควันบุหรี่ชนิดที่ผ่านไส้กรอง โดยสามารถสรุปได้ว่า โมเดลการศึกษานี้เป็นการจำลองการสูบบุหรี่แบบมือสองซึ่งทำในช่วงวันที่ 7 และวันที่ 14 ที่รมควันบุหรี่แบบไม่ผ่านไส้กรองและผ่านไส้กรอง ซึ่งแนวโน้มที่คล้ายคลึงกันในการลดลงของตัวรับวิตามินดีและการกระตุ้นแมฟไคเนสในกลุ่มการทดลองทั้งสอง แสดงให้เห็นถึงความสามารถที่ลดลงของไส้กรองบุหรี่ในการป้องกันโปรตีนและเซลล์จากความเสียหายหลังจากรมควันบุหรี่ไป 14 วัน รวมทั้งการเปลี่ยนแปลงทางพยาธิวิทยาต่อพยาธิกำเนิดของโรคถุงลมโป่งพองในระยะเริ่มต้นและความรุนแรงของโรคที่เกิดขึ้นถูกพบในการศึกษาครั้งนี้ ซึ่งแนวทางที่ดีที่สุดในการป้องกันโรคเรื้อรังที่จะเกิดขึ้นในระบบทางเดินหายใจนั้นคือการเลิกบุหรี่

สาขาวิชา วิทยาศาสตร์การแพทย์

ปีการศึกษา 2560

ลายมือชื่อ นิสิต .....

ลายมือชื่อ อ.ที่ปรึกษาหลัก .....

# # 5774060930 : MAJOR MEDICAL SCIENCE

KEYWORDS: VITAMIN D RECEPTOR / CIGARETTE SMOKE EXPOSURE / MITOGEN ACTIVATED PROTEIN KINASE

FATIST OKRIT: Vitamin D receptors distribution and MAPK activation in cigarette smoke induced emphysema rats. ADVISOR: ASSOC. PROF. SOMPOL SANGUANRUNGSIRIKUL, M.D.,M.Sc., pp.

Rat model was used in this study in order to investigate subcellular vitamin D receptors (VDR) distribution and mitogen activated protein kinase (MAPK) alteration in the lungs of emphysema development after cigarette smoke exposure for 7 days (acute) and 14 days (subacute). Thirty male Wistar rats were randomly divided into 3 groups per each time point; 1) control (air exposed), 2) no-filter (smoke exposed without cigarette filter) and 3) filter (smoke exposed with cigarette filter) (n=5 per group). Each rat was daily and constantly exposed to 6 cigarettes smoke for 7 or 14 days. After 24 hours of the last exposure, rats were euthanized by intraperitoneal injection with overdose sodium pentobarbital. The left lung was collected for pathological examination and immunohistochemistry. The right lung was salvaged for determination of VDR distribution and cascade proteins of MAPK pathway. Results on day 7<sup>th</sup> of cigarette smoke exposure showed declining trend of cytoplasmic VDR in both cigarette smoke groups whereas nuclear VDR only observed in no-filter group. MAPK cascade proteins such as p-ERK, p-JNK and p-p38 were increased in no-filter group while only p-JNK was found in both subcellular areas of filter group. This was consistent with pathological finding that alveolar macrophage and peribronchiolar epithelium proliferation significantly increased ( $p<0.05$ ) in no-filter group after 7 days smoke exposure. Furthermore, tracheal epithelial change and lung parenchymal infiltration tended to increase in both cigarette smoked groups. For 14 days of cigarette smoke exposure, the results demonstrated decrease cytoplasmic VDR in both cigarette smoked groups in the way same as in 7 days period but only nuclear VDR was significantly ( $p<0.05$ ) decreased especially in filter groups. In addition, both p-ERK and p-JNK of MAPK cascades in cytoplasm and nucleus were activated in both cigarette smoked groups. On the other hand, cytoplasmic p-p38 was prone to increase only in filter group but not nuclear p-p38 in both groups. These proteins outcomes were consistence with histopathological changes observed in both no-filter and filter groups on 14 days exposure that exhibited significantly ( $p<0.05$ ) increased of alveolar macrophages, tracheal epithelial cell changes and peribronchiolar epithelial cell proliferation. Lung parenchymal infiltration had tended to increase after exposed to both cigarette smoke types. Immunohistochemistry showed the reduction trend of VDR in both cigarette smoke groups on 7 days and significantly decreased ( $p<0.05$ ) on 14 days in filter group. In conclusion, this study demonstrated that the second-hand smoker model for 7 and 14 days of cigarette smoke exposure with or without filter. The similar tendencies of VDR depletion and MAPK activation in both cigarette smoke types confirmed that there was no benefit of using cigarette filter to prevent damaging proteins as well as protect cells undergone 14 days smoke exposure. The histological changes of early emphysema pathogenesis and the severity of disease found in this study suggested the best way to prevent chronic respiratory diseases is to quit smoking.

Field of Study: Medical Science

Student's Signature .....

Academic Year: 2017

Advisor's Signature .....

## ACKNOWLEDGEMENTS

Beginning with the powerful word “Bismillahirrahmannirrahim” which means in the name of Allah, the most gracious and merciful. I can’t deny that this master degree is a good opportunity that he gives me to prove myself and grow up again. My feeling permeates with appreciation and thankfulness for all lessons and assistances.

I would like to express my sincere gratitude to my advisor Assoc. Prof. Sompol Sanguanrungrasirikul for giving me encouragement, valuable instructions and all continual supports which enable me to achieve my master degree study. My gratefulness also expands to Assoc. Prof. Puchavit Chantranuwat for his excellent suggestion about knowledge and skills in histopathology interpretation.

I also would like to thank my thesis committees Prof. Vilai Chentanez, Assoc. Prof. Wilai Anomasiri, Asst. Prof. Wacharee Limpanasithikul and Prof. Juraiporn Somboonwong for their splendid commends and give more insight correction for this thesis.

My special thanks go to Prof. Duangporn Werawatganon, Asst. Prof. Chanchai Boonla, Dr. Depicha Jindatip, Mr. Manud Sonsomdeang, Mr. Wasin Manuprasert, Mr. Chakriwong Ma-on, Mrs. Wanida Buasorn, Ms. Apinya Butrlee and Mrs. Manita Saleeon for their educate more laboratory techniques and facilitate all laboratory instruments.

I would like to express from my heartfelt to the 72th Anniversary of His Majesty King Bhumibol Adulyadej Scholarship, 90th Anniversary of the Chulalongkorn University Fund (Ratchadaphiseksomphot endowment fund) and Ratchadapiseksompoth Fund, Faculty of Medicine, Chulalongkorn University, grant number 2560-023 for the financial supports.

Finally, I am much obliged to my family and friends not only in Medical Science program, but also including everyone who always provide their love, furtherance and all supports to me in every part of my life.



## CONTENTS

	Page
THAI ABSTRACT .....	iv
ENGLISH ABSTRACT .....	v
ACKNOWLEDGEMENTS .....	vi
CONTENTS .....	vii
LIST OF FIGURE.....	1
LIST OF TABLE .....	5
LIST OF ABBREVIATION.....	6
CHAPTER I INTRODUCTION.....	8
Background and rationale .....	8
Research questions.....	10
Objectives.....	10
Hypotheses.....	10
Conceptual framework .....	11
Key words .....	11
Limitation of this study.....	12
Expected benefit and application .....	12
Suggestion for further investigation.....	12
CHAPTER II LITERATURE REVIEW .....	13
1. Chronic obstructive pulmonary disease .....	13
2. Cigarettes smoke and its harmful components .....	13
3. Cigarette filter & no-filter .....	14
4. Vitamin D receptors: structure, distribution and mediated-actions.....	15

	Page
4.1 VDR structure .....	16
4.2 VDR distribution .....	16
4.3 VDR mediated actions .....	17
4.3.1 Genomic action .....	17
4.3.2 Nongenomic action .....	18
4.4 Classical actions of vitamin D .....	19
4.5 Non-classical actions of vitamin D .....	20
5. The classical MAP kinases (MAPKs) cascades .....	21
5.1 Extracellular regulated kinase (ERK) .....	21
5.2 c-Jun N-terminal kinases (JNK) .....	22
5.3 p38 MAPK cascades .....	22
6. Cigarette smoke and MAPK activation in the lungs .....	22
Chapter III MATERIALS AND METHOD .....	25
1. Research design and methods .....	25
1.1 Animals .....	25
1.2 Experimental protocol .....	27
1.3 Cigarette smoke exposure .....	27
2. Lung pathological study .....	28
2.1 Tissues collection and fixation .....	28
2.2 Tissues processing .....	29
2.3 Sectioning and H&E staining procedures .....	30
2.4 Lung pathological evaluation .....	31
3. Immunohistochemistry .....	33

	Page
3.1 Deparaffinization and rehydration .....	33
3.2 Antigen retrieval .....	34
3.3 Blocking endogenous target activity and non-specific protein.....	34
3.4 Sample labeling.....	34
3.5 Counterstain.....	35
3.6 Mounting.....	36
3.7 Quantitative evaluation .....	36
4. Western Blot analysis .....	36
4.1 Sample preparation.....	36
4.1.1 Whole cells extraction.....	36
4.1.2 Cytoplasmic and nuclear protein extraction .....	36
4.2 Total protein calculation by bicinchoninic acid (BCA) assay .....	37
4.3 Electrophoresis method (SDS-PAGE).....	39
4.4 Protein transfer to PVDF membrane.....	39
4.5 Immunoblotting.....	40
4.6 Protein detection and analysis.....	41
5. Statistical analysis.....	42
Chapter IV RESULTS .....	43
1. The effects of cigarette smoke exposure on lung histopathological changes .....	43
1.1 Tracheal epithelial cell changes.....	45
1.2 Peribronchiolar epithelial cell proliferation.....	52
1.3 Lung parenchymal inflammatory cell infiltration.....	59
1.4 Alveolar macrophage count .....	66

2. Western blot analysis of VDR distribution and MAPK protein expression .....	73
2.1 Whole cell VDR distribution and MAPK protein expression in lung tissue after cigarette smoke exposure on 7 and 14 days.....	73
2.2 VDR distribution between cytoplasmic and nuclear compartments in lung tissue after cigarette smoke exposure on 7 and 14 days .....	77
2.3 p-ERK (p42, sensitive form) between cytoplasmic and nuclear compartments in lung tissue after cigarette smoke exposure on 7 and 14 days .....	80
2.4 p-ERK (p44, less sensitive form) between cytoplasmic and nuclear compartments in lung tissue after cigarette smoke exposure on 7 and 14 days .....	82
2.5 p-JNK (p46, less sensitive form) between cytoplasmic and nuclear compartments in lung tissue after cigarette smoke exposure on 7 and 14 days .....	84
2.6 p-JNK (p54, sensitive form) between cytoplasmic and nuclear compartments in lung tissue after cigarette smoke exposure on 7 and 14 days .....	86
2.7 p-p38 between cytoplasmic and nuclear compartments in lung tissue after cigarette smoke exposure on 7 and 14 days.....	88
3. Immunohistochemistry of lung VDR distribution in early phase after cigarette smoke exposure with no-filter and filter types induced emphysema model...	91
4. The summary data of histopathological changes, VDR distribution and MAPK protein expression after 7 and 14 days cigarette smoke exposure with no- filter and filter.....	95
Chapter V DISCUSSION AND CONCLUSION .....	97

1. Effects of acute and subacute cigarette smoke exposure with no-filter and filter on lung histopathological alterations in rat model .....	97
2. The alterations of VDR distribution after 7 and 14 days of cigarette smoke exposure with no-filter and filter in lung rat.....	97
3. Immunohistochemistry of VDR distribution in lung sections after cigarette smoke exposure with two different types on 7 and 14 days.....	98
4. The activation of ERK1/2 MAPK protein expression after early phase cigarette smoke exposure with no-filter and filter in lung rat. ....	99
5. The activation of JNK MAPK protein expression after early phase cigarette smoke exposure with no-filter and filter in lung rat. ....	100
6. The activation of p38 MAPK protein expression after early phase cigarette smoke exposure with no-filter and filter in lung rat. ....	101
7. Conclusion .....	105
.....	106
REFERENCES .....	106
APPENDIX.....	117
Appendix 1 Research tools .....	118
Appendix 2 Materials and equipment.....	119
Appendix 3 Chemicals and reagents .....	120
Appendix 4 Whole cell, cytoplasmic and nuclear protein extraction protocol .....	122
Appendix 5 The formula for gel preparation (gel size 1.5 mm).....	125
Appendix 6 Buffer and reagents preparation for the western blot analysis .....	126
VITA.....	128

## LIST OF FIGURE

	Page
<b>Figure 1</b> Vitamin D receptor structure .....	16
<b>Figure 2</b> Genomic vs nongenomic actions of vitamin D mediated by VDR.....	19
<b>Figure 3</b> The schematic of classical and non-classical actions of vitamin D which involved with COPD patients .....	21
<b>Figure 4</b> The association between cigarette smoke and MAPK activation and lung injury of COPD.....	23
<b>Figure 5</b> Sample size calculation from StatsToDo computer program .....	26
<b>Figure 6</b> Experimental protocol .....	27
<b>Figure 7</b> Cigarette smoke exposure system .....	28
<b>Figure 8</b> Tissue processing procedure .....	30
<b>Figure 9</b> Hematoxylin and eosin staining process in lung tissue sections .....	31
<b>Figure 10</b> Deparaffinization and rehydration procedure for IHC .....	33
<b>Figure 11</b> Series of dehydration and clearing procedure for IHC.....	35
<b>Figure 12</b> The examples of optical density values measurement from Microplate reader and standard curve of 9 standards plot .....	38
<b>Figure 13</b> Protein transferring on PVDF membrane by wet tank system.....	40
<b>Figure 14</b> Acute and subacute effect of cigarette smoke exposure with no-filter and filter on tracheal epithelial cells changes .....	45
<b>Figure 15</b> Tracheal epithelial cells changed of control group after room air exposure for 7 days .....	46
<b>Figure 16</b> Tracheal epithelial cells changed of no-filter group after cigarette smoke exposure for 7 days .....	47
<b>Figure 17</b> Tracheal epithelial cells changed of filter group after cigarette smoke exposure for 7 days .....	48
<b>Figure 18</b> Tracheal epithelial cells changed of control group after room air exposure for 14 days .....	49
<b>Figure 19</b> Tracheal epithelial cells changed of no-filter group after cigarette smoke exposure for 14 days.....	50

<b>Figure 20</b> Tracheal epithelial cells changed of filter group after cigarette smoke exposure for 14 days.....	51
<b>Figure 21</b> Acute and subacute effect of cigarette smoke exposure with no-filter and filter on bronchiolar epithelial cells proliferation .....	52
<b>Figure 22</b> Peribronchiolar epithelial cells of control group after room air exposure for 7 days .....	53
<b>Figure 23</b> Peribronchiolar epithelial cells of no-filter group after cigarette smoke exposure for 7 days .....	54
<b>Figure 24</b> Peribronchiolar epithelial cells of filter group after cigarette smoke exposure for 7 days .....	55
<b>Figure 25</b> Peribronchiolar epithelial cells of control group after room air exposure for 14 days .....	56
<b>Figure 26</b> Peribronchiolar epithelial cells of no-filter group after cigarette smoke exposure for 14 days .....	57
<b>Figure 27</b> Peribronchiolar epithelial cells of filter group after cigarette smoke exposure for 14 days .....	58
<b>Figure 28</b> Acute and subacute effect of cigarette smoke exposure with no-filter and filter to lung parenchymal inflammatory cells infiltration .....	59
<b>Figure 29</b> Lung parenchymal inflammatory cells infiltration of control group after room air exposure for 7 days .....	60
<b>Figure 30</b> Lung parenchymal inflammatory cells infiltration of no-filter group after cigarette smoke exposure for 7 days .....	61
<b>Figure 31</b> Lung parenchymal inflammatory cells infiltration of filter group after cigarette smoke exposure for 7 days .....	62
<b>Figure 32</b> Lung parenchymal inflammatory cells infiltration of control group after room air exposure for 14 days .....	63
<b>Figure 33</b> Lung parenchymal inflammatory cells infiltration of no-filter group after cigarette smoke exposure for 14 days .....	64
<b>Figure 34</b> Lung parenchymal inflammatory cells infiltration of filter group after cigarette smoke exposure for 14 days .....	65

<b>Figure 35</b> Acute and subacute effect of cigarette smoke exposure with no-filter and filter to alveolar macrophages count in the alveolar spaces .....	66
<b>Figure 36</b> Alveolar macrophages count of control group after room air exposure for 7 days .....	67
<b>Figure 37</b> Alveolar macrophages count of no-filter group after cigarette smoke exposure for 7 days .....	68
<b>Figure 38</b> Alveolar macrophages count of filter group after cigarette smoke exposure for 7 days .....	69
<b>Figure 39</b> Alveolar macrophages count of control group after room air exposure for 14 days .....	70
<b>Figure 40</b> Alveolar macrophages count of no-filter group after cigarette smoke exposure for 14 days .....	71
<b>Figure 41</b> Alveolar macrophages count of filter group after cigarette smoke exposure for 14 days .....	72
<b>Figure 42</b> Effect of cigarette smoke exposure with no-filter and filter to whole cell VDR distribution on 7 and 14 days of lung rats .....	74
<b>Figure 43</b> Effect of cigarette smoke exposure with no-filter and filter to whole cell p-ERK protein expression on 7 and 14 days of lung rats .....	74
<b>Figure 44</b> Effect of cigarette smoke exposure with no-filter and filter to whole cell p-JNK protein expression on 7 and 14 days of lung rats .....	75
<b>Figure 45</b> Effect of cigarette smoke exposure with no-filter and filter to whole cell p-p38 protein expression on 7 and 14 days of lung rats .....	76
<b>Figure 46</b> Effect of cigarette smoke exposure with no-filter and filter to VDR distribution in cytoplasm (cVDR) and nucleus (nVDR) after 7 days exposed of lung rats .....	78
<b>Figure 47</b> Effect of cigarette smoke exposure with no-filter and filter to VDR distribution in cytoplasm (cVDR) and nucleus (nVDR) after 14 days exposed of lung rats.....	79
<b>Figure 48</b> Cytoplasmic and nuclear p-ERK (p42) protein expression after cigarette smoke exposure with no-filter and filter on 7 days of lung rats .....	80



<b>Figure 49</b> Cytoplasmic and nuclear p-ERK (p42) protein expression after cigarette smoke exposure with no-filter and filter on 14 days of lung rats .....	81
<b>Figure 50</b> Cytoplasmic and nuclear p-ERK (p44) protein expression after cigarette smoke exposure with no-filter and filter on 7 days of lung rats .....	82
<b>Figure 51</b> Cytoplasmic p-ERK (p44) protein expression after cigarette smoke exposure with no-filter and filter on 14 days of lung rats .....	83
<b>Figure 52</b> Cytoplasmic and nuclear p-JNK (p46) protein expression after cigarette smoke exposure with no-filter and filter on 7 days of lung rats .....	84
<b>Figure 53</b> Cytoplasmic and nuclear p-JNK (p46) protein expression after cigarette smoke exposure with no-filter and filter on 14 days of lung rats .....	85
<b>Figure 54</b> Cytoplasmic and nuclear p-JNK (p54) protein expression after cigarette smoke exposure with no-filter and filter on 7 days of lung rats .....	86
<b>Figure 55</b> Cytoplasmic and nuclear p-JNK (p54) protein expression after cigarette smoke exposure with no-filter and filter on 14 days of lung rats .....	87
<b>Figure 56</b> Cytoplasmic and nuclear p-p38 protein expression after cigarette smoke exposure with no-filter and filter on 7 days of lung rats .....	89
<b>Figure 57</b> Cytoplasmic and nuclear p-p38 protein expression after cigarette smoke exposure with no-filter and filter on 7 days of lung rats .....	90
<b>Figure 58</b> Immunohistochemistry of VDR expression in alveolar type II cells after 7 days of cigarette smoke exposure .....	92
<b>Figure 59</b> Immunohistochemistry of VDR expression in alveolar type II cells after 14 days of cigarette smoke exposure .....	93
<b>Figure 60</b> Quantitative immunohistochemistry of VDR distribution in alveolar type II cells of lung rats after cigarette smoke exposure on 7 and 14 days .....	94

## LIST OF TABLE

	Page
<b>Table 1</b> Pathological scores evaluation .....	32
<b>Table 2.1</b> Histopathological examination data of all groups after 7 days exposure .....	43
<b>Table 2.1</b> Histopathological examination data of all groups after 14 days exposure .....	44



## LIST OF ABBREVIATION

APS	= Ammonium persulfate
BSA	= Bovine serum albumin
CER	= Cytoplasmic extraction reagent
COPD	= Chronic obstructive pulmonary disease
CSE	= Cigarette smoke extract
DBP	= Vitamin d binding protein
DRIP	= Vitamin d receptor interacting protein
ERK	= Extracellular signal-regulated kinase
FGF <sub>23</sub>	= Fibroblast growth factor 23
g	= Gram
GOLD	= Global initiative for Chronic obstructive lung disease
IL-1	= Interleukin 1
JNK	= c-Jun NH <sub>2</sub> -terminal kinase
LBD	= Ligand binding domain
MARRS	= Membrane-associated rapid response steroid
MAPK	= Mitogen activated protein kinase
mg	= Milligram
MMP	= Matrix metalloproteinase
MMP2	= Matrix metalloproteinase 2
MMP9	= Matrix metalloproteinase 9
MMP12	= Matrix metalloproteinase 12
NCoR	= Nuclear corepressor
NER	= Nuclear extraction reagent
NF-κB	= Nuclear factor kappa B
NLS	= Nuclear localization signal
PI3K	= Phosphatidylinositol-3-kinase
PKC	= Protein kinase C
PTH	= Parathyroid hormone
p38	= p38 mitogen activated protein kinase

RXR	= Retinoid X receptor
SD	= Standard deviation
SDS-PAGE	= Sodium dodecyl sulfate poly acrylamide gel electrophoresis
SMRT	= Silencing mediator of retinoic acid and thyroid receptor
SRC	= Steroid receptor coactivator
TEMED	= Tetramethylethylenediamine
TGF- $\beta$	= Transforming growth factor $\beta$
TNF- $\alpha$	= Tumor necrosis factor $\alpha$
T-PER	= Tissue protein extraction reagent
VDR	= Vitamin D receptor
VDRE	= Vitamin D responsive elements
VDRm	= Membrane vitamin D receptor
VDRn	= Nuclear vitamin D receptor
1,25(OH) <sub>2</sub> D <sub>3</sub>	= 1,25-dihydroxy vitamin D <sub>3</sub>
$\mu$ g	= Microgram
°C	= Degree Celsius

## CHAPTER I INTRODUCTION

### Background and rationale

Cigarette smoke is the major risk factor of chronic obstructive pulmonary disease (COPD). Nowadays, it is the fifth leading cause of death worldwide and it is predicted to become the third leading cause of mortality by the year 2020 (1) as a cigarette consists of many components of more than 7,000 substances (2) which were associated with a lot of human pathologies such as airway inflammation, COPD, atherosclerosis and age-related disorder. Also, terrible effects of the components of cigarette smoke would damage an airway, mucous cell and lead to air space enlargement including cellular toxicity and cell death (3). In addition, the smoke affects the malfunction of vitamin D receptor (VDR) and reduces of vitamin D metabolism in smokers and be a part of pathogenesis of COPD (4, 5).

Vitamin D receptor is an intracellular receptor which can evoke the biological actions via binding with active vitamin D, or called "1,25 dihydroxy-vitaminD<sub>3</sub> (1,25(OH)<sub>2</sub>D<sub>3</sub>). This is not only a crucial role in classical function through controlling the calcium and phosphate homeostasis, especially in bones, intestine and kidney but also has non-classical functions such as maintaining cell differentiation, inflammation and cell apoptosis in human pathogenesis (6-8).

According to the knockout mice model of Isaac et al., demonstrated that deficiency of VDR in mouse lung could lead to an increase number of inflammatory cells, nuclear factor kappa B (NF-κB) and then induced up-regulation of matrix metalloproteinase (MMPs) MMP2, MMP9 and MMP12. Therefore, the knockout VDR in lung mice has sensitivity to emphysema/COPD because there have been increased the air space enlargement and decreased in lung function (9). All mentioned above represent that the VDR is one of the important factors which is related to the

pathogenesis of COPD. In smokers, vitamin D has a non-classical action in the lungs which is a part of the homeostasis to modify the abnormality of the inflammatory lung. Remarkably, if the effects of the smoke make VDR can't bind to active vitamin D from the non-classical action is attenuated so this outcome may also be affected to the distribution of VDR.

Thus, cigarette smoke exposure model is the most appropriate model to study the pathogenesis of emphysema/COPD in rat and these several exposure systems are available. Animal models of cigarette smoke exposure compose of two types: 1) an exposure with non-filter generating the smoke directly through the burning of the cigarette to the animals and 2) an exposure through the filter generating smoke from cigarette pass the commercial cigarette filter to the animals in the chamber (10, 11). These two cigarette smoke exposure forms were performed to imitate human smoking situations when they smoke and inhale smoke from the environment.

Mitogen activated protein kinases or MAPKs are intracellular transducing molecules consisting of three main subtypes which are extracellular signal-regulated kinase (ERK), p38 and c-Jun NH<sub>2</sub>-terminal kinase (JNK). These involves with various cellular activities such as cell proliferation, differentiation, and cell survival (12). In COPD/emphysema, there have been discovered about these three MAPKs which are activated among stress and inflammatory conditions (13). Marumo et al., demonstrated that the cigarette smoke can induce lung inflammation, apoptosis, proteinase expression and lung injury via up-regulation of p38 MAPK only in mice (14). Uh et al., reported that the cigarette smoke extracts (CSE) reduced the levels of cytoplasmic VDR distribution in A549 cell which also up-regulation of extracellular regulated kinase (ERK) (5). However, there have no study on effects of two different cigarette smoke induced emphysema rats to VDR distribution and all three MAPK alterations.

Consequently, this study was conducted to investigate the association between filter and no-filter cigarette smoke exposure to subcellular VDR distribution and MAPK protein expression in acute and subacute cigarette smoke induced emphysema rats (in vivo model).

### Research questions

1. Whether cigarette smoke exposure with no-filter and filter can change the histopathology in the lungs of cigarette smoke induced emphysema rats.
2. Whether exposure of cigarette smoke with no-filter and filter can alter the levels of VDR distribution in the lungs of cigarette smoke induced emphysema rats.
3. Whether no-filter cigarette smoke exposure group can enhance the levels of MAPK subtype expression higher than cigarette smoke with filter group in the lungs of cigarette smoke induced emphysema rats.

### Objectives

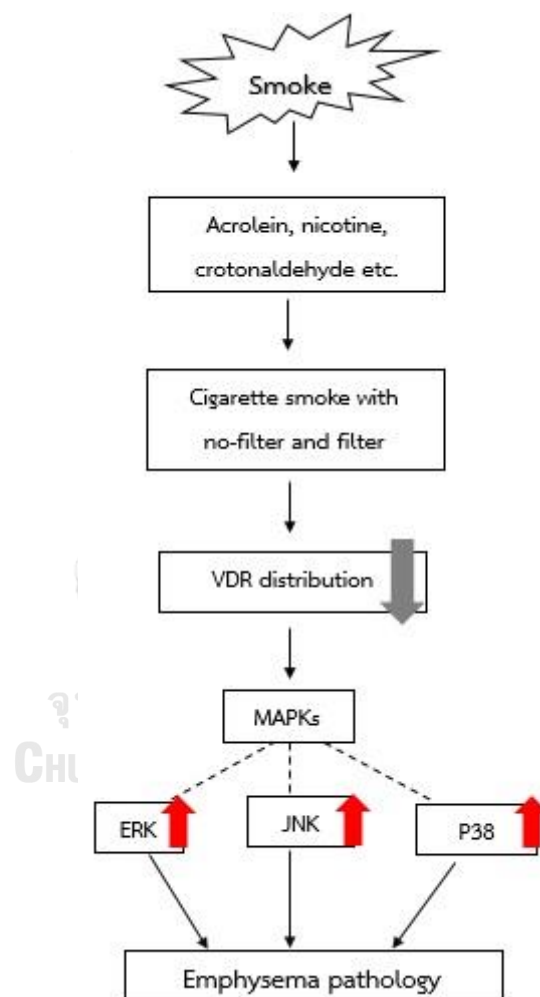
1. To investigate the effects of cigarette smoke exposure with no-filter and filter to lung histopathological changes in cigarette smoke induced emphysema rats.
2. To investigate the effects of cigarette smoke exposure to the alteration of VDR distribution in cigarette smoke with no-filter and filter from the model of emphysema rats.
3. To investigate the association between mitogen activated protein kinase (MAPK) subtype expression and two different cigarette smoke types induced emphysema rats.

### Hypotheses

1. Cigarette smoke exposure with no-filter can change histopathological score more than the smoke with filter in cigarette smoke induced emphysema rats.

2. Cigarette smoke exposure can alter the levels of cytoplasmic and nuclear VDR distribution in alveolar epithelial cells from emphysema rat model.
3. No-filter cigarette smoke exposure can increase the levels of MAPK subtypes expression higher than the smoke with filter induced emphysema rats.

### Conceptual framework



### Key words

vitamin D receptor (VDR) distribution, cigarette smoke exposure, mitogen activated protein kinases (MAPKs)



### **Limitation of this study**

This study didn't measure total particulate matter (TPM) of the smoke that passed through filter or no-filter in the inhalation chamber to the animal. The volumes of TPM may affected to the variation of histopathology or protein expression in both cigarette smoke groups.

### **Expected benefit and application**

1. To know the association between vitamin D receptors distribution and the alteration of MAPK subtypes expression in two cigarette smoke exposure with no-filter and filter induced emphysema rats.
2. To provide the information about two different cigarette smoke exposure which may involve with the distribution of vitamin D receptor affecting the severity of histopathology.

### **Suggestion for further investigation**

To ensure which exactly MAPK cascade is major dominant in associated with emphysema pathogenesis caused by cigarette smoke induced VDR depletion. Further study will apply knock down or knock out techniques to attenuate VDR action and treat cigarette smoke as the same protocol in current study. At last, three target of MAPK cascades will investigate for providing clearly information about MAPK cascades relate early emphysema.

## CHAPTER II LITERATURE REVIEW

### 1. Chronic obstructive pulmonary disease

The high prevalence of chronic obstructive pulmonary disease occurred all around the world caused by a major factor “cigarette smoke” and could lead to the mortality and morbidity for inducible death in the fifth series of the diseases within 2020 (1). The Global Initiative for Chronic Obstructive Lung Disease (GOLD) guideline gave the definition of COPD that is “a preventable and treatable disease with some significant extrapulmonary effects that may contribute to the severity in individual patients”. COPD is a progressive disease happened together with an abnormal inflammatory response in the lung to the harmful particles or gases (15).

The classification of COPD composes of two major types: “chronic bronchitis” and “emphysema”. The diagnosis of chronic bronchitis is the inflammation of the bronchial tubes with the production of cough for over a specific number of months and years, while the diagnosis of emphysema is the architecture of parenchyma destruction which effect to inadequate gas exchange in alveolar tissues (15).

The report of Isaac et al. indicated the significance of VDR in emphysema/COPD pathologies. After they knockout VDR from the lung mice, the result showed the alteration of architecture of alveolar wall, activation of pro-inflammatory mediators, extracellular matrix remodeling and changes of respiratory mechanic which induced to early emphysema/COPD (9). So, this data advises that VDR is implicated in physiological lung function and involves with the homeostasis of vitamin D.

### 2. Cigarettes smoke and its harmful components

Cigarette smoke is a complex mixture of more than 7,000 chemical substances fused in the aerosol particles or independent in the gas phase. The researchers know at least 69 chemicals which are the carcinogens and the toxicants can induce multiple cellular process alteration encompasses oxidative stress (imbalance of oxidant and antioxidant), unusual cellular repair, abnormal alveolar maintenance function, extracellular matrix malfunction (imbalance of protease and anti-protease), cell apoptosis, and lung inflammation deal with many diseases (16, 17).

For instance, the chemical components which can be found in the tobacco smoke are involved with the oxidative stress and inflammation. Moreover, the function of these mixed substances can demolish many biomolecules which become mutations, the alteration of gene transcription and apoptosis (18). According to the study of Kern et al., they reported that after exposed the aqueous cigarette smoke extract (CSE) on human lung epithelial (HBE1) cells, these cells occurred apoptosis and pro B lymphoid cells occurred necrotic cell death at more than 10  $\mu\text{M}$  in culture medium lacking serum (19).

Consequently, Hansdottir et al. and Moretto et al., illustrated that cigarette smoke and its components can damage lung tissue and trigger the inflammation in airway epithelial cells through p38 MAPK pathway including demolish vitamin D metabolism in the lungs that leads to the pathology of emphysema/COPD (4, 20). Therefore, these events may be interfered and relate to the function of vitamin D and protein VDR interaction in alveolar epithelial cells.

### **3. Cigarette filter & no-filter**

At the beginning in 1950s, it was the first produced cigarette filter to reduce the smoke yields that entered into human body. Almost of the commercial cigarette filters are made of mono-filament cellulose acetate and the property of this cellulose acetate can filtrate the smoke components as tar and nicotine about 40-50% when compare to non-filter cigarettes (21). Two main types of the smoke fractions that contain in the non-filter cigarette smoke are tar and gas phase fractions in contrast to the cigarette with filter generally has the smoke in the gas phase. In addition, there have been found the volumes of carcinogenic constituents and free radicals in the tar phase than the gas phase which leads to the study of cyto-genotoxicity involved with the pathological process of inflammation and carcinogenesis in vitro and in animal models (22).

According to the study of Adams et al., they analyzed 12 toxic substances between cigarette smoke with filter and non-filter, the result showed all toxic components of the smoke in cigarette filter reduced significantly when compared to cigarette with non-filter (23). Like the study of Cavallo et al., they evaluated the effects

of cigarette smoke extract (CSE) from commercial cigarette filter and without filter to the cyto-genotoxicity in different lung cell types; human basal alveolar epithelial cells (A549) and human bronchial epithelial cells (BEAS-2B). Non-filter cigarette smoke had more amounts of the particles than cigarette with filter which decreases the viability of the cell especially in BEAS-2B cells and had higher levels of membrane damage including significantly direct to DNA damage at 5-10% CSE concentrations in both cell types from non-filter cigarettes (22).

Thus, cigarette smoke with filter and non-filter study design is the appropriate scientific tool which can apply in the animal study in order to mimic the second-hand smoke people who inhaled the smoke through exhaled smoke from smokers and directly inhaled the smoke from the smoldering cigarette, respectively. Up to now, there is uncertainly clear that filter or no-filer are influent to COPD pathogenesis caused by second-hand smoke. Thus, the dominant point is the protective role of the filter involves with the different levels of smoke particles when it penetrates into human lungs which maybe affects to the alteration of various proteins in the target cells during pathological process.

#### **4. Vitamin D receptors: structure, distribution and mediated-actions**

Vitamin D receptor is an intracellular receptor which binds with active vitamin D “1,25(OH)<sub>2</sub>D<sub>3</sub>” for beginning their biological functions. Since 1969, the scientist found that vitamin D receptors extensively distribute in more than 30 tissues/organ (7). Then it can help them answers a question about roles of vitamin D. Primarily, gene expression is regulated through action of 1,25(OH)<sub>2</sub>D<sub>3</sub> which is mediated by VDR and it has the region where is located specific DNA sequences called “vitamin D response elements (VDRE)”(24). Moreover, vitamin D/VDR interaction has the classical actions and non-classical actions which involve in the homeostasis of many parts in the body system.

#### 4.1 VDR structure

The VDR is a member of nuclear receptor family of transcription factors which has molecular weight approximately 50-60 kDa (25). The structure of VDR composes of two main domains which are DNA binding domain and ligand binding domain. Firstly, DNA binding domain has two zinc finger regions where the proximal (N-terminal) zinc finger prefers specificity to VDRE while the distal zinc finger and the residue region are the specific sites to bind with RXR (Retinoid X Receptor) (Fig1.) (24). Area after distal zinc finger is the ligand binding domain (LBD) which is an important area for the binding region of  $1,25(\text{OH})_2\text{D}_3$  and RXR. At the end of C-terminal, it is a main stimulation region now known as “AF-2 domain”. The widespread of VDR coactivators such as the steroid receptor coactivator (SRC) and VDR-interacting protein (DRIP or Mediator) families have to bind with AF-2 domain for the activation (26).

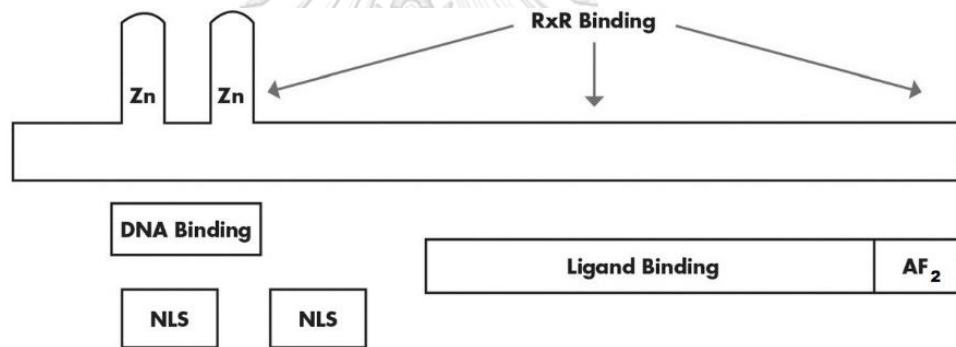


**Figure 1** VDR Structure. The DNA-binding domain or N-terminal region consisting of two zinc fingers that functions like the other steroid hormone receptors. NLS or Nuclear localization signals are found in this region. More than half of the molecule are related to the ligand binding domain and AF-2 domain which is dominant position at C-terminal. The coactivators such as the SRC family and DRIP will bind with specifically AF-2 domain (24).

#### 4.2 VDR distribution

The distribution of VDRs are overspread throughout the various tissues in human body although many of these tissues are not primarily targets for  $1,25(\text{OH})_2\text{D}_3$ . Notably, the experiment about  $1,25(\text{OH})_2\text{D}_3$  and VDR in different cell types revealed that  $1,25(\text{OH})_2\text{D}_3$  can change all these tissue functions that reflected the outstanding

effects of  $1,25(\text{OH})_2\text{D}_3$ . Li et al. have been studied in animal models which knockout VDR causing severe vitamin D deficiency. It represents an important role of VDR which can be the mediator with vitamin D action (27). Moreover, there have been found that the level of VDR was lower in the lungs of COPD patients when compared to the lung of the smokers (9).

The hormonal form of vitamin D like other steroid hormone interacts with VDR to regulate the transcription of target genes and adapt many cell functions. This process called genomic actions. Even though there has been paradoxical data, the unliganded VDR is located in the nucleus or cytoplasm. Later, many techniques have been developed such as microwave energy fixation of tissues (28) which has specificity and sensitivity. Finally, they can detect VDR both in cytoplasm and nucleus.

### **4.3 VDR mediated actions**

#### **4.3.1 Genomic action**

The genomic action is happened in the nucleus by the function of  $1,25(\text{OH})_2\text{D}_3$  and vitamin D receptor (VDR).  $1,25(\text{OH})_2\text{D}$  is an active vitamin D which function reciprocally to the other steroid hormones. In the blood circulation,  $1,25(\text{OH})_2\text{D}$  have small amounts which are bound to the carrier protein called “Vitamin D binding proteins (sDBP)” and are translated to the target tissue. When it comes to the target tissue,  $1,25(\text{OH})_2\text{D}$  will isolate from sDBP and bind to VDR in the cytoplasm of the cell. The binding of  $1,25(\text{OH})_2\text{D}$  and VDR induces the complex of receptor-hormone in form of heterodimerization and translocate to the cell nucleus with partner proteins call “the retinoid X receptor (RXR)”. The VDR-RXR complex plays the role in the transcription factor in the nucleus. At the promoter region of the target genes in the nucleus, the VDR-responsive elements (VDREs) will respond to bind with those complex which can magnetize various cofactors that provoke the expression of genes (Fig.2) (29). The VDRE has two influent effects on VDR and RXR complex; activators or repressors. For the activators, they are composed of two significant activators complex: the steroid receptor complex (SRC) contains three types which are SRC1, SRC2 and SRC3 activators (30) and the vitamin D receptor activator complex (DRIP) known as

“mediator”(31). Also, corepressors have two subgroups: the nuclear corepressor (NCoR) and silencing mediator of retinoic acid and thyroid receptor (SMRT) will be replaced when lacking of  $1,25(\text{OH})_2\text{D}_3$  for binding with VDR.

VDRs are expressed in many tissues and they have the essential role in the biological activity of vitamin D which indicates that the actions of vitamin D happen in various tissues not only preservation of mineral homeostasis, but also extraosseous action. Lastly,  $1,25(\text{OH})_2\text{D}_3$  controls gene expression by genomic action at the transcription level mediate through VDR yet (32).

#### 4.3.2 Nongenomic action

The genomic action cannot clarify all the actions of  $1,25(\text{OH})_2\text{D}_3$  via the interaction between receptor-hormone complex. This situation does not relate with the transcription and arise outside the nucleus of the cells called rapid response or nongenomic action. Nongenomic action occurs within seconds and minutes that associates with the stimulation of receptors on the membranes to respond the physiological levels of  $1,25(\text{OH})_2\text{D}_3$ . For instance, rapid transportation of calcium in the intestine occurs through activation of calcium-dependent protein kinase C (PKC) activity, Jun-activated kinase (JNK) and extracellular response-activated kinase (ERK). These Jun-activated kinase (JNK) and extracellular response-activated kinase (ERK) are the mitogen-activated protein kinase (MAPK) subtypes implicates with the nongenomic mechanisms of  $1,25(\text{OH})_2\text{D}_3$  which also play a role on target cells (Fig.2) (32).

Presently, There have been found the new specific binding protein for  $1,25(\text{OH})_2\text{D}_3$  that maintains  $\text{Ca}^{2+}$  transport named membrane-associated rapid response steroid (MARRS) where this membrane vitamin D receptor (VDRm) cannot be found in the nucleus but resided around the cell surface and perinuclear area (33). While there have been known about the manifested of VDRm on nongenomic actions, there was still an argue whether the nuclear VDR (VDRn) cooperate with the nongenomic action of  $1,25(\text{OH})_2\text{D}_3$ . The study of Buitrago et al. revealed that the participation of VDRn in C2C12 murine myoblast when was knocked down VDRn by RNA interference (RNAi) resulting in dismissing of  $1,25(\text{OH})_2\text{D}_3$  induced up-regulation of p38, ERK1/ERK2, src and PI3K. This indicated the association role of VDRn in mediateing nongenomic actions.

After  $1,25(\text{OH})_2\text{D}_3$  activation in MC3T3-E1 osteoblasts study found the movement of VDRn from the caveolae to the nucleus, no data showed VDRm movement. This represents that this transferring can be the option of VDRn to collaborate in genomic and nongenomic signaling pathways (34). Thus, there may be the probable cross talk during the genomic and nongenomic of  $1,25(\text{OH})_2\text{D}_3$  signaling that encourage the biological action of  $1,25(\text{OH})_2\text{D}_3$  in different target tissues.

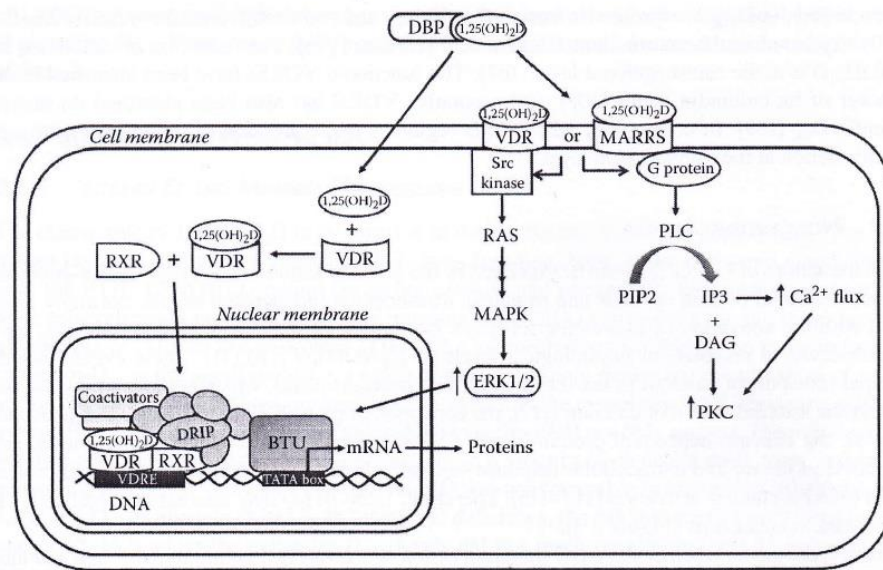


**Figure 2** Genomic versus nongenomic actions of vitamin D mediated by VDR (32).

#### 4.4 Classical actions of vitamin D

Vitamin D has an important role in controlling balance of calcium and metabolism of bones (35). Cholecalciferol or vitamin D<sub>3</sub> is a vitamin derived from 7-dehydrocholesterol which is synthesized in skin. Inactive vitamin D is attained from diet and skin synthesis. The primary reaction is hydroxylation which occurs in a liver and changes vitamin D<sub>3</sub> to 25-hydroxyvitamin D (25-OHD) via 25-hydroxylase enzyme thus 25-hydroxy-vitamin D represents the level of vitamin D in a body. The secondary hydroxylation occurs in the kidney where 25-OHD is converted to an active vitamin D<sub>3</sub> that is 1,25-dihydroxyvitamin D ( $1,25(\text{OH})_2\text{D}_3$ ) or calcitriol and regulated by parathyroid hormone (PTH) and levels of calcium and phosphorus in the serums (36, 37). When  $1,25(\text{OH})_2\text{D}_3$  appears in blood circulation, it increases the potential of renal calcium, intestinal calcium and phosphorus absorption. After that, the enzyme 25-



hydroxyvitamin D-24-hydroxylase (CYP24) is activated and it catabolizes both 25-hydroxyvitamin D and 1,25-dihydroxyvitamin D into an inactive form calcitroic acid which excretes bile from the gall bladder (35). Likewise,  $1,25(\text{OH})_2\text{D}_3$  binding with the VDR can act on various locations such as the small intestine, kidney, bones and the others tissues. After that, it stimulates absorption of calcium and phosphorus from diet and also promotes the reabsorption of calcium in the renal region (Fig.3) (38, 39).

#### 4.5 Non-classical actions of vitamin D

Vitamin D receptor (VDR) is activated by other ligands so that it's showed the uncorrelated between the distribution of VDR and mineral metabolism. The combination of  $1,25(\text{OH})_2\text{D}_3$  and VDR is specificity to the transcription process in more than 200 genes which is related to cellular growth, differentiation, proliferation, anti-inflammation, anti-fibrosis, maturation, inhibited renin-angiotensin axis and angiogenesis (Fig.3) (7, 40, 41). In the term of emphysema/COPD, non-classical action of vitamin D/VDR related with lung tissue remodeling and inflammatory response (9). Apart from above,  $1,25(\text{OH})_2\text{D}_3$  can control the homeostasis of extracellular matrix in the other tissues beyond bones including lung and skin tissue through the modulation of transforming growth factor- $\beta$  (TGF- $\beta$ ), matrix metalloproteinase (MMP) and plasminogen activator system (40). Interestingly, if the non-classical action of vitamin D/VDR complex cannot function in the lung, the VDR will lose to bind with vitamin D. This is because the smoking, resulting in attenuation of activity of vitamin D, causes malfunction in emphysema rat.

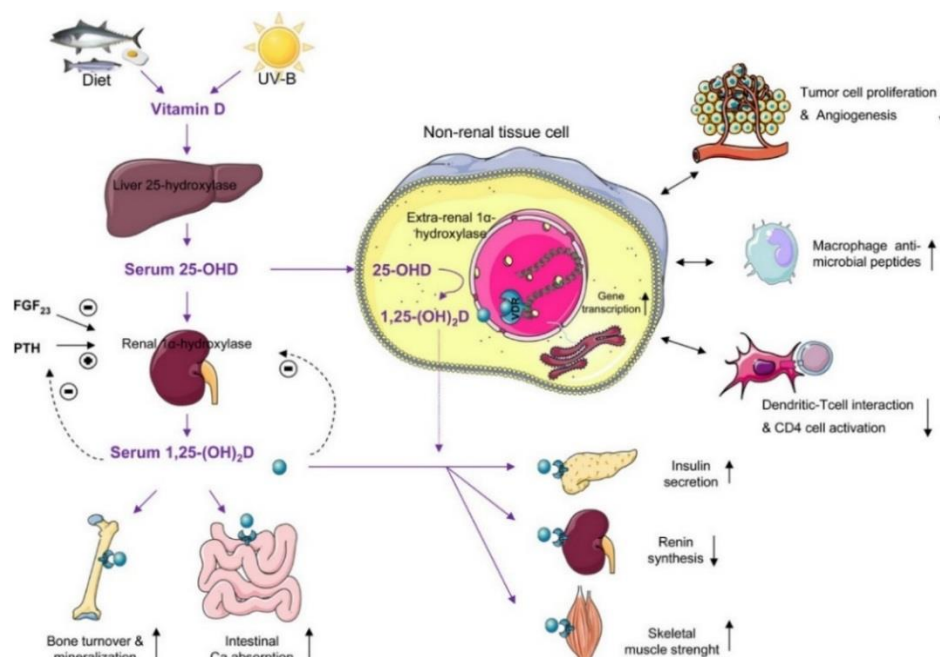


**Figure 3** The schematic of classical and non-classical actions of vitamin D which involved with COPD patients (40).

## 5. The classical MAP kinases (MAPKs) cascades

The relevant conditions that is principally occurred in emphysema/COPD such as inflammation, imbalance of proteinase-antiprotease and/or oxidant-antioxidant cause lungs and airways damage. The possible changes of the cellular response and the expression of epithelial target genes will be involved to interaction between the cells after lung injury and parenchyma walls destruction which conducted by MAPKs signal transduction. Moreover, the outstanding of these cascades is activated by many stimulators including cigarette smoke, stress, mitogens and other environmental toxins that can motivate to similar cascades (42).

MAPKs or mitogen activated protein kinases can be divided into six subgroups but the main interest of almost study is three major subgroups which are extracellular signal-regulated kinases (ERK), c-Jun N-terminal kinases (JNK) and p38 MAPK.

### 5.1 Extracellular regulated kinase (ERK)

The dominant feature of MAP kinase in mammalian is ERK which consisting of two 90% similarity genes sequence: ERK-1 (p44) and ERK-2 (p42). The ERK cascade is

stimulated by mitogens and after growth factor bound to receptor or non-receptor tyrosine kinase is activated by autophosphorylation, it starts this cascade. The consequence of this ERK cascade often relates with cell proliferation (42).

### 5.2 c-Jun N-terminal kinases (JNK)

For JNK pathway is highly correlated with controlling of apoptosis program which is induced by UV light, cell stress, TNF- $\alpha$ , IL-1 and osmotic shock. Also, the inhibition of protein transformation, growth factor and change of temperature may affect stress to the cell that leads to activation and phosphorylation to many substrates, including mitochondrial Bcl-2 (42). But the information about the roles of JNK signaling in biological action is still inconclusive in the emphysema.

### 5.3 p38 MAPK cascades

Two main activating factors of P38 MAPK are inflammatory cytokines and environmental stress which affect alteration of transcription, protein synthesis, expression of cell surface receptor and cytoskeletal structure including influence the rate of cell survival or manage of programmed cell death (43). Especially, the roles of p38 MAPK is well known as it involved with the production of cytokines in immune cells. The study of Lee et al. revealed the capability of p38 enzymes in regulating TNF- $\alpha$  target genes which related to the inflammation (44).

## 6. Cigarette smoke and MAPK activation in the lungs.

Cigarette smoke is the one of stimulator which can activate many MAPK cascades among the lung injury condition in COPD. It is also doubted that cigarette smoke can alter ligand-receptor interaction or directly affect membrane-bound receptors. It is now known that cigarette smoke is related with rapid response in many kinase cascades which occurred within minutes. In this (fig.4), it shows the relationship between cigarette smoke and MAPK signaling in epithelial cells and inflammatory responses to cigarette smoke (42).

The study of Mercer et al. in animal model and human study showed that there have been significantly increased of ERK1/2 in pulmonary of mice after cigarette

smoke exposure for 10 days and unsealed of significantly escalate of ERK1/2 in airways and alveolar epithelial cells of emphysema patients, respectively (45). In another study, Marumo et al. showed the significantly up-regulated of p38 MAPK in both acute and chronic cigarette smoke exposure in C57BL/6 mice which developed lung inflammation (14). In contrast, Mochida-Nishimura et al. studied on the baseline of MAPK in alveolar macrophage of smokers and nonsmokers showing level of p38 MAPK of smokers significantly lower than nonsmokers whereas the activity of ERK1/2 and JNK MAPK are not different when compared between these two groups (46). These data recommended that cigarette smoke can activate through different MAPK cascades in various cells of the lungs.

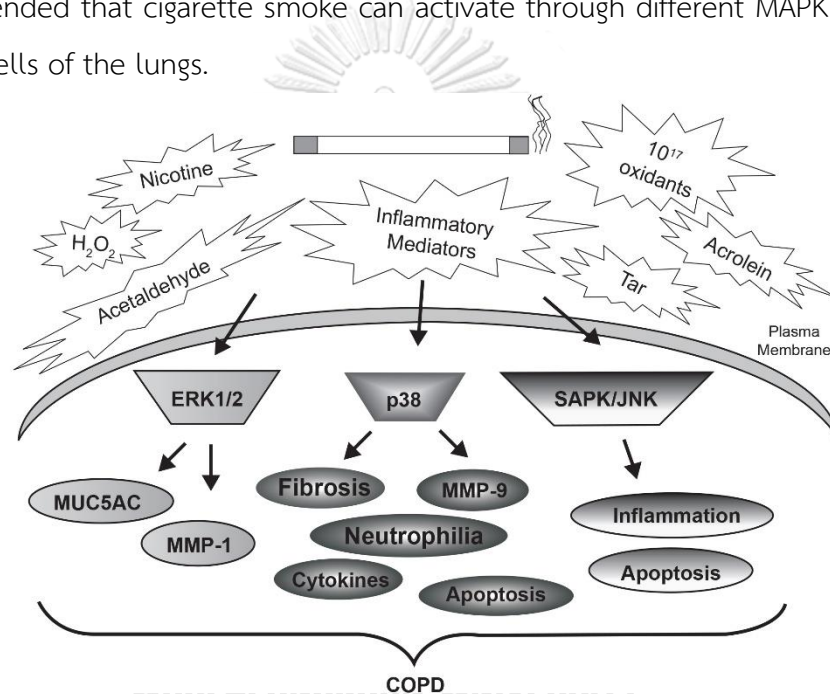


**Figure 4** The association between cigarette smoke and MAPK activation and lung injury of COPD (42).

The steroid hormone 1,25(OH)<sub>2</sub>D<sub>3</sub> support biological responses via stimulation of MAPK cascades through steroid receptor coactivator (Src) in various cell types to induce non-genomic effects. In the recent years, Buitrago et al. suggested that non-transcriptional actions of 1,25(OH)<sub>2</sub>D<sub>3</sub> associated with VDR in infection C2C12 murine myoblasts that reduces the expression of VDR. When lacking of VDR, it indicates that 1,25(OH)<sub>2</sub>D<sub>3</sub>-dependent activity of ERK vanished so it should be noted that VDR may involve in rapid response of 1,25(OH)<sub>2</sub>D<sub>3</sub> and associated with the responses of cells survival and proliferation in skeletal muscle cells (34).

Uh and his colleagues who are the first group studied about the effect of cigarette smoke extracts (CSE) to the translocation of VDR which is one of the distribution of VDR data in cytoplasm and nucleus of A549 cells. Thus, they discovered that cigarette smoke extracts have influent to VDR distribution by inhibiting the translocation of VDR from nucleus to cytoplasm (5). Furthermore, they showed the result that ERK pathways activation significantly increased by CSE but the JNK and p38 were not activated. Together with, when nuclear VDR was knocked down in myoblast cell line, it caused the upregulation of p38 and ERK which some of these cascades may involve with our condition (34). It's still inconclusive about which cascades are related to VDR distribution after cigarette smoke exposure in vivo experiment.

Although, there have been studied the effects of cigarette smoke extract to VDR distribution and alteration of MAPKs cascades but it was in vitro studied which different circumstance from in vivo. Moreover, this in vivo model related with the homeostasis which had the interacting between various cellular communication and adaptation in the lungs. Consequently, this is the first interesting study that performed to investigate the effect of the filter and non-filter cigarette smoke exposure to VDR distribution and MAPK alteration in cigarette smoke induced early emphysema rats.

## Chapter III MATERIALS AND METHOD

### 1. Research design and methods

This study was conducted Thirty male Wistar rats, 210-250 g body weight. Before experimental process, the animals had to acclimatize in the appropriate environment for 1 week. After that, the animals were randomly divided into 6 groups and exposed under cigarette smoke instrument which modified from Brito et al study. Each Wistar rat was exposed to 6 cigarettes per day (3 cigarettes per time point at 10.00 am and 14.00 pm, respectively) with filter and no-filter system for 7 and 14 days, each cigarette was generated smoke approximately 15 minutes (47).

#### 1.1 Animals

Thirty male Wistar rats (body weight 210-250g) were obtained from the National Laboratory Animal Center, Salaya Campus, Mahidol University, Nakhonpathom, Thailand. The experimental procedures were conducted in accordance with the guidelines for experimental animals by National Research Council of Thailand, and authorized by the Committee of animal care, Faculty of Medicine, Chulalongkorn University (license number 009/2559). Each Wistar rat lived in the stainless cage in a room at 25°C with 12:12 hour light-dark cycle and fed ad libitum for normal diet and water. Before the beginning of experiment, rats were acclimatized in the real place of the experiment for one week and their body weights were recorded daily at the same time during the experimental period.

**Sample size determination:** the number of rats per group and per time point were performed as Brito et al. (47). They demonstrated that cigarette smoke exposure to rats was revealed significantly increase in emphysematous changes compared to a control group (emphysematous changes was  $0.00 \pm 0.00$  from control group and  $1.40 \pm 0.51$  from experimental group;  $n=10/\text{group}$ ). This study, we chose mean ( $\bar{x}$ ), and standard deviation ( $s$ ) from emphysematous changes values in both experimental group and control group respectively. Because the emphysematous change is the major one of histopathological character of emphysema. Using the analysis of variance

to determine the sample size for each group(48). Thus, in this study we chose the number of rats per group per time point = 5.

**Single calculation : sample size estimation**

Probability of Type I Error ( $\alpha$ )	<input type="text" value="0.01"/>
Power ( $1 - \beta$ )	<input type="text" value="0.8"/>
Number of Groups in the Analysis	<input type="text" value="3"/>
Largest Difference Between any Two Means	<input type="text" value="1.40"/>
Expected Background Standard Deviation	<input type="text" value="0.51"/>

**Sample Size for Analysis of Variance**

Probability of Type I Error ( $\alpha$ ) = 0.01  
 Power ( $1 - \beta$ ) = 0.8  
 Number of groups (between group df + 1) = 3  
 Largest difference to be detected = 1.40  
 Within group Standard Deviation = 0.51

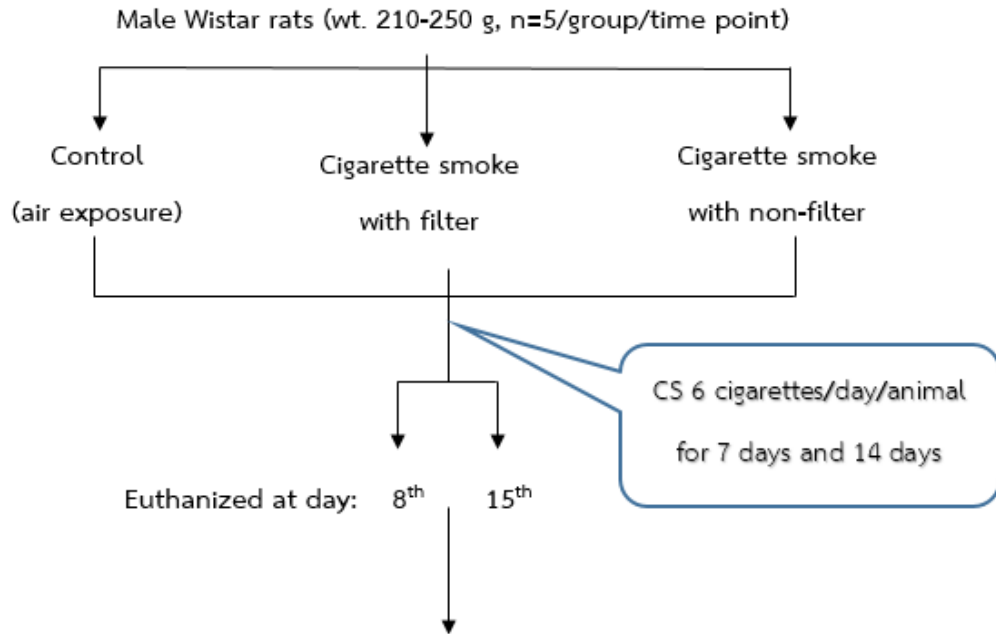
**Calculated parameters**

beta ( $\beta$ ) = 0.2  
 between group df (u) = 2  
 effect size (Diff / SD) = 2.7451  
 effect size (Cohen f) = 1.2941  
 Sample size required (per group) = 5

Figure 5 Sample size calculation from StatsToDo computer program (48).

## 1.2 Experimental protocol

This flow chart below is the detail about experimental design.



The following parameters were studied.

- Histopathology: H&E staining
- VDR distribution: Western blot
- MAPK subtypes: Western blot
- VDR localization: Immunohistochemistry

Figure 6 Experimental procedure.

## 1.3 Cigarette smoke exposure

Thirty male Wistar rats (6-8 weeks, 210-250g body weight) were used in the cigarette smoke exposure protocol followed by Brito et al. (47). Wistar rats were randomly divided into six groups which subdivided into two periods 7 days; 1) CS with filter, 2) CS without filter and 3) control groups and 14 days; 4) CS with filter, 5) CS without filter and 6) control groups. The exposure system generated the smoke composing of six components which are the inhalation chamber, air compressor, conduction pipes, cigarette filter articulation, cigarette cradle, ash and smoke storage box.



For the cigarette smoke with filter group, the animals were placed in the inhalation chamber then inserted the commercial cigarette filter to the cigarette filter articulation and the cigarette was lightened at the proximal portion of the connection pipe. Switch on the air compressor to inhale the smoke constantly from storage box and push through the distal part to the animal in the chamber. In parts of the cigarette smoke without filter group, the cigarette was not covered with the filter which directly expose to the animal in the chamber. Each cigarette generates smoke approximately 15 minutes at every 10.00 and 14.00 throughout 7 and 14 days. For the control group, the animals were exposed to room air in the chamber as both cigarette smoke group with the same period for all of experiment procedures.



**Figure 7** Cigarette smoke exposure system (47).

## 2. Lung pathological study

### 2.1 Tissues collection and fixation

On 8<sup>th</sup> and 15<sup>th</sup> day at the end of the experiment, rats were euthanized by intraperitoneal injection (IP) with overdose sodium pentobarbital (>100mg/kg) and collected both lungs of animal. From the previous publication, the left lung was inflated with 10% neutral buffer formalin at constant pressure 25 cmH<sub>2</sub>O for 15 minutes through intratracheal instillation (49) and then tied the trachea with the thread to prevent fixative leakage. Immersed the left lung in 10% neutral buffered formalin for

24-48 hours to complete the fixation process. This step used to preserve original properties of the tissues for the next studies.

## 2.2 Tissues processing

After fixation process, the lung tissues were performed by automated tissue processor. Firstly, the tissues were passed through gradient alcohol concentration; 70% (15 min), 95% (15 min) and 100% (15, 15, 30 and 45 min respectively) to reduce water content in the tissue which called “dehydration” step. Because melted paraffin wax has the insoluble qualification or hydrophobic, so the water in the tissue should be removed before it can be penetrated with wax that resulting in the distortion of the tissue during cutting process. Secondly, xylene is used to be an intermediate solvent which is miscible with melted paraffin wax and alcohol. We called this step “Clearing” because xylene is a good clearing agent to make tissues transparency from their high refractive index and it has the role in removing fat from tissue which emerge as an obstacle for paraffin wax infiltration. From our method, we immersed the tissues in the series of xylene as following 20, 20 and 45 min respectively. Thirdly, the paraffin wax has long been used for many years as the base-histological waxes which has melting point at 60°C and can be penetrated into the tissue at this temperature then gradually to cool at 20°C which provides the sections firm and easily to cut with microtome. For the routine wax infiltration process, Paraplast™ were used as typical histological waxes for wholly substitute the clearing agents by immersion for 30, 30 and 45 min serially. Finally, the last process was set up to establish the tissue into a “block” which facilitated to grip the block for microtome cutting. Thus, the tissue had to place on accurate orientation in a mould for good histological interpretation, put a cassette on top of the mould and topped up more paraffin wax with immediately transfer to the cold plate for solidify. In addition, the complete blocks can certainly to remove by observation from conveniently pull the blocks out of the mould (50).

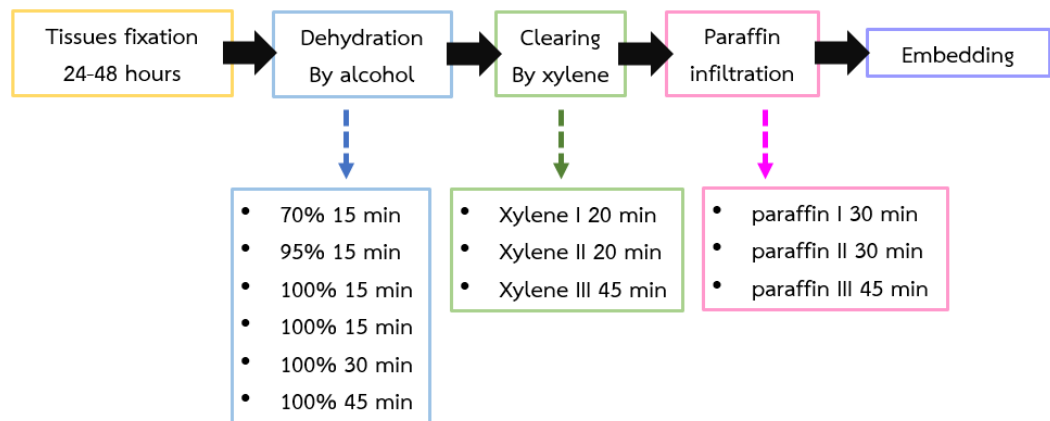
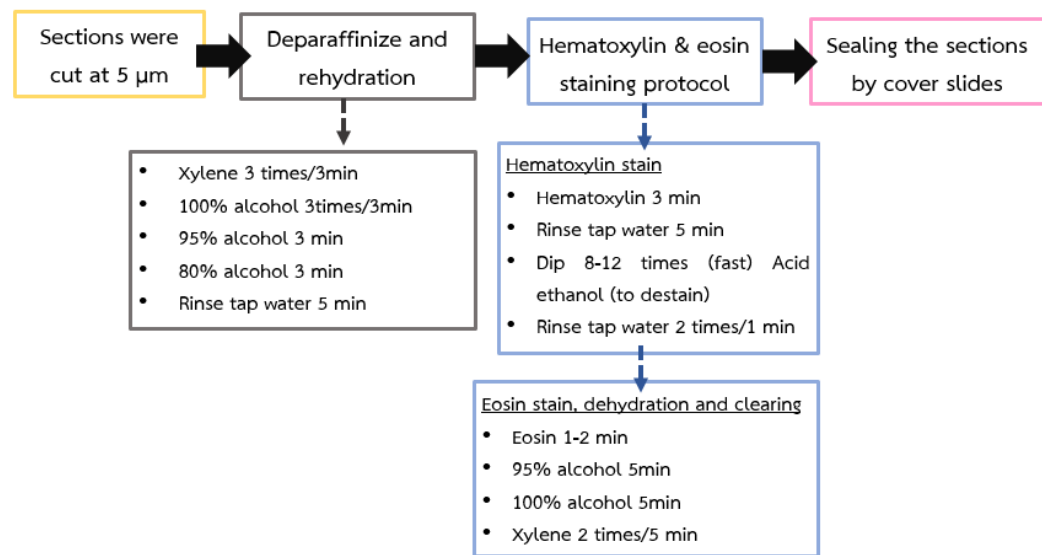


Figure 8 Tissue processing procedure (50).

### 2.3 Sectioning and H&E staining procedures

Microtome is medical pathology instrument used to cut blocked tissue precisely. The tissues were excised into the sections of five  $\mu\text{m}$  of left basal lungs to determine histopathological analysis by microscopy. The sections were floated on warm water surface in a histology floatation bath to expand them and gather up on microscope slide. After that, prepared the sections as dry as possible readily available for staining.

Hematoxylin and eosin (H&E) staining method is a popular method that suitable to estimate pathogenesis of lung rats in this study. Initially, the slides were filled in a slide holder and continued to deparaffinize and rehydrate process from the chart below. The sections were stained nucleus and cytoplasm by hematoxylin and eosin solutions respectively. For the last step, the slides were mounted with cover slip and dry overnight in hood until analysis by microscopy.



**Figure 9** Hematoxylin and eosin staining process in lung tissue sections.

#### 2.4 Lung pathological evaluation

In order to estimate tracheal epithelial cell changes, peribronchiolar proliferation, lung parenchymal infiltration and alveolar macrophage count. All parameters were analyzed by using semiquantitative method from the previous studies (51, 52) as shown in the table below and blinded by experience pathologist. The pathological scores are composed of 0-no change, 1-minimal, 2-moderate, 3-severe and 4-very severe.

Firstly, tracheal epithelial cell changes were graded, where 0 indicated no change of tracheal epithelial cell, 1 indicated focal squamous cell metaplasia, 2 indicated squamous cell metaplasia with hyperplasia, 3 indicated squamous cell metaplasia with hyperplasia and acute inflammation, and 4 indicated squamous cell metaplasia with hyperplasia and diffuse various inflammatory cells. Secondly, peribronchiolar epithelial cell proliferation was graded, where 0 indicated normal two-layers epithelium, 1 indicated squamous dysplasia with focal to full thickness of epithelium by squamous cell, 2 indicated mild dysplasia with the lowest abnormalities with basal expansion, increase cellularity and limited to bottom third of epithelium, 3 indicated moderate dysplasia with more abnormalities, extending to lower two thirds of epithelium, and 4 indicated severe dysplasia with cellular pleomorphism, frequent nuclei, basal zone to upper third of epithelium and superficial cell flattening. Thirdly,

lung parenchymal infiltration was graded by neutrophil and leukocytes infiltration, where 0 indicated no injury, 1 indicated injury to 25% of the field, 2 indicated injury to 50% of the field, 3 indicated injury to 75% of the field, and 4 indicated diffuse injury. Lastly, alveolar macrophage count was graded, where 0 indicated no macrophage in alveolar spaces, 1 indicated 1-4 cells of macrophage in alveolar spaces, 2 indicated 5-9 cells of macrophage in alveolar spaces, 3 indicated more than 10 cells of macrophage in alveolar spaces, and 4 indicated abundant cells of macrophage in alveolar spaces. The observation of all histological features was seen by using microscopy at 40X magnification with randomly ten fields per cut to cumulative scores for average score calculation.

**Table 1** Pathological scores evaluation Dogan and Kerr et al (51, 52).

Pathological features / Score	0: No change	1: Mild	2: Moderate	3: Severe	4: Very severe
Tracheal epithelial cell changes	No change	Focal squamous cell metaplasia (S2 met)	Squamous cell metaplasia + hyperplasia	Squamous cell metaplasia + hyperplasia + acute inflame	Squamous cell metaplasia with hyperplasia + diffuse inflammatory cells
Peribronchiolar epithelial cell proliferation	Normal two-layers epithelium	Squamous dysplasia	Mild dysplasia	Moderate dysplasia	Severe dysplasia
Lung parenchymal infiltration	No injury	Injury to 25% of the field	Injury to 50% of the field	Injury to 75% of the field	Diffuse injury
Alveolar macrophage count	0 cell	1-4 cells	5-9 cells	≥10 cells	Abundant cells

### 3. Immunohistochemistry

Immunohistochemistry (IHC) is the confirmatory method that used to assist in studying the localization of antigens (proteins) in cells of tissue sections depend on binding of specific antibodies to antigens (53). Immunohistochemistry process consisted of seven procedures to completely perform until being visualized with microscopy analysis.

#### 3.1 Deparaffinization and rehydration

Tissue sections at 3  $\mu\text{m}$  thickness were deparaffinized and rehydrated through gradient of xylene and alcohol concentration as Figure 11. Then, all sections were rinsed in tap water for 5 min.

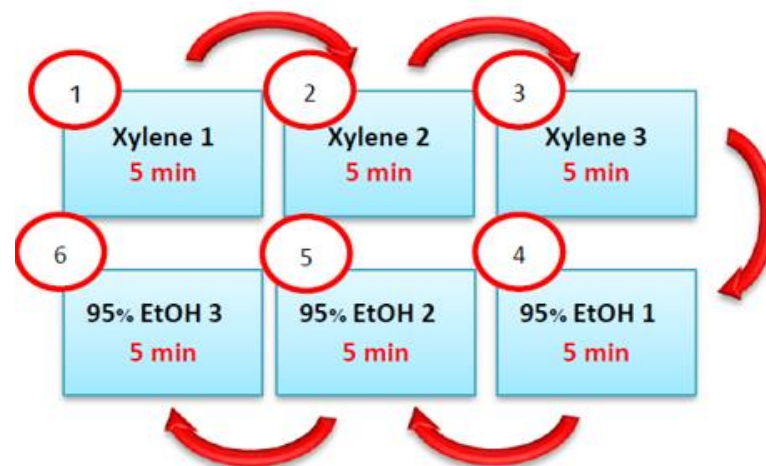


Figure 10 Deparaffinization and rehydration procedure for IHC.

### 3.2 Antigen retrieval

Antigen retrieval citrate buffer pH 6.0 (DAKO envision kit, USA) was conducted to cover all sections and took into the microwave by using heat-induced epitope retrieval. Microwave was set at hi-power 100P for 3 min and continue microwaving low-power 30P for 10 min. Then, left the sections at room temperature for 30 min and running in tap water to eliminate surplus retrieval buffer for 5 min.

### 3.3 Blocking endogenous target activity and non-specific protein

To prevent false positive interpretation, blocking endogenous activity is an important step to concentrate and using hydrogen peroxide blocking endogenous peroxidase. These endogenous cells' component can interfere the antigens detection by generating background staining. After retrieve antigens, sections were placed on IHC performing chamber that containing water to moisture sections. Dako pen (DAKO envision kit) was used to whirl around the tissue sections to prevent leakage and save of substrates throughout IHC process. 3% Hydrogen peroxide (H<sub>2</sub>O<sub>2</sub>) was used to block endogenous peroxidase for 10 min at room temperature. The sections were rapidly removed hydrogen peroxide and run in tap water for 5 min. Then, the slides were washed in wash buffer for 5 min. After that, the slides were incubated with antibody diluent for blocking non-specific protein about 10 min at room temperature.

### 3.4 Sample labeling

After removing antibody diluent, cover circled areas were then incubated at 4°C overnight with primary antibody by using Polyclonal, anti-rabbit VDR (cat. no. NBP1-51322; 1:300 dilution; Novus Biologicals, Littleton, USA). The slides were removed primary antibody and rinse in wash buffer 2 times for 5 min/wash. To amplify primary antibody signal, commercial secondary antibody from DAKO envision system was incubated for 30 min at room temperature. Envision detection system (peroxidase labeled polymer) was used to detected antigen targets through chromogenic method relied on antibodies conjugated to enzymes. Envision system HRP (Anti-rabbit) was covered on circle areas in humidity chamber for 30 min at room temperature and subsequently washed by wash buffer 2 times for 5 min/wash. Substrate chromogen

detection include diaminobenzidine (DAB) was prepared by using DAB substrate buffer 1 ml to DAB liquid 1 drop from this formula: Sample (n) x 2 x 100  $\mu$ l = total DAB. Prepared DAB was dripped 100  $\mu$ l of DAB substrates on cover circle areas and incubated for 5 min to precipitate brown color on tissue samples. Suddenly, all slides were transferred to run in tap water 10 min for inactivation of DAB reaction.

### 3.5 Counterstain

Counterstain gives prominently contrast to the prior stain and usually supplement after staining of antibody. Therefore, hematoxylin was generally used as a counterstain detection for IHC detection. This step carried on by steeping all slides in hematoxylin jar for 1-2 min and then running in tap water for 5 min. Afterwards, all slides were passed through dehydration and clearing processes followed by figure 11 below to prepare for mounting step.

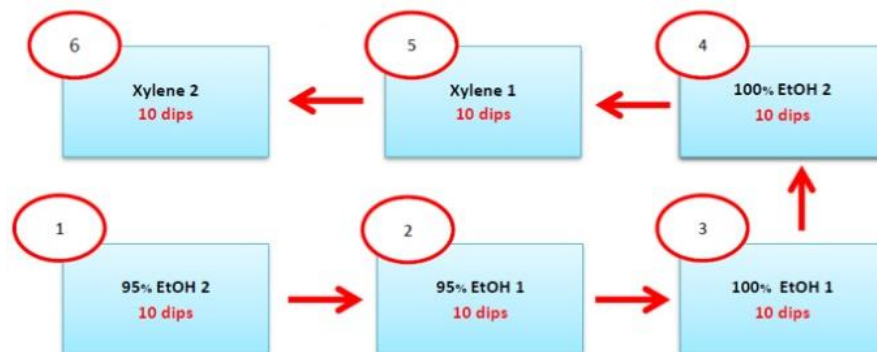


**Figure 11** Series of dehydration and clearing procedures for IHC.



### 3.6 Mounting

After completed slides staining processes, the sample should be protected from damaging for long term preservation by applying the suitable mounting solution. For a good visualization, the cover slip glasses should be sealed the samples without bubbles and others artifacts.

### 3.7 Quantitative evaluation

Samples were analyzed and capture through microscopy in TIFF format files and transferred to the computer for estimation. Positive cells of pneumocytes type II were counted in five randomly fields and expressed as positive cells per lung tissues area ( $\mu\text{m}^2$ ).

## 4. Western Blot analysis

### 4.1 Sample preparation

#### 4.1.1 Whole cells extraction

For total protein extraction from tissue samples was used T-PER protein extraction reagent (Thermo Scientific, Rockford, IL, USA). All procedures were performed step by step followed by the data sheet. Firstly, the tissue samples were weighted, used a ratio of ~ 1g of tissue to 20 mL T-PER Reagents. Secondly, the tissue samples were homogenized after adding T-PER Reagent in the suitable volumes. Thirdly, the samples were centrifuged at  $10,000 \times g$  for 5 minutes to pellet cell/tissue debris. Finally, the supernatants were collected at  $-80 \text{ }^\circ\text{C}$  until used and carried out with western blot analysis or further purification.

#### 4.1.2 Cytoplasmic and nuclear protein extraction

Nuclear and cytoplasmic proteins were separated by using NE-PER nuclear and cytoplasmic extraction reagents kit (Thermo Scientific, Rockford, IL, USA) followed the guideline in the manufacturer. The frozen lung tissue weight 20-100 mg was cut in small pieces and placed in a microcentrifuge tube. Tissue was washed with ice-cold PBS and centrifuged at  $500 g$  for 5 minutes. Then, they were removed and discarded by the supernatant with a pipette. After that, left the pellet as dry as possible and

homogenized tissue by Dounce homogenizer or tissue grinder in appropriate volume of cytoplasmic extraction reagent I (CER I). Next, immediately vortex the tube on the highest setting for 15 seconds for suspending the cell pellet and incubating on ice for 10 minutes. After adding cytoplasmic extraction reagent II (CER II), all tubes were centrifuged at 16,000 g for 5 minutes. The supernatants were used as the cytoplasm and stored at  $-80^{\circ}\text{C}$  until it is used. All pellet tubes were added with nuclear extraction reagent (NER) in ice-cold and vortex 5 seconds at the highest setting for suspending the insoluble fraction. Recurrent vortex for 15 seconds, the samples were placed on ice and carry on vortex for 15 seconds every 10 minutes for 40 minutes. Then, all samples were centrifuged at 16,000 g for 10 minutes and suddenly transferred the supernatant (nuclear extract) fraction into clean pre-chilled tubes on ice which were stored at  $-80^{\circ}\text{C}$  until it is used. This supernatant was the nucleus protein which carried on to analyzed by western blot in further study step.

#### **4.2 Total protein calculation by bicinchoninic acid (BCA) assay**

Total protein concentration was measured by The Thermo Scientific™ Pierce™ BCA protein assay (Thermo Scientific, Rockford, IL, USA) which suitable for the colorimetric detection and quantification of total protein concentration. This method was highly sensitive and compatible with the cuprous cation ( $\text{Cu}^{1+}$ ) for colorimetric detection by using this specific detergent. The essential component of this detergent, bicinchoninic acid was bound with the reduction of  $\text{Cu}^{2+}$  to  $\text{Cu}^{1+}$  via an alkaline medium containing protein and expressed the purple color which represented reaction formed of the chelation of two molecules BCA with one cuprous ion. This complex form displays an absorbance at 562 nm that give approximately linear directions of increasing protein concentration from protein standard range (20-2000  $\mu\text{g}/\text{mL}$ ). Hence, total protein concentration from the sample of interest can be estimated by comparing with protein standards (54).

To calculate unknown total protein concentration for each sample, standards blanks and samples were transferred to 96-well plate by using 1:10 ratio so added 6  $\mu\text{l}$  of those samples, 54  $\mu\text{l}$  of diluent and 200  $\mu\text{l}$  of BCA working reagent with gently shook to mix well. After that, 96-well plate was incubated at  $37^{\circ}\text{C}$  for 30 minutes and

microplate reader (Microplate *spectrophotometer*, Thermo scientific) was used to interpret the absorbance at 562 nm followed by manual guide. All optical density (O.D.) values of 9 standards were plotted by subtracting blanks values to generate the standard curve. The standard curve equation was acquired to calculate the total protein concentration of all samples represented from Figure 12.

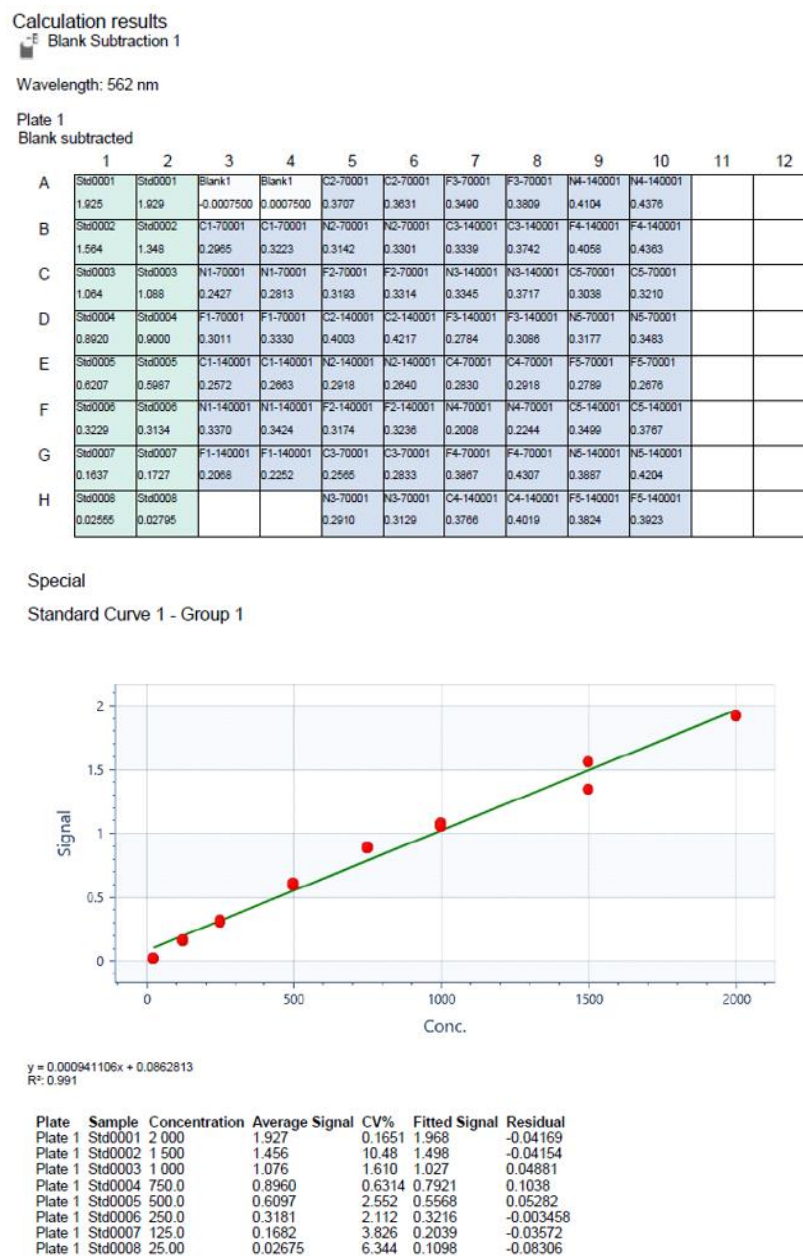


**Figure 12** The examples of optical density values measurement from microplate reader and standard curve of 9 standards plot.

### 4.3 Electrophoresis method (SDS-PAGE)

Electrophoresis system was adopted to compile all proteins together and loaded among optimum condition to separating proteins by their molecular weight which necessary to selecting properly power supply and maintaining the temperature during separation process. For the running gel, composed of two parts such as 10% polyacrylamide gel for separating gel and 5% for stacking gel (see the formula in Appendix 5).

The running gel was prepared by mixing all substrates excepted Tetramethylethylenediamine (TEMED) and Ammonium persulfate (APS) because both of these play an important role in polymerization of acrylamide and bis-acrylamide cross linkage. TEMED and APS were lastly added in running gel due to TEMED had a property to catalyzing free radicals from APS that it can accelerate acrylamide polymerization. The running gel was filled between 2 glasses plate and permitted to set about 45 to 60 min. The stacking gel was also prepared and filled on the top of running gel then inserting the comb carefully on stacking gel and let the gel set as equal time as separating gel. After running gel already set, the comb was removed and sample lysates were loaded equivalent volumes of 50  $\mu\text{g}/\mu\text{l}$  into the wells of sodium dodecyl sulfate polyacrylamide gel electrophoresis (SDS-PAGE) following short boiling of the samples. Protein marker was also loaded on the left side of the gel as molecular weight comparable during protein running. Running buffer (see formula in Appendix 6) was loaded to complete this electrophoresis system. Protein samples were aggregated by using 80 V for 30 min in stacking gel and separated at 120V for 90 min in separating gel respectively.

### 4.4 Protein transfer to PVDF membrane

The polyvinylidene fluoride (PVDF) was applied as transfer membrane because there are various characteristics such as highly protein binding capacity, high sensitivity to detect, better for retention of protein absorption and higher chemical resistance. After electrophoresis protein separation, proteins were transferred to PVDF membrane (Immobilon-P PVDF membrane, Merck Millipore) using wet tank transfer system (Mini Trans-Blot<sup>®</sup> Cell, Bio-rad). Initially, PVDF membrane was activated with methanol for 1

min and transferred to washing with DDW as equal time. Then, 1X transfer buffer volume 1.5 L was added into clean box for soaking all equipment such as filter paper, gel holder cassette, foam pads including membrane before protein transferring procedure. From the cathode (-) to anode (+) side, one foam pad was placed on the bottom followed by two wet filter papers and the gel was placed at the next order. Then, membrane was placed on the gel accompanied by another two wet filter papers with foam pad on the top of transferring system. After sealing gel holder cassette, transfer buffer was poured into transfer tank at the recommended point. The electroblotted was set constant voltage at 90V and run for 90 min. The membrane was removed and washed in 1xPBS with 0.1%Tween (PBST) to eliminate over transfer buffer.



**Figure 13** Protein transferring on PVDF membrane via wet tank system.

#### 4.5 Immunoblotting

Immunoblotting is a scientific technique that used to tagging specific antibodies to specific protein of interest in protein mixture samples. After protein transfer step, membrane was incubated with 1% bovine serum albumin (BSA) for blocking non-specific protein overnight. The membranes were transferred to primary antibody solution which prepared between specific antibodies and 1%BSA in 1XPBST. The following primary antibodies were used; Polyclonal, anti-rabbit VDR (cat. no. NBP1-51322; 1:1,000 dilution; Novus Biologicals, Littleton, USA), monoclonal, anti-rabbit p-ERK1/2 (cat. no. 4376; 1:1,000 dilution; Cell Signaling Technology, Inc., Danvers MA, USA), monoclonal, anti-rabbit p-JNK (cat. no. 4668; 1:1,000 dilution; Cell Signaling Technology, Inc., Danvers MA, USA), monoclonal, anti-rabbit p-p38 (cat. no. 4511; 1:1,000 dilution; Cell Signaling Technology, Inc., Danvers MA, USA), monoclonal, anti-

rabbit  $\beta$ -actin (cat. no. 4970; 1:10,000 dilution; Cell Signaling Technology, Inc., Danvers MA, USA) and monoclonal, anti-rabbit Lamin B1 (cat. no. ab133741; 1:10,000 dilution; Abcam, Cambridge MA, USA). The membranes were incubated at room temperature for 1 hour in PBST with 1%BSA. After washing three times with PBST, the membranes were incubated with secondary antibody (Anti-rabbit IgG, HRP-linked Antibody, cat. no. 7074; 1:10,000 dilution; Cell Signaling Technology, Inc., Danvers MA, USA) for 60 min at room temperature. The membranes were then washed six times 10 min/wash in PBST to reduce background appearance.

#### 4.6 Protein detection and analysis

Molecular Imager<sup>®</sup> ChemiDoc Touch (Bio-rad) was developed to detect protein signals based on Superignal West Femto maximum sensitivity substrate (Thermo Scientific) or enhanced chemiluminescence kit (ECL). The membrane was inserted in the tray and dropped appropriate volumes of prepared ECL all over the membrane. Incubated membrane in the machine around 75 seconds and chose automatically chemiluminescence tap to detecting protein signals. All image results were imported to the computer in TIFF format and band densities were analyzed via Image Lab<sup>™</sup> 5.2 (Bio-rad) analysis program. Each band density was analyzed by using volume tools mode and automatically subtracted background values in every band for an accurate estimation and avoid bias. The levels of VDR protein expression was shown as ratio between relative density of VDR to  $\beta$ -actin (VDR/actin ratio) for whole cell and cytoplasm whereas Lamin B1 (LMB1) was used as normalized protein in part of nucleus. Relative density of three targeted MAPK was shown in the ratio of phosphorylated form to  $\beta$ -actin and Lamin B1 as described above. In addition, cytoplasmic of p-ERK, p-JNK and p-p38 were reported as p-ERK/ $\beta$ -actin, p-JNK/ $\beta$ -actin and p-p38/ $\beta$ -actin whereas nuclear of p-ERK, p-JNK and p-p38 were reported as p-ERK/LMB1, p-JNK/LMB1 and p-p38/LMB1 respectively.

## 5. Statistical analysis

All data were expressed as mean  $\pm$  standard error of measurement (SEM). One-way analysis of variance (one-way ANOVA) was inducted to compare the differences of all histological parameters, immunohistochemistry results, VDR distribution and MAPK subtypes protein expression among all groups of animals followed by Tukey's HSD *post hoc test*. Differences statistically significant were reported at  $p < 0.05$  and statistical analysis was performed by SPSS software version 22.



## Chapter IV RESULTS

### 1. The effects of cigarette smoke exposure on lung histopathological changes

To evaluate the effects of cigarette smoke with no-filter and filter on lung histopathological changes in acute (7 days) and subacute (14 days) emphysema rat models. The left basal lung sections were stained with H&E method which provided the results as shown in table 2.1 and 2.2.

After 7 days smoke exposed to rats' lung, the results demonstrated that the prior event that obviously occurred in this condition was alveolar macrophage infiltrated into the alveolar spaces. No-filter and filter groups were significantly ( $p < 0.05$ ) escalated of alveolar macrophage when compared to control group. After that, there was significantly ( $p < 0.05$ ) augmented of peribronchiolar epithelial cell proliferation in no-filter group and tended to increase in filter group as compared with control. Besides, tracheal epithelial cell changes and lung parenchymal infiltration showed increasing trended in both cigarette smoked exposure groups when compared with control. Eventually, all lung histopathology parameters of no-filter group be liable to severe more than filter group in acute (7 days) phase.

**Table 2.1** Histopathological examination data of all groups after 7 days exposure

	7 Days		
	Control	No-filter	Filter
Tracheal epithelial changes	0.00±0.00	1.40±0.51	1.00±0.31
Peribronchiolar epithelial proliferation	0.00±0.00	*2.40±0.67	0.80±0.80
Lung parenchymal infiltration	0.50±0.00	0.80±0.12	0.90±0.29
Alveolar macrophages count	0.52±0.08	*1.60±0.16	*1.48±0.31

Data were expressed as mean ± SEM; n=5 for each group.

\* $p < 0.05$  when compared to control group.



After 14 days of cigarette smoked exposure, not only both no-filter and filter groups were significantly ( $p < 0.05$ ) increased of alveolar macrophage count, but also tracheal epithelial cell changes became another one parameter which significantly increased ( $p < 0.05$ ) in both cigarette smoked groups as compared with control. Furthermore, peribronchiolar epithelial cell proliferation of no-filter group was significantly ( $p < 0.05$ ) increased after 14 days smoke exposure whereas filter group was prone to increase when compared with control. Nevertheless, lung parenchymal infiltration had tended to increase of both cigarette smoked groups but not significantly different. Lastly, the subacute (14 days) phase after cigarette smoked exposure showed nearly alveolar macrophage influx of both cigarette smoked groups and higher severity of residues parameters of no-filter group than filter group.

**Table 2.2** Histopathological examination data of all groups after 14 days exposure

	14 Days		
	Control	No-filter	Filter
Tracheal epithelial changes	0.00±0.00	*2.20±0.49	*1.60±0.40
Peribronchiolar epithelial proliferation	0.00±0.00	*2.60±0.40	1.40±0.51
Lung parenchymal infiltration	0.50±0.00	1.00±0.00	0.90±0.18
Alveolar macrophages count	0.64±0.11	*1.64±0.14	*1.80±0.32

Data were expressed as mean  $\pm$  SEM; n=5 for each group.

\* $p < 0.05$  when compared to control group.

### 1.1 Tracheal epithelial cell changes

Cigarette smoke exposure with no-filter and filter on 7 and 14 days can alter tracheal epithelial cells changes by altering various criteria such as the altering of pseudostratified ciliated columnar epithelial cells to squamous cell metaplasia, hyperplasia and diffusion of inflammatory cells into the lamina propria. The current study showed the trend of increased tracheal epithelial cells changes of no-filter ( $1.40 \pm 0.51$  vs  $0.00 \pm 0.00$ ) and filter groups ( $1.00 \pm 0.31$  vs  $0.00 \pm 0.00$ ) on 7 days when compared with control. Moreover, on 14 days, there were significantly increased of tracheal epithelial cells changes score in both no-filter ( $2.20 \pm 0.49$  vs  $0.00 \pm 0.00$ ) and filter groups ( $1.60 \pm 0.40$  vs  $0.00 \pm 0.00$ ) when compared with control.

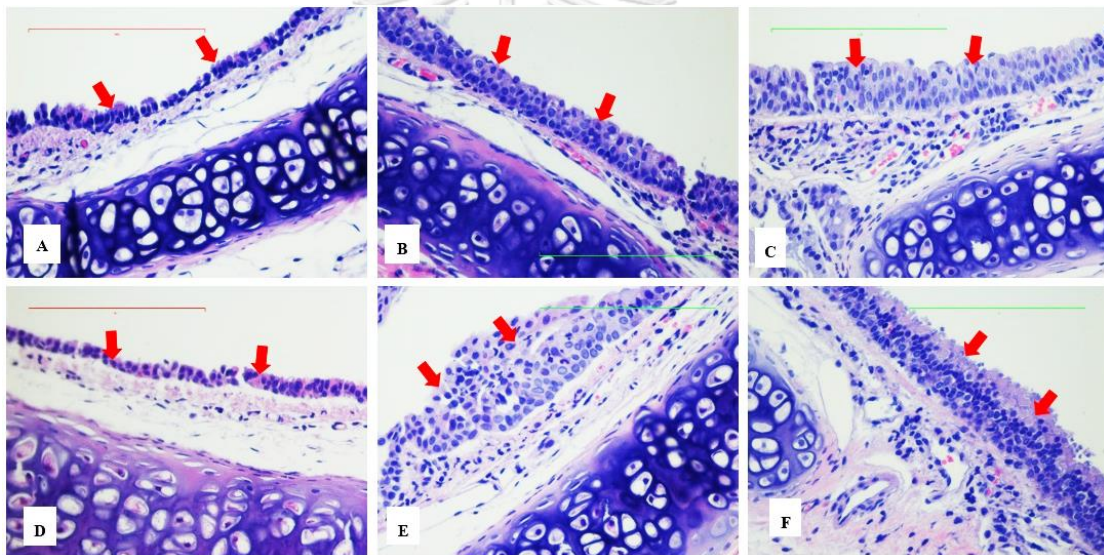


**Figure 14** Acute and subacute effect of cigarette smoke exposure with no-filter and filter on tracheal epithelial cells changes. The left panel showed tracheal epithelial cells of control groups that exposed with room air condition on 7 and 14 days (A,D). The middle panel represented tracheal epithelial cells changes of no-filter groups that exposed to cigarette smoke on 7 and 14 days (B,E). The right panel exhibited tracheal epithelial cells changes of filter groups that exposed to cigarette smoke on 7 and 14 days respectively (C,F).  $n=5$  animals per group. Magnification 40x.

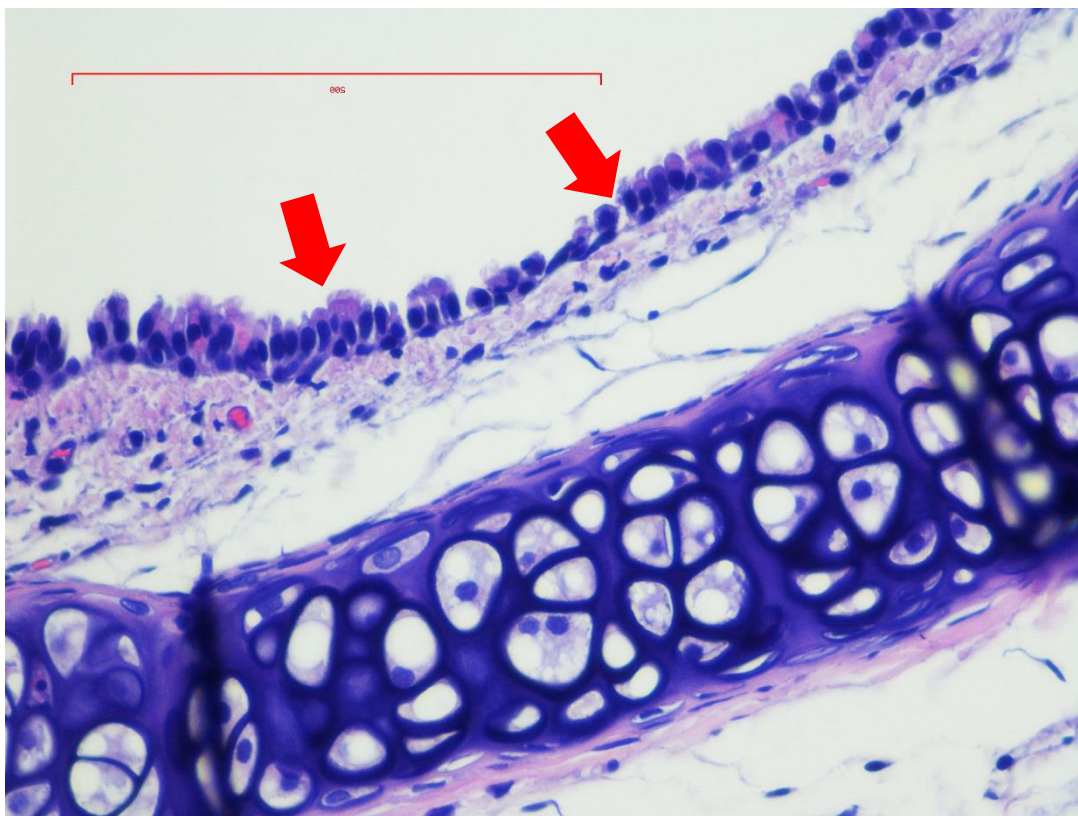


**Figure 15** Tracheal epithelial cells changed of control group after room air exposure for 7 days. Red arrows indicated the epithelial cells that used to grade histopathological score. n=5 animals per group. Magnification 40x.

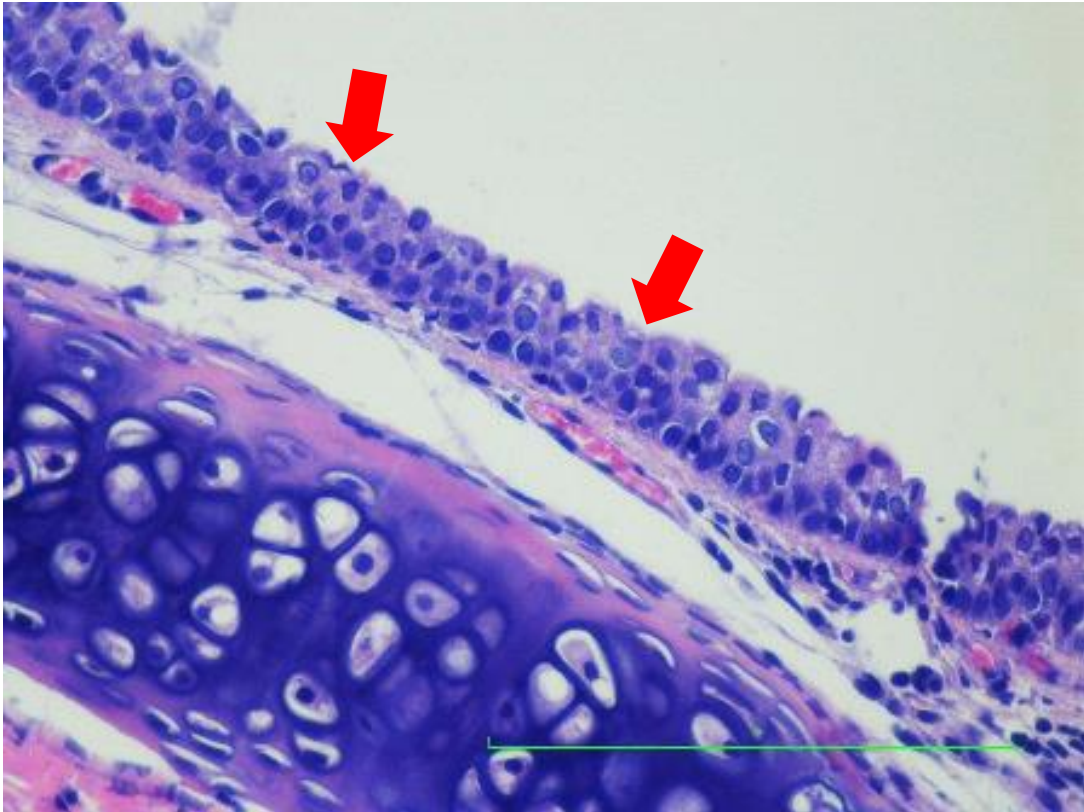


**Figure 16** Tracheal epithelial cells changed of no-filter group after cigarette smoke exposure for 7 days. Red arrows indicated the epithelial cells that used to grade histopathological score. n=5 animals per group. Magnification 40x.

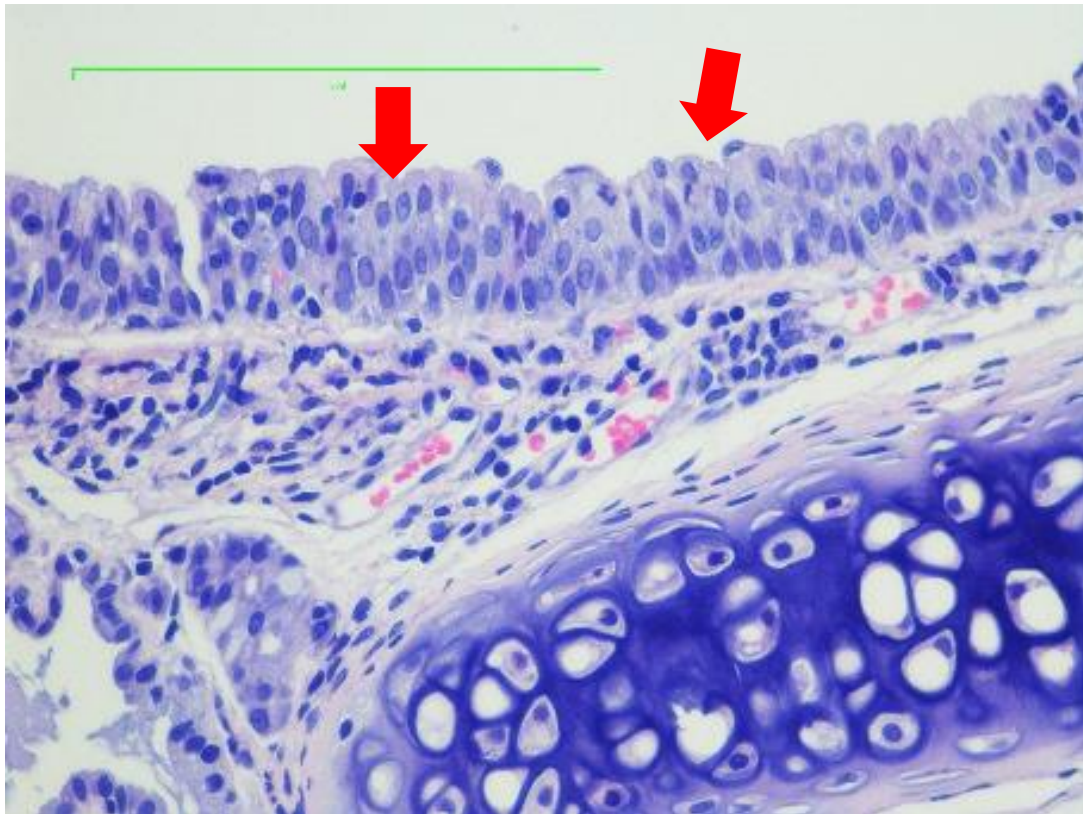


**Figure 17** Tracheal epithelial cells changed of filter group after cigarette smoke exposure for 7 days. Red arrows indicated the epithelial cells that used to grade histopathological score. n=5 animals per group. Magnification 40x.

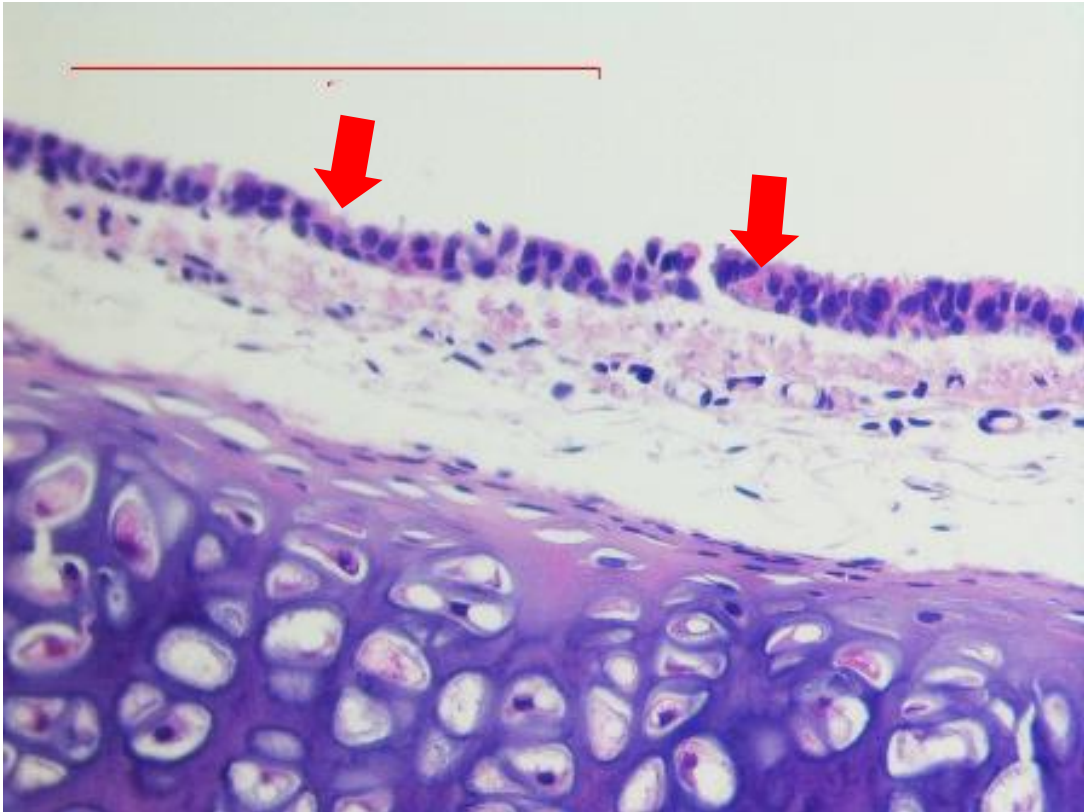


**Figure 18** Tracheal epithelial cells changed of control group after room air exposure for 14 days. Red arrows indicated the epithelial cells that used to grade histopathological score. n=5 animals per group. Magnification 40x.

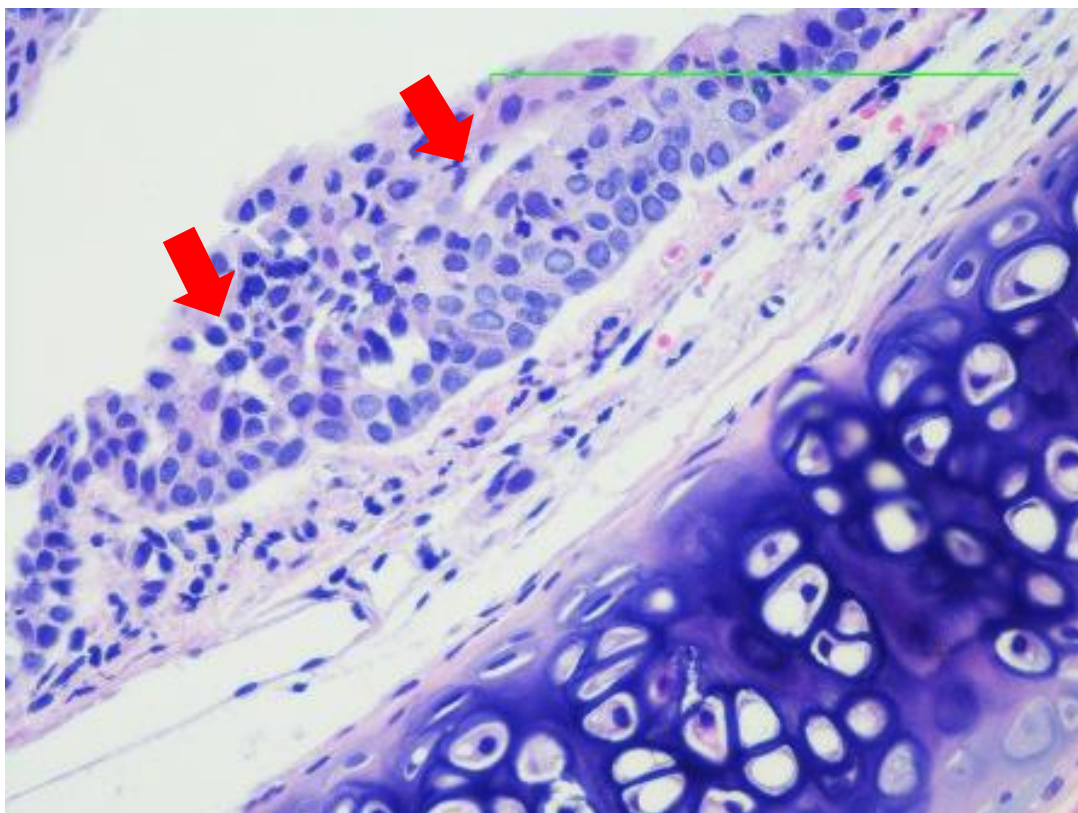


**Figure 19** Tracheal epithelial cells changed of no-filter group after cigarette smoke exposure for 14 days. Red arrows indicated the epithelial cells that used to grade histopathological score. n=5 animals per group. Magnification 40x.

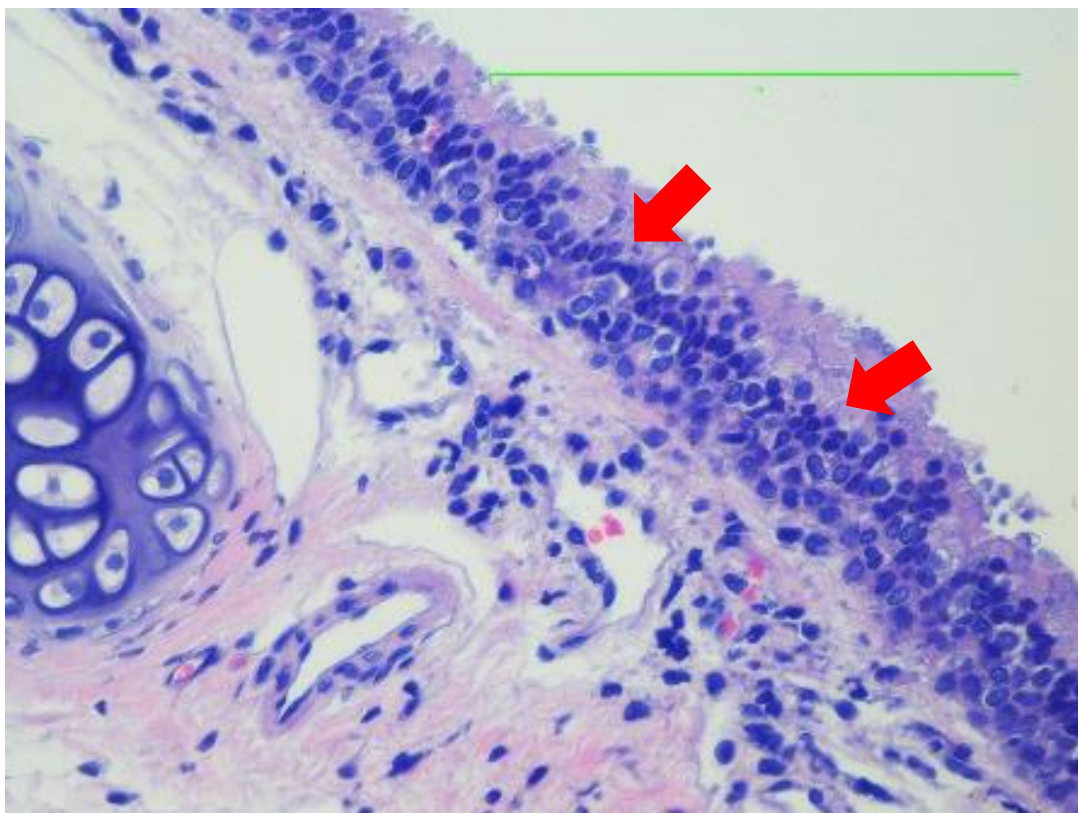


**Figure 20** Tracheal epithelial cells changed of filter group after cigarette smoke exposure for 14 days. Red arrows indicated the epithelial cells that used to grade histopathological score. n=5 animals per group. Magnification 40x.



## 1.2 Peribronchiolar epithelial cell proliferation

This study applied the bronchiolar epithelial cells proliferation to the pathological parameter from two cigarette smoke exposure types on acute and subacute phase. The results showed that not only significantly increased of bronchiolar epithelial cell proliferation of no-filter group when compared with control ( $2.40 \pm 0.67$  vs  $0.00$ ) on 7 days, but also filter group ( $0.80 \pm 0.80$  vs  $0.00$ ) was expressed a tendency of proliferative effect as the same time. Furthermore, there were significantly more extended of peribronchiolar epithelial cells proliferation in no-filter group as compared with control ( $2.60 \pm 0.40$  vs  $0.00$ ) on 14 days together with the inclination of peribronchiolar epithelial cells proliferation of filter group ( $1.40 \pm 0.51$  vs  $0.00$ ) on 14 days when compared with control.

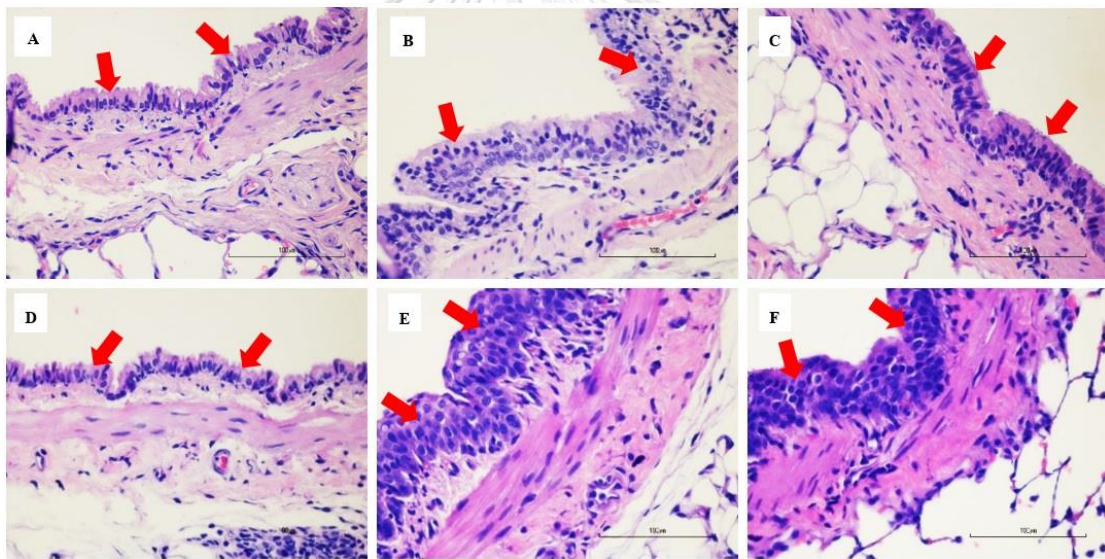


**Figure 21** Acute and subacute effect of cigarette smoke exposure with no-filter and filter on peribronchiolar epithelial cells proliferation. The left panel demonstrated peribronchiolar epithelial cells of control group that exposed with room air condition on 7 and 14 days (A,D). The middle panel showed peribronchiolar epithelial cells proliferation after cigarette smoke exposure of no-filter group on 7 and 14 days (B,E). The right panel presented peribronchiolar epithelial cells proliferation after cigarette smoke exposure of filter group on 7 and 14 days respectively (C,F).  $n=5$  animals per group. Magnification 40x.

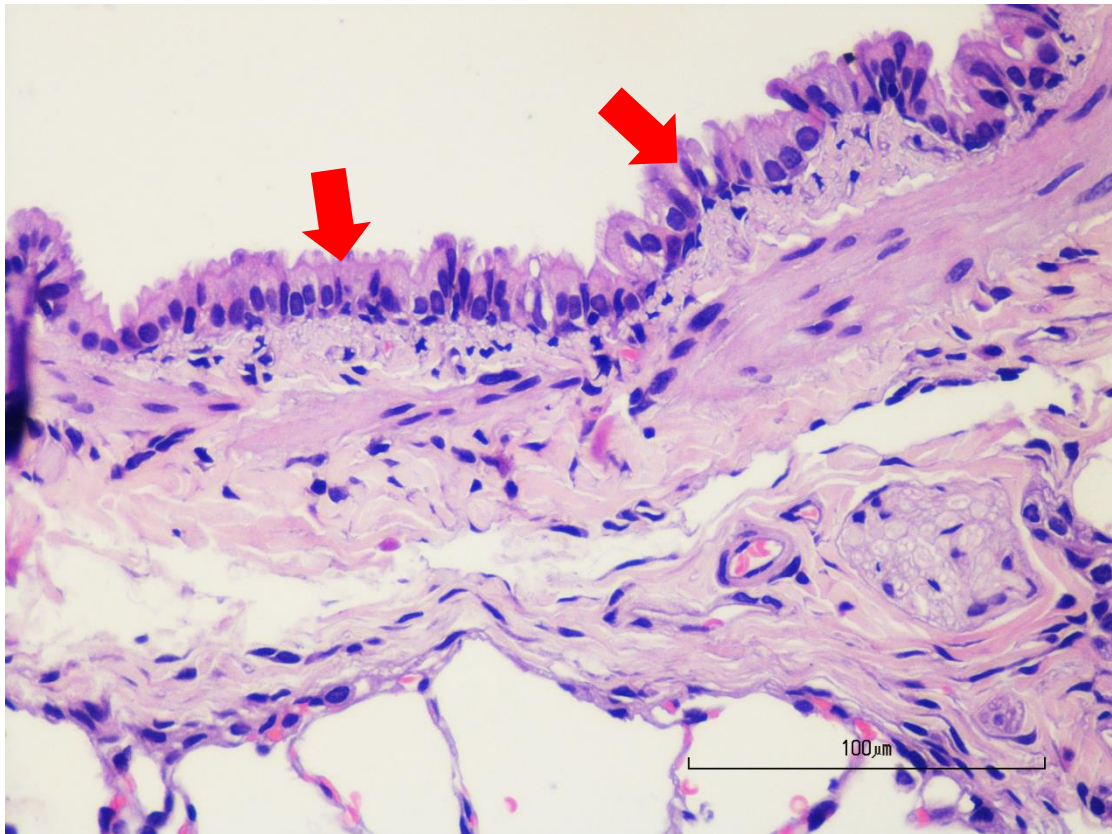


**Figure 22** Peribronchiolar epithelial cells of control group after room air exposure for 7 days. Red arrows indicated the epithelial cells that used to grade histopathological score. n=5 animals per group. Magnification 40x.

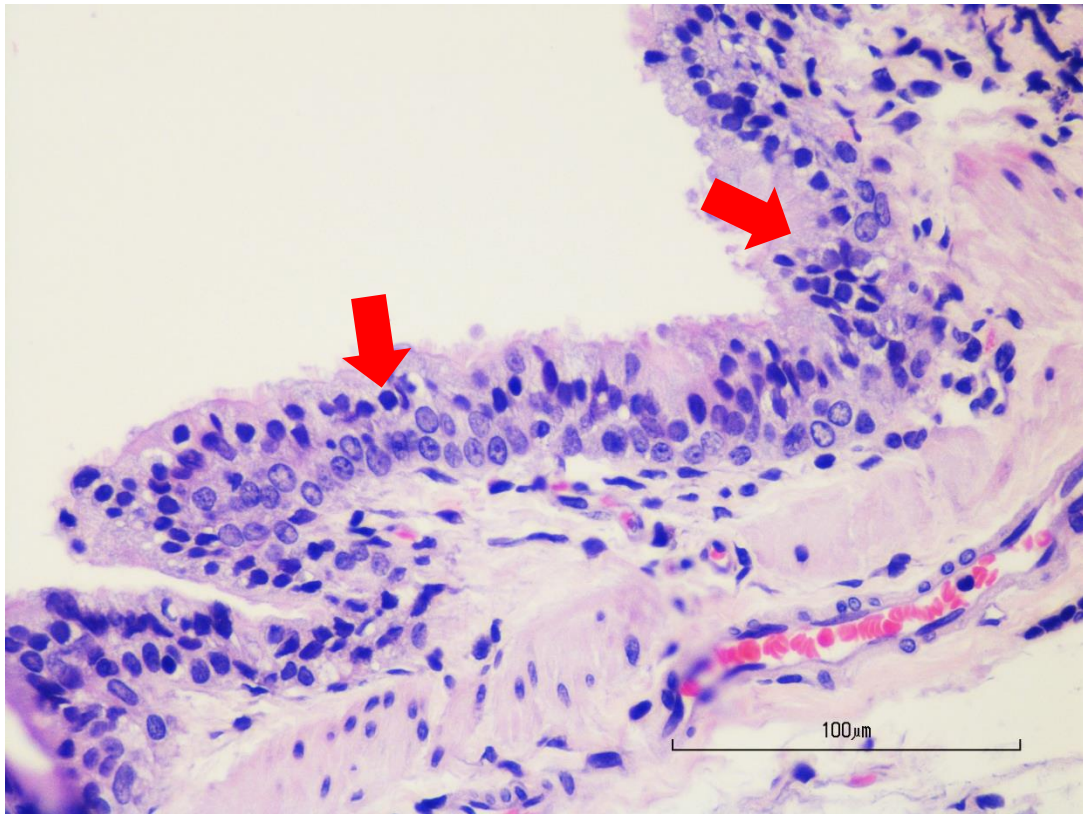


**Figure 23** Peribronchiolar epithelial cells of no-filter group after cigarette smoke exposure for 7 days. Red arrows indicated the epithelial cells that used to grade histopathological score. n=5 animals per group. Magnification 40x.

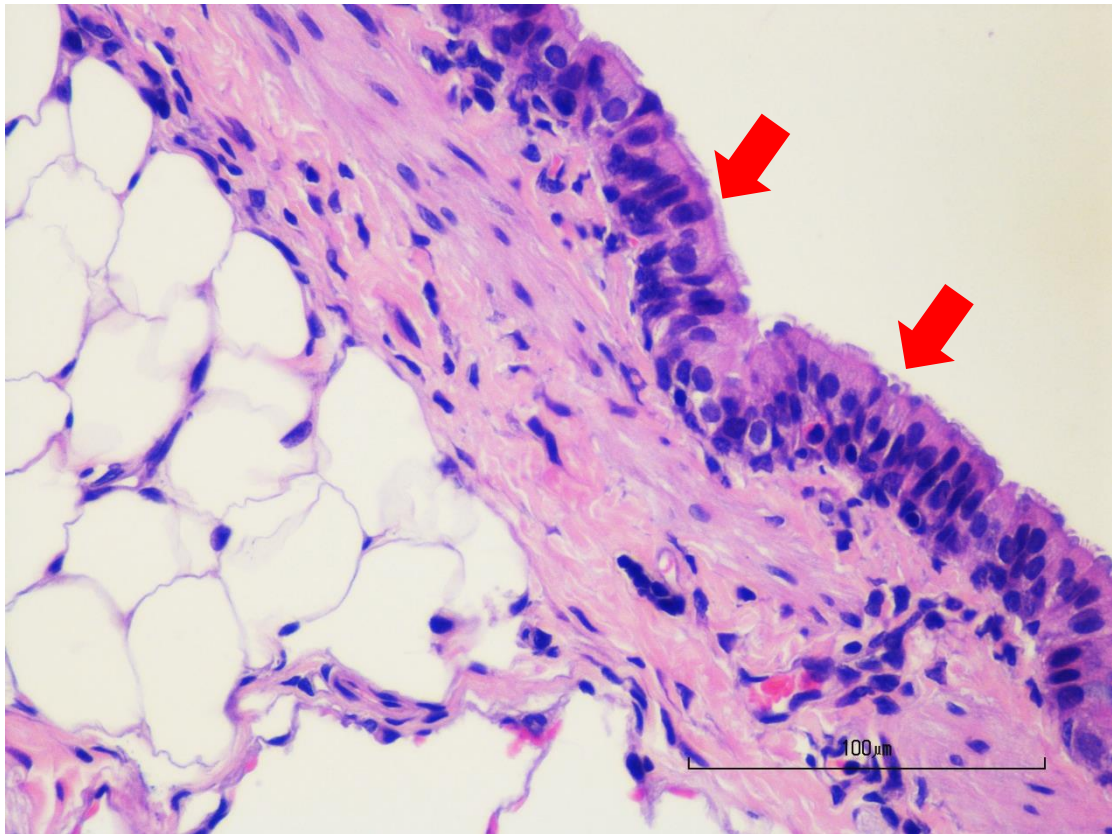


**Figure 24** Peribronchiolar epithelial cells of filter group after cigarette smoke exposure for 7 days. Red arrows indicated the epithelial cells that used to grade histopathological score. n=5 animals per group. Magnification 40x.

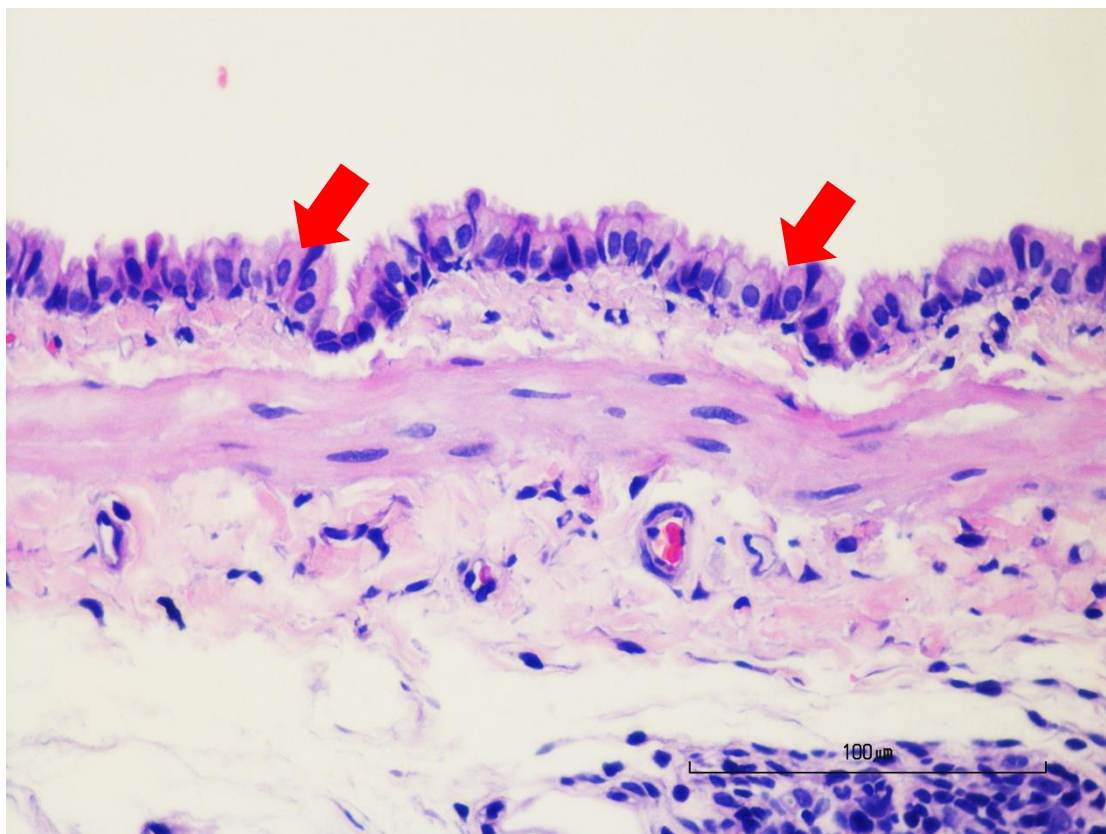


**Figure 25** Peribronchiolar epithelial cells of control group after room air exposure for 14 days. Red arrows indicated the epithelial cells that used to grade histopathological score. n=5 animals per group. Magnification 40x.

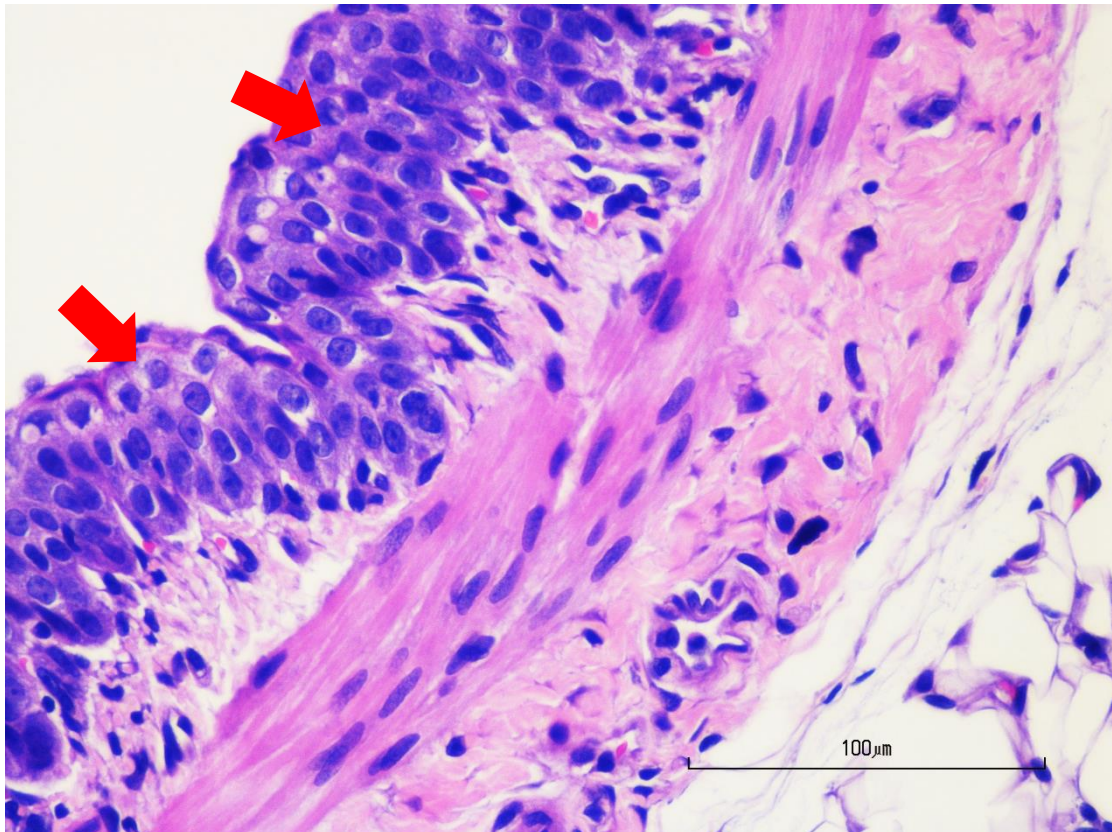


**Figure 26** Peribronchiolar epithelial cells of no-filter group after cigarette smoke exposure for 14 days. Red arrows indicated the epithelial cells that used to grade histopathological score. n=5 animals per group. Magnification 40x.

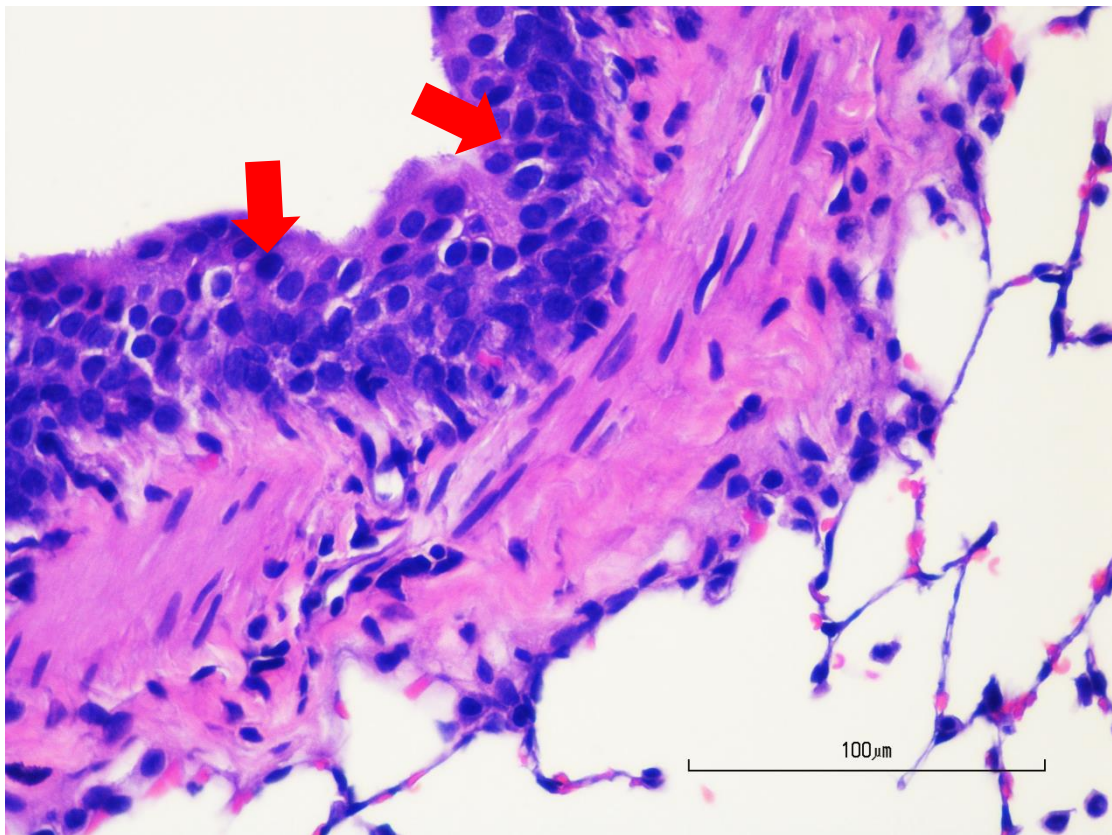


**Figure 27** Peribronchiolar epithelial cells of filter group after cigarette smoke exposure for 14 days. Red arrows indicated the epithelial cells that used to grade histopathological score, n=5 animals per group. Magnification 40x.

### 1.3 Lung parenchymal inflammatory cell infiltration

Lung parenchymal inflammatory cell infiltration was used as one of the inflammatory parameter via determining of neutrophils and leukocytes that infiltrate into the lung parenchyma after cigarette smoke exposure. The results of this parameter suggested that the tendency of lung parenchymal inflammatory cell infiltration in both no-filter (7D:  $0.80 \pm 0.12$ , 14D:  $1.00 \pm 0.00$ ) and filter groups (7D:  $0.90 \pm 0.29$ , 14D:  $0.90 \pm 0.18$ ) were increased when compare to control group after exposed to cigarette smoke on 7 and 14 days respectively.

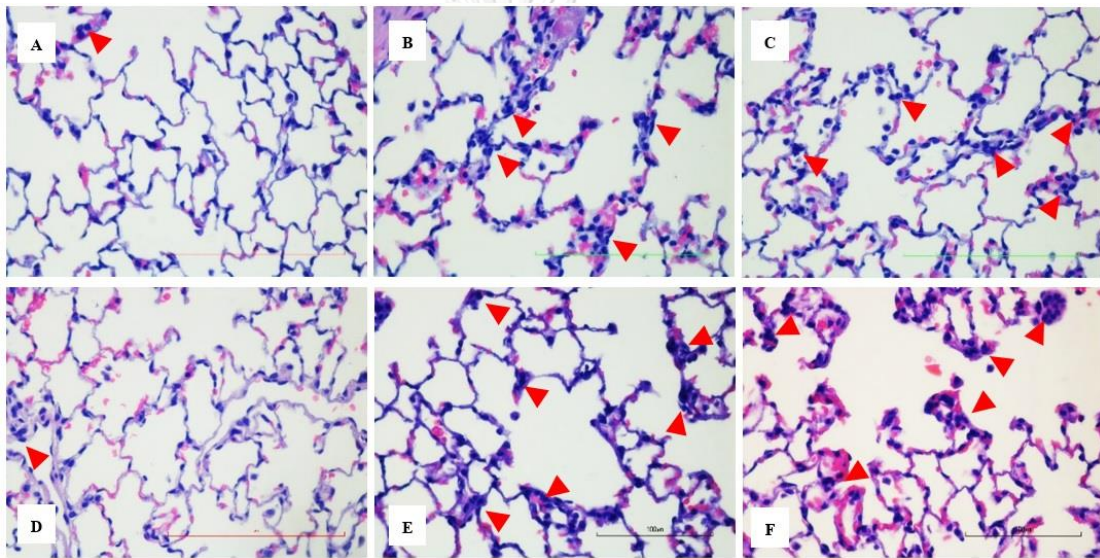


**Figure 28** Acute and subacute effect of cigarette smoke exposure with no-filter and filter to lung parenchymal inflammatory cells infiltration. The left panel showed lung parenchymal infiltration of control groups that exposed with room air condition on 7 and 14 days (A,D). The middle panel showed lung parenchymal inflammatory cells infiltration after cigarette smoke exposure of no-filter groups on 7 and 14 days (B,E). The right panel presented lung parenchymal inflammatory cells infiltration after cigarette smoke exposure of filter groups on 7 and 14 days respectively (C,F). The red arrows indicated the areas of inflammatory cells infiltration. n=5 animals per group. Magnification 40x.



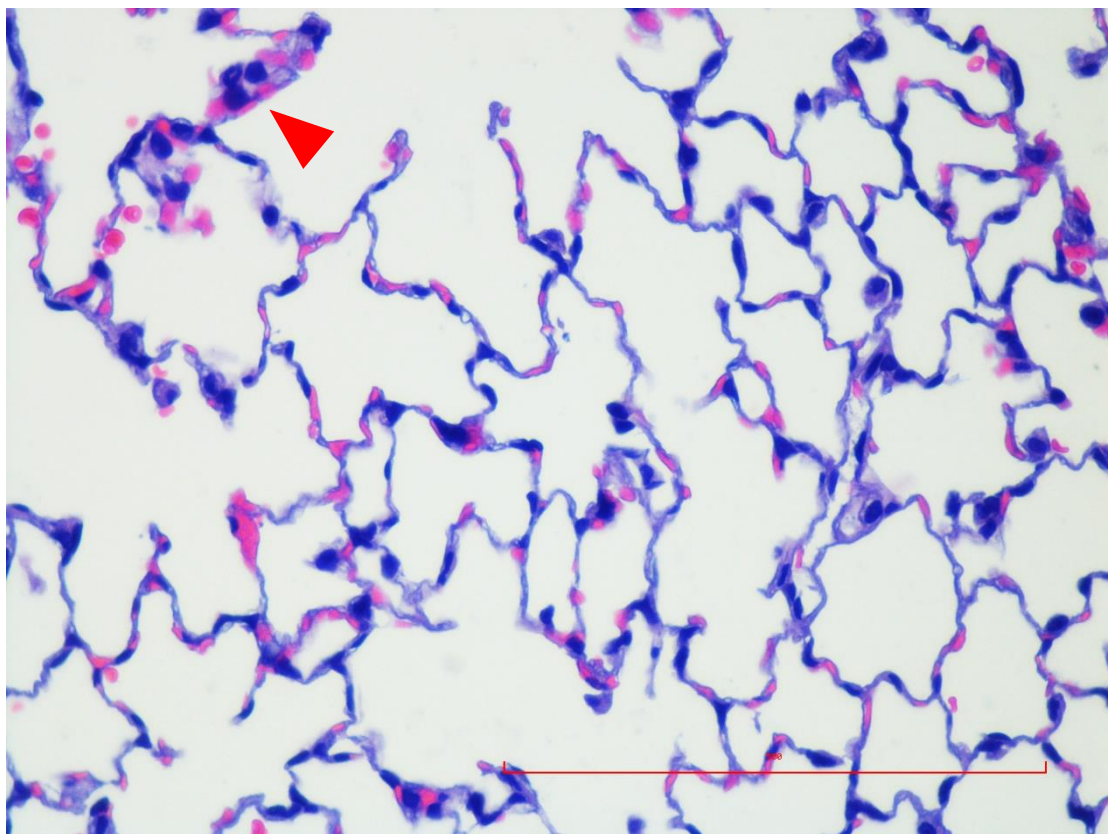


**Figure 29** Lung parenchymal inflammatory cells infiltration of control group after room air exposure for 7 days. Red arrows indicated the area of inflammatory cells infiltration that used to grade histopathological score. n=5 animals per group. Magnification 40x.

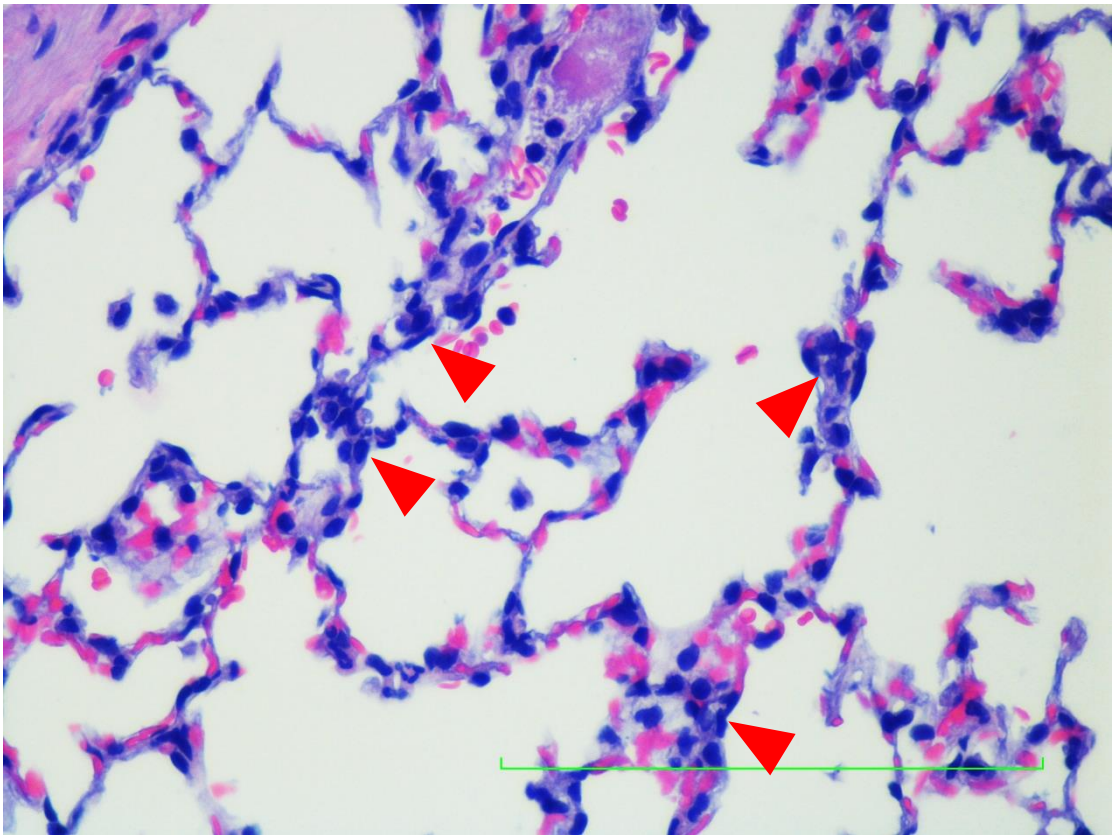


**Figure 30** Lung parenchymal inflammatory cells infiltration of no-filter group after cigarette smoke exposure for 7 days. Red arrows indicated the area of inflammatory cells infiltration that used to grade histopathological score. n=5 animals per group. Magnification 40x.

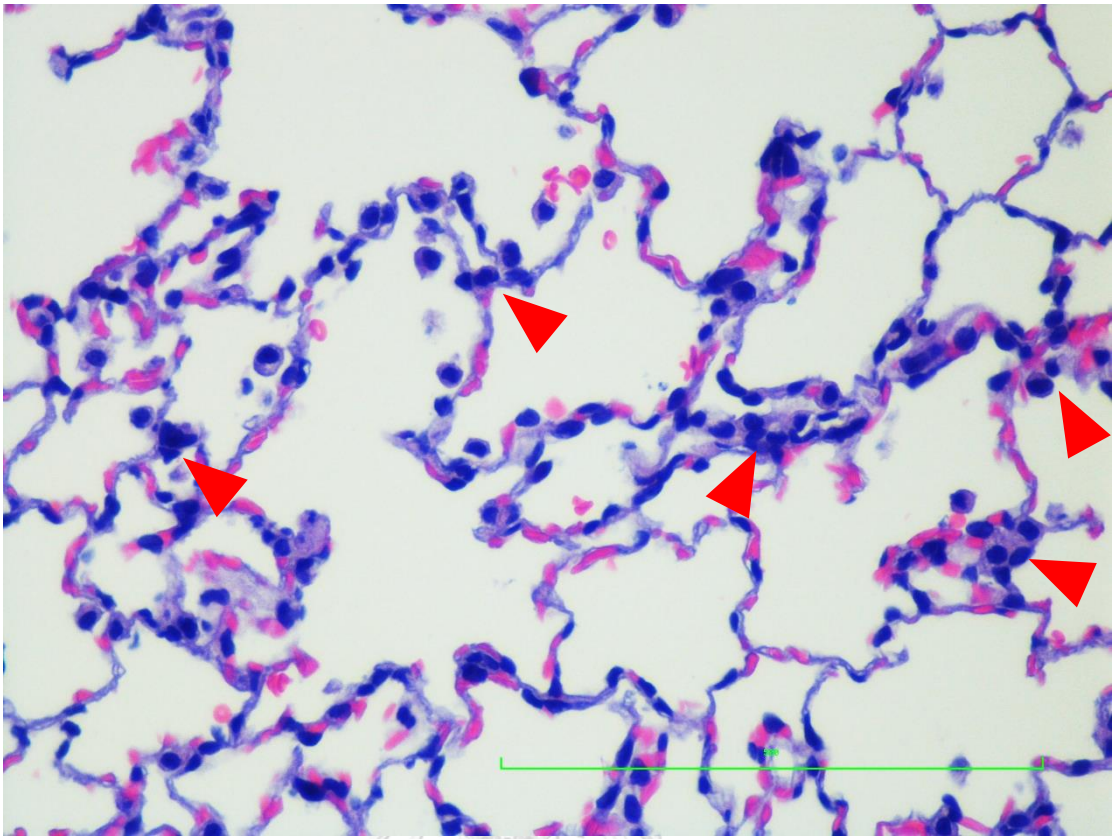


**Figure 31** Lung parenchymal inflammatory cells infiltration of filter group after cigarette smoke exposure for 7 days. Red arrows indicated the area of inflammatory cells infiltration that used to grade histopathological score. n=5 animals per group. Magnification 40x.

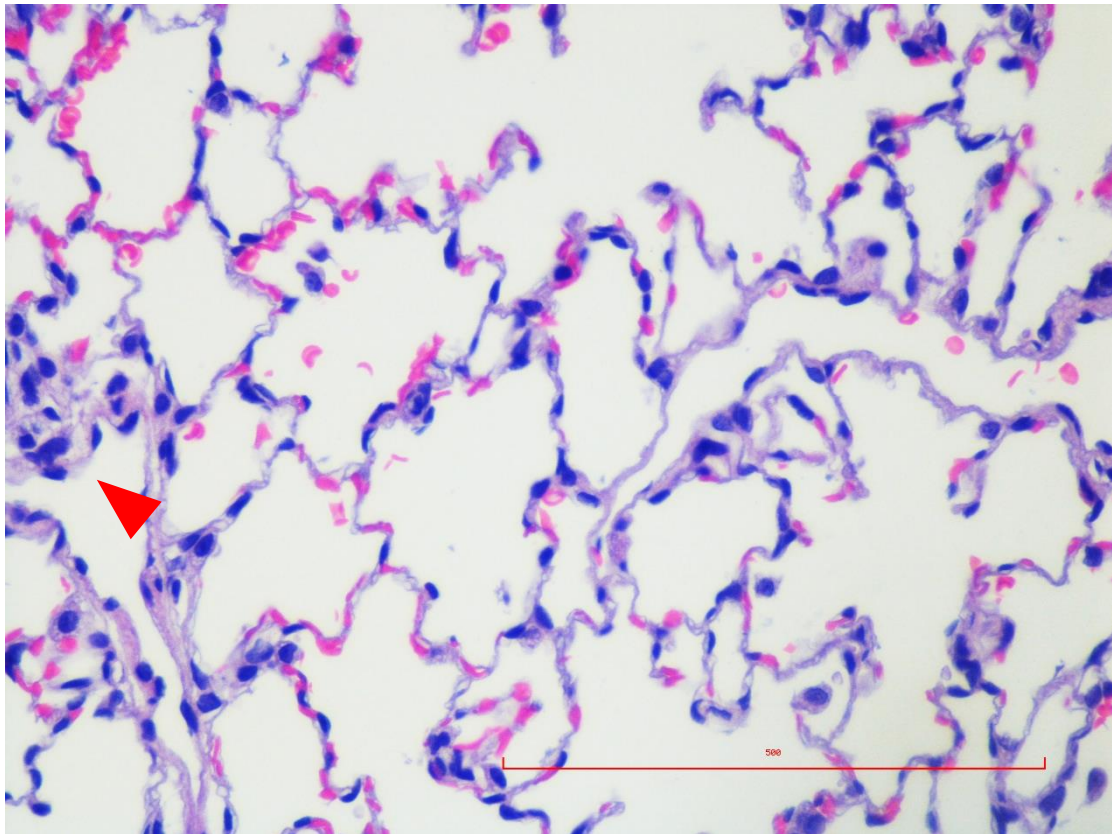


**Figure 32** Lung parenchymal inflammatory cells infiltration of control group after room air exposure for 14 days. Red arrows indicated the area of inflammatory cells infiltration that used to grade histopathological score. n=5 animals per group. Magnification 40x.

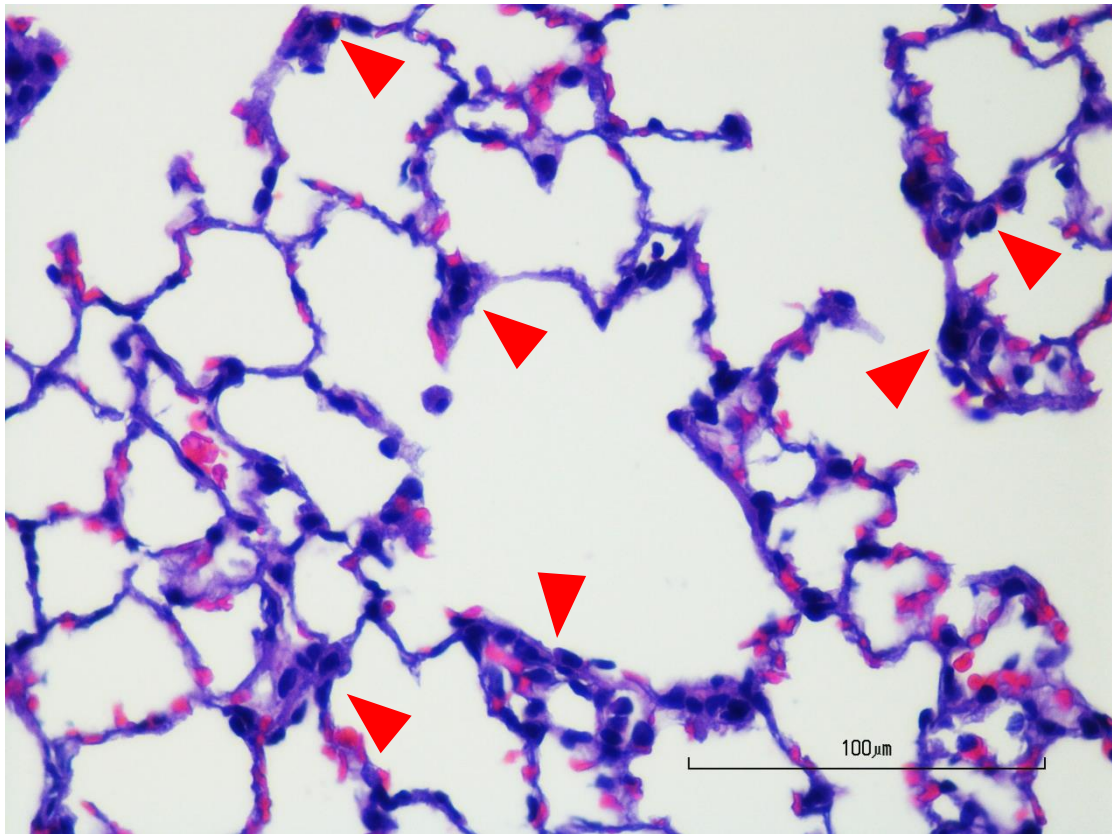


**Figure 33** Lung parenchymal inflammatory cells infiltration of no-filter group after cigarette smoke exposure for 14 days. Red arrows indicated the area of inflammatory cells infiltration that used to grade histopathological score. n=5 animals per group. Magnification 40x.

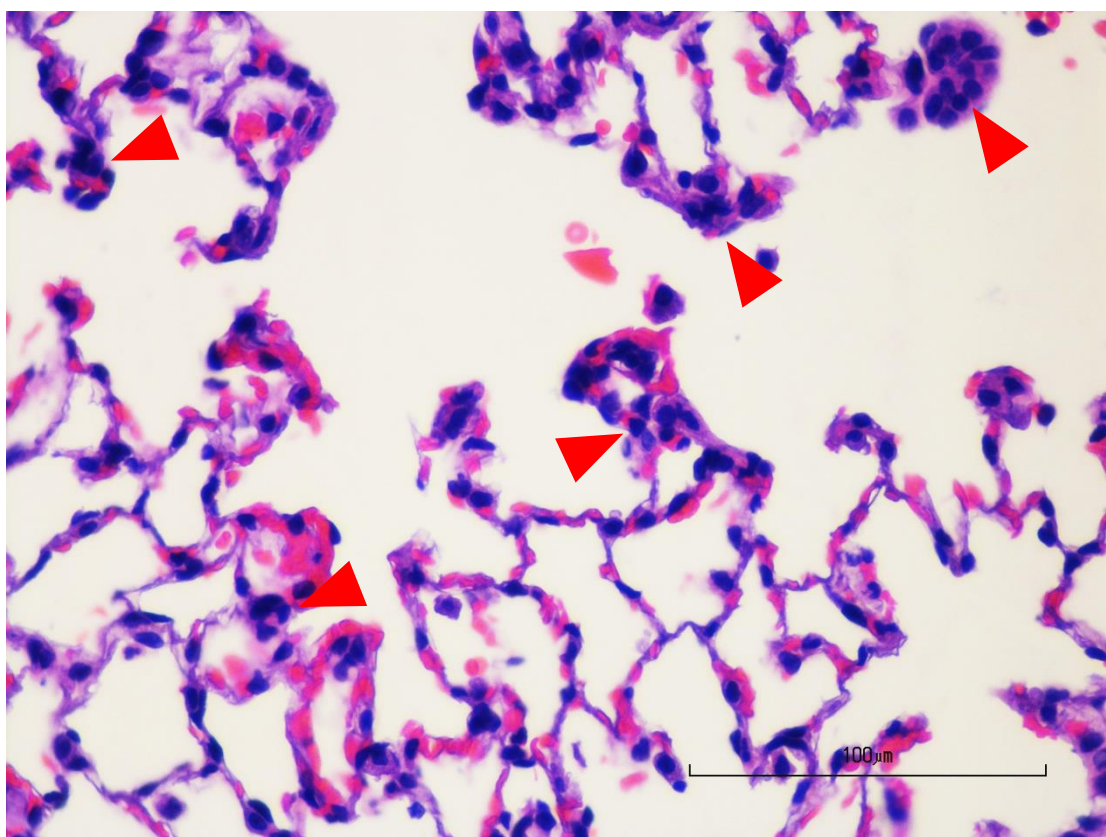


**Figure 34** Lung parenchymal inflammatory cells infiltration of filter group after cigarette smoke exposure for 14 days. Red arrows indicated the area of inflammatory cells infiltration that used to grade histopathological score. n=5 animals per group. Magnification 40x.

#### 1.4 Alveolar macrophage count

Alveolar macrophage count was used as another parameter to ensure inflammatory process by counting the influx of alveolar macrophages into the alveolar spaces. The results demonstrated that there were significantly escalated of alveolar macrophage count of both no-filter ( $1.60 \pm 0.16$  vs  $0.52 \pm 0.08$ ) and filter ( $1.48 \pm 0.31$  vs  $0.52 \pm 0.08$ ) groups on 7 days after cigarette smoke exposure when compared with control. Likewise, the alveolar macrophage count of both no-filter ( $1.64 \pm 0.14$  vs  $0.64 \pm 0.11$ ) and filter ( $1.80 \pm 0.32$  vs  $0.64 \pm 0.11$ ) groups were significantly increased like dose dependent manner for 14 days after cigarette smoke exposure.

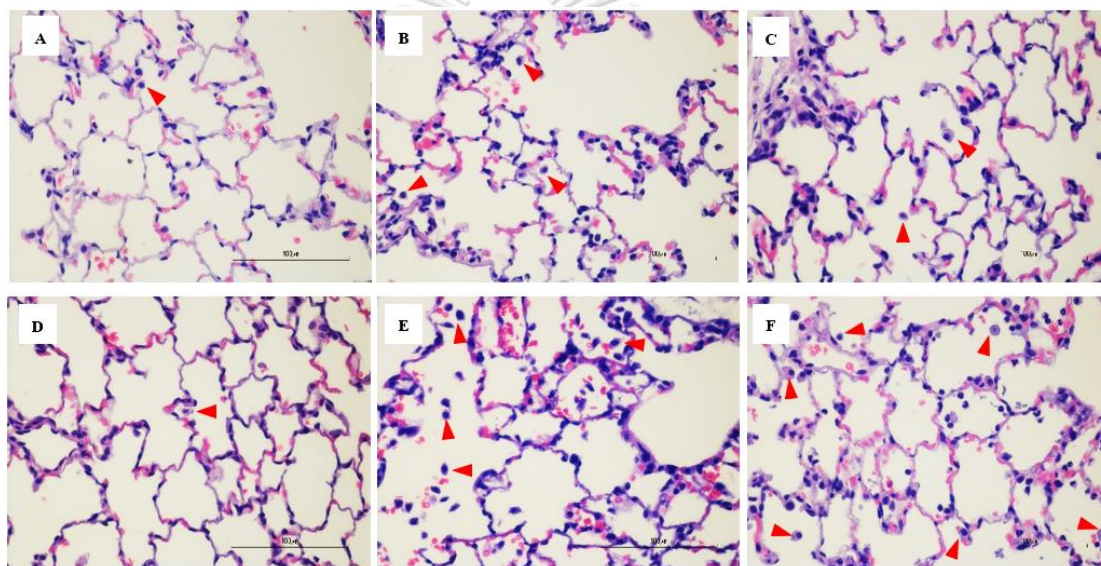


**Figure 35** Acute and subacute effect of cigarette smoke exposure with no-filter and filter to alveolar macrophages count in the alveolar spaces. The left panel showed slightly alveolar macrophage in alveolar spaces of control groups that exposed with room air condition on 7 and 14 days (A,D). The middle panel showed alveolar macrophage infiltration in the alveolar spaces after cigarette smoke exposure of no-filter groups on 7 and 14 days (B,E). The right panel presented alveolar macrophage infiltration in the alveolar spaces after cigarette smoke exposure of filter groups on 7 and 14 days respectively (C,F). The red arrows indicated the alveolar macrophages in the alveolar spaces of the samples. n=5 animals per group. Magnification 40x.

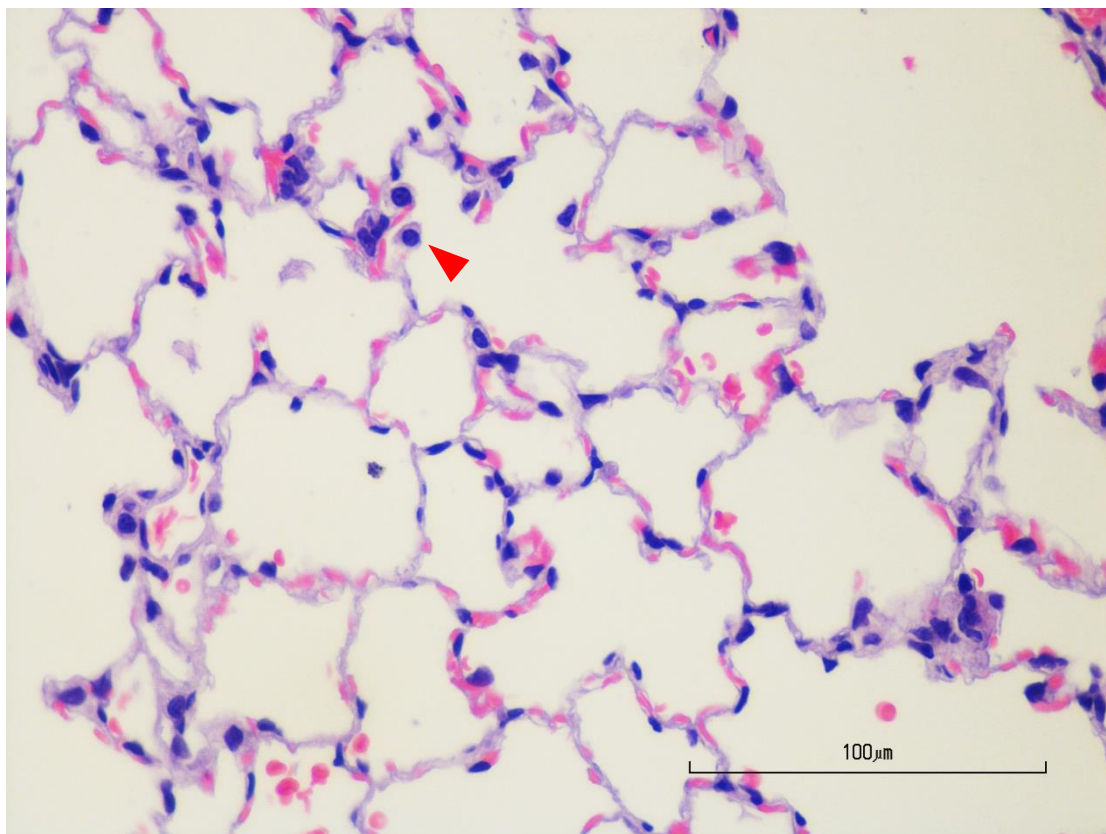


**Figure 36** Alveolar macrophages count of control group after room air exposure for 7 days. Red arrows indicated macrophage in the alveolar space that used to grade histopathological score. n=5 animals per group. Magnification 40x.



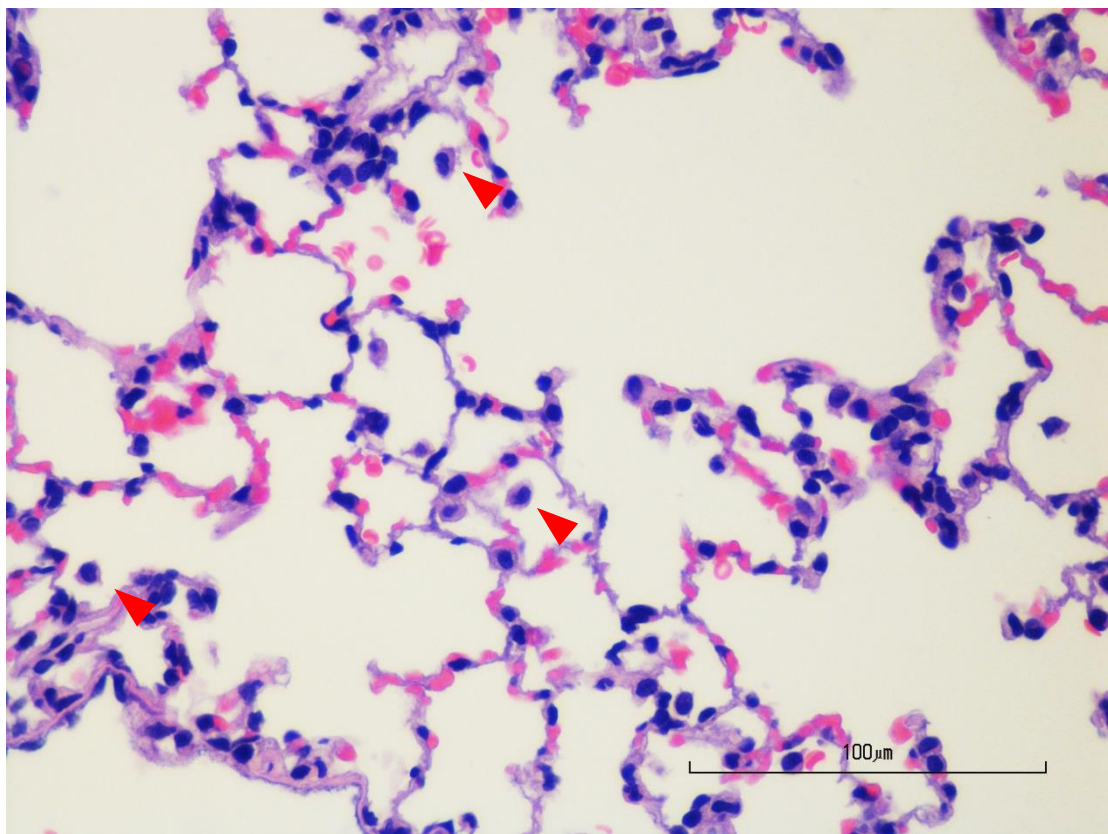


**Figure 37** Alveolar macrophages count of no-filter group after cigarette smoke exposure for 7 days. Red arrows indicated macrophages in the alveolar space that used to grade histopathological score. n=5 animals per group. Magnification 40x.

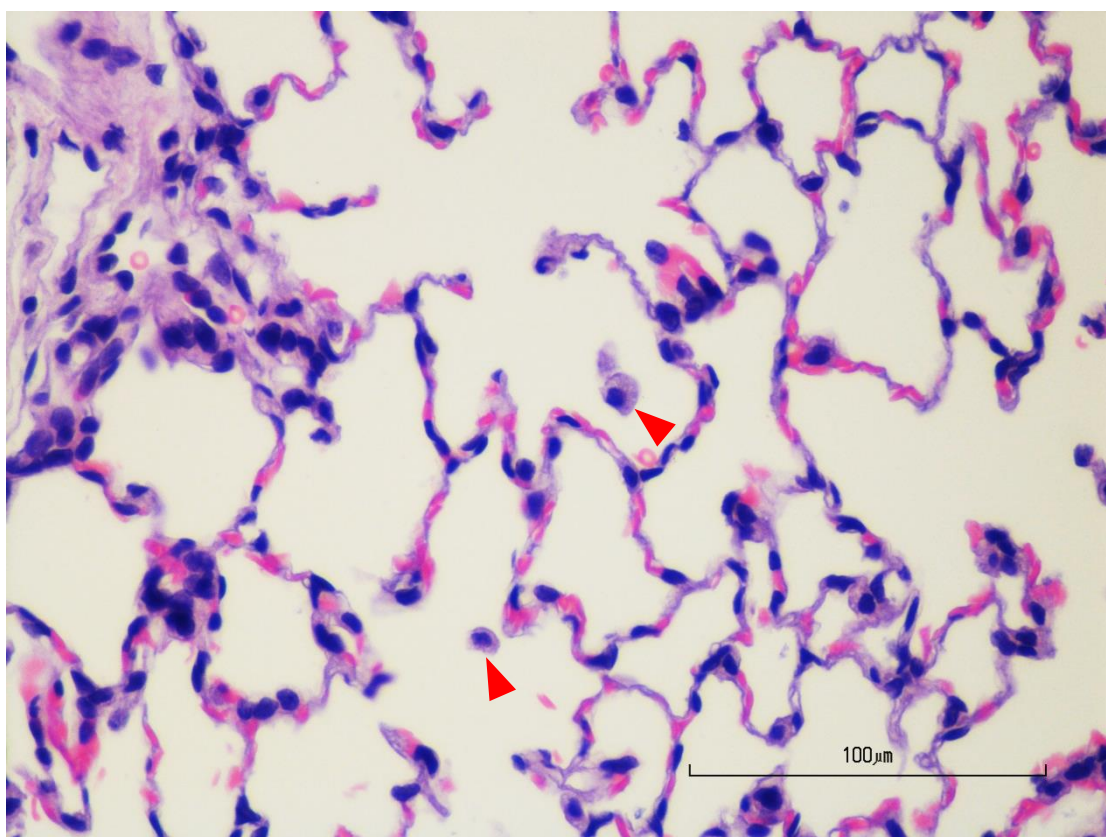


**Figure 38** Alveolar macrophages count of filter group after cigarette smoke exposure for 7 days. Red arrows indicated macrophages in the alveolar space that used to grade histopathological score. n=5 animals per group. Magnification 40x.

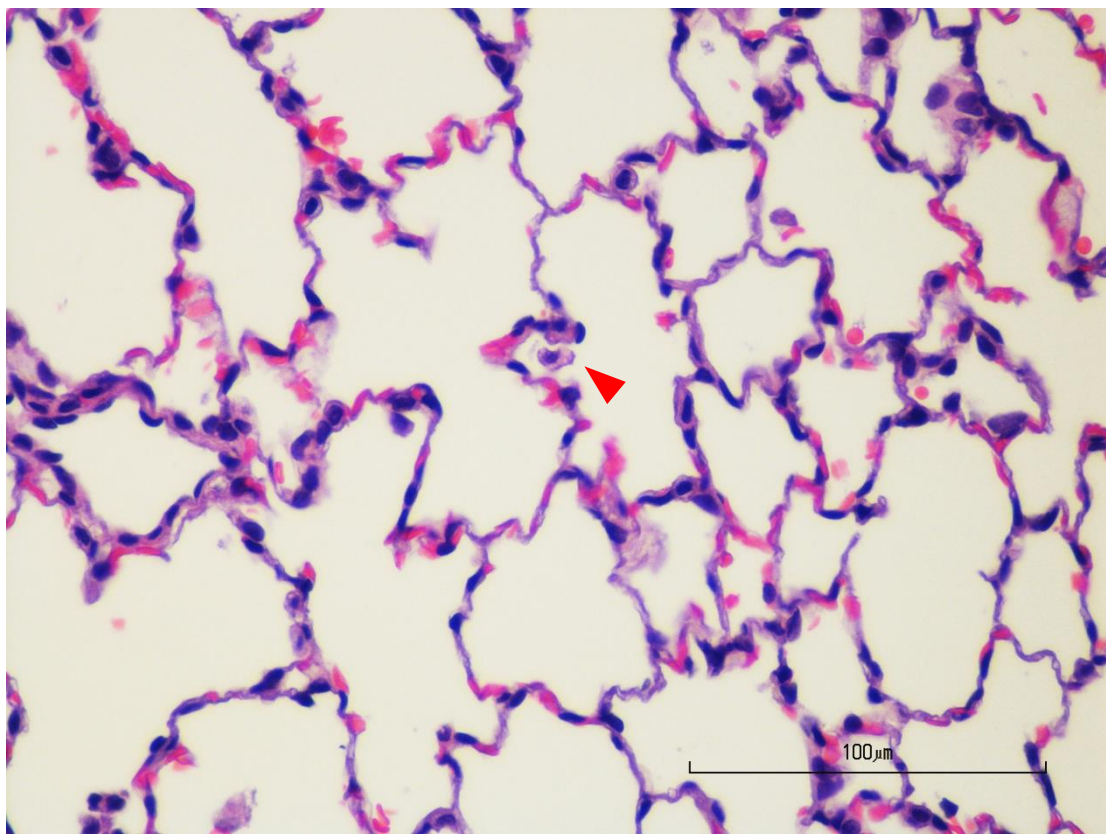


**Figure 39** Alveolar macrophages count of control group after room air exposure for 14 days. Red arrows indicated macrophage in the alveolar space that used to grade histopathological score. n=5 animals per group. Magnification 40x.

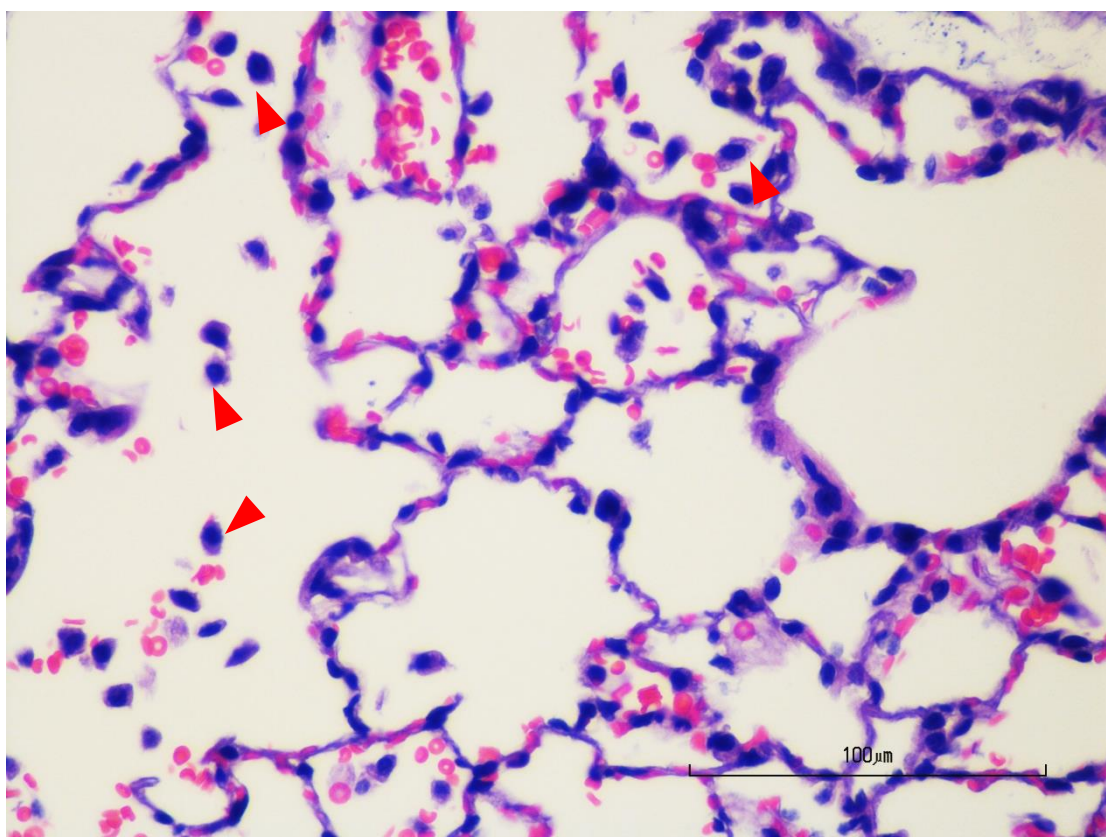


**Figure 40** Alveolar macrophages count of no-filter group after cigarette smoke exposure for 14 days. Red arrows indicated macrophages in the alveolar space that used to grade histopathological score. n=5 animals per group. Magnification 40x.

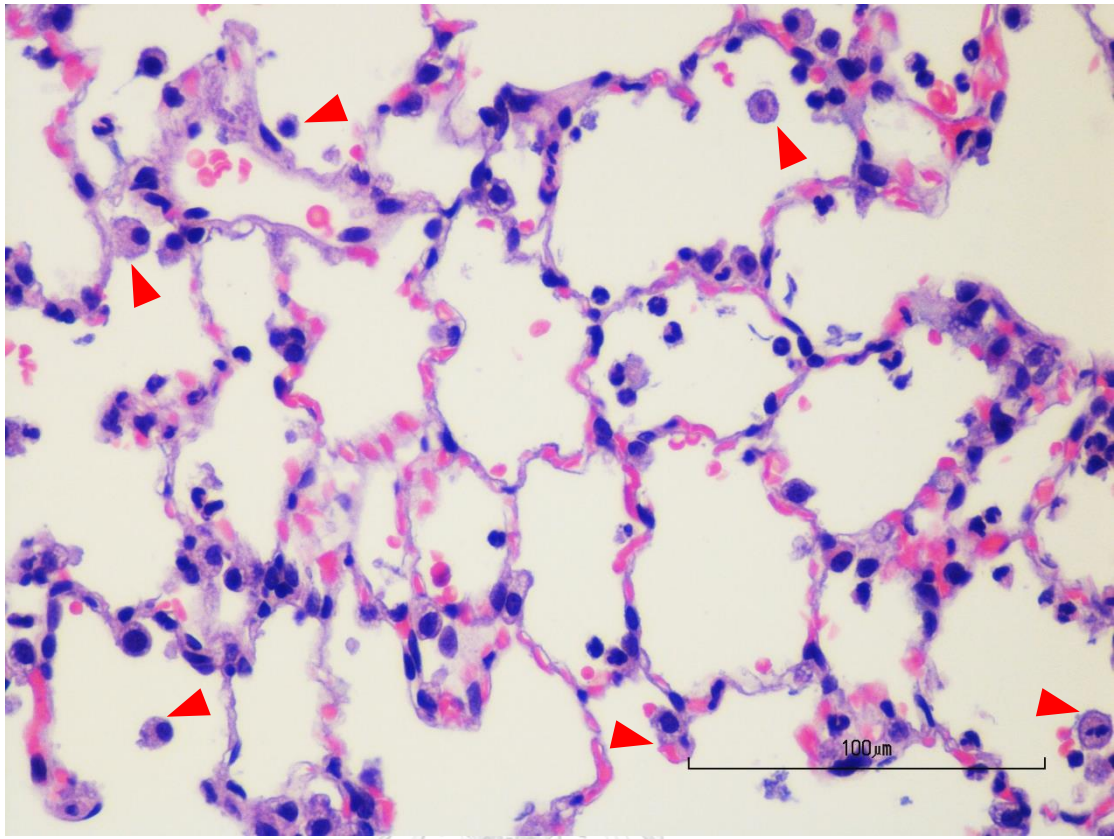


**Figure 41** Alveolar macrophages count of filter group after cigarette smoke exposure for 14 days. Red arrows indicated macrophages in the alveolar space that used to grade histopathological score. n=5 animals per group. Magnification 40x.

## 2. Western blot analysis of VDR distribution and MAPK protein expression

### 2.1 Whole cell VDR distribution and MAPK protein expression in lung tissue after cigarette smoke exposure on 7 and 14 days

The right lung was used to determine VDR distribution, whole cell VDR distribution showed equally level of VDR distribution between control and filter groups on 7 days with slightly reduced in no-filter group. While, 14 days results exhibited declination trend of VDR expression in filter group which contrary to no-filter group when compared with control (Figure 42).

The band intensities of whole cell p-ERK protein expression not differed level of cigarette smoked groups on 7 days when compared with control group. In contrast, cigarette smoked with no-filter and filter groups showed meagerly increased level of p-ERK than control group on 14 days (Figure 43).

Whole cell p-JNK expression showed higher level of no-filter group whilst filter group was similar level of p-JNK when compared to control on 7 days. Moreover, both of cigarette smoked groups were upregulated of p-JNK protein level on 14 days after smoke exposed as compared with control group (Figure44).

At last, whole cell p-p38 protein expression of no-filter group was significantly ( $p < 0.05$ ) escalated on 7 days and significantly ( $p < 0.05$ ) decreased on 14 days when compared with control and the same group on 7 days. While filter group displayed slightly increased of p-p38 protein levels on 7 days and significantly ( $p < 0.05$ ) increased on 14 days when compared with control and no-filter group in similar period (Figure45).

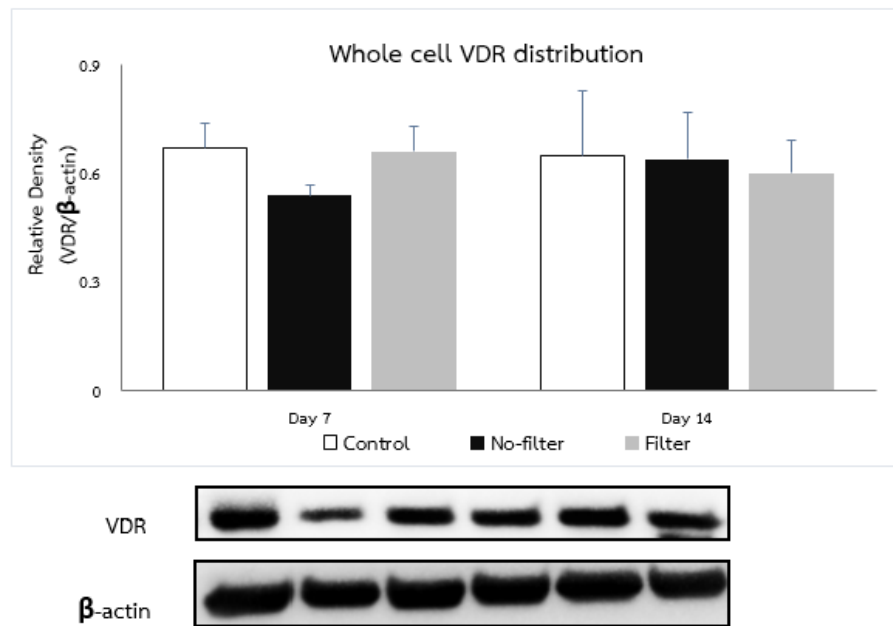


**Figure 42** Effect of cigarette smoke exposure with no-filter and filter to whole cell VDR distribution on 7 and 14 days of lung rats.

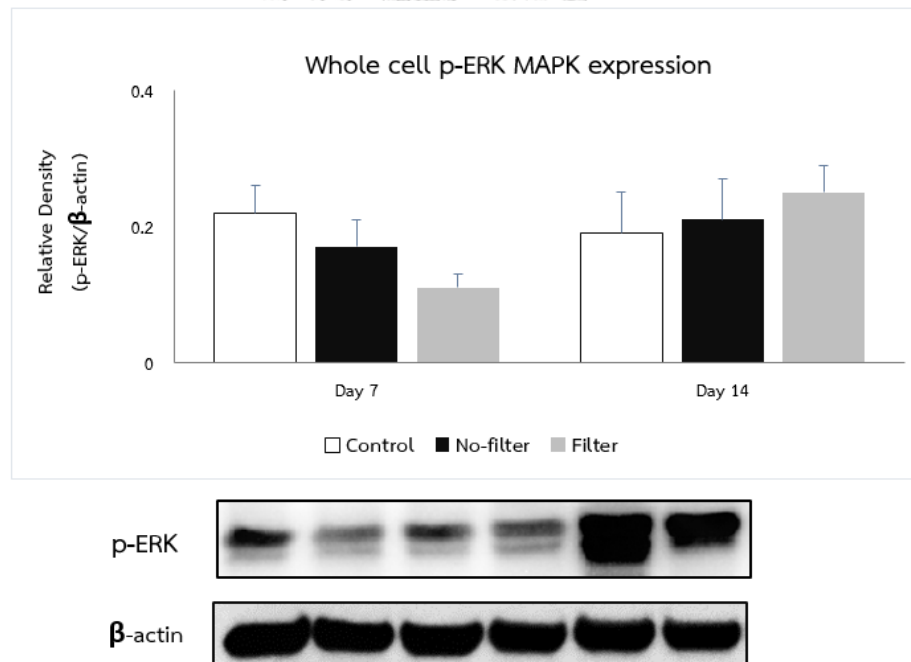


**Figure 43** Effect of cigarette smoke exposure with no-filter and filter to whole cell p-ERK protein expression on 7 and 14 days of lung rats.

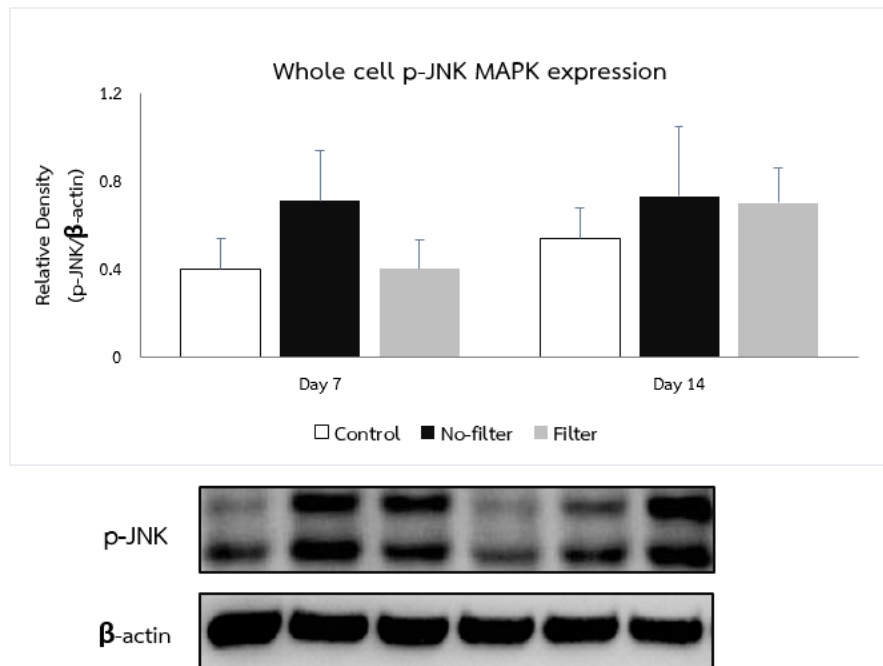


**Figure 44** Effect of cigarette smoke exposure with no-filter and filter to whole cell p-JNK protein expression on 7 and 14 days of lung rats.



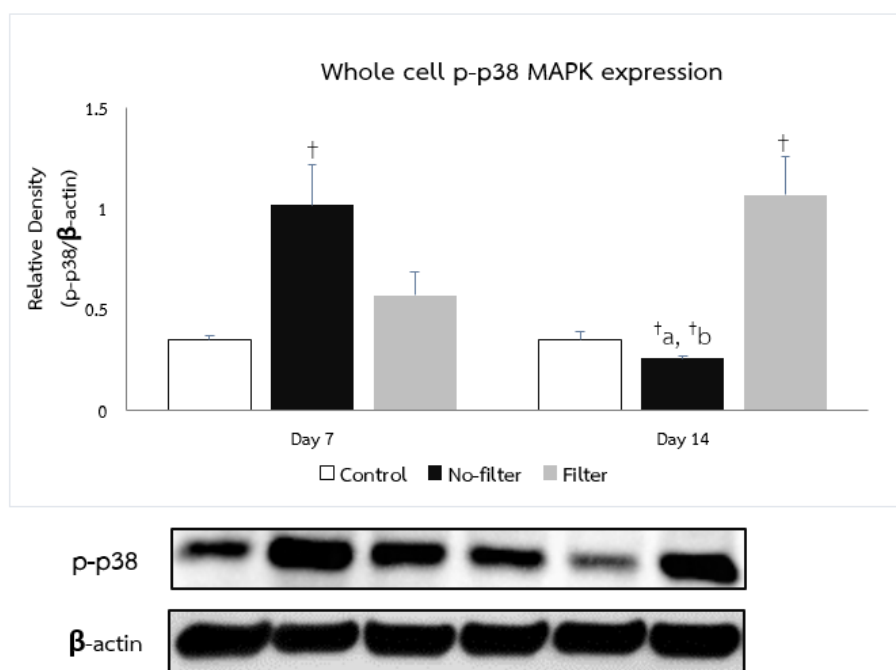


**Figure 45** Effect of cigarette smoke exposure with no-filter and filter to whole cell p-p38 protein expression on 7 and 14 days of lung rats.

†,  $p < 0.05$  when compared with control group

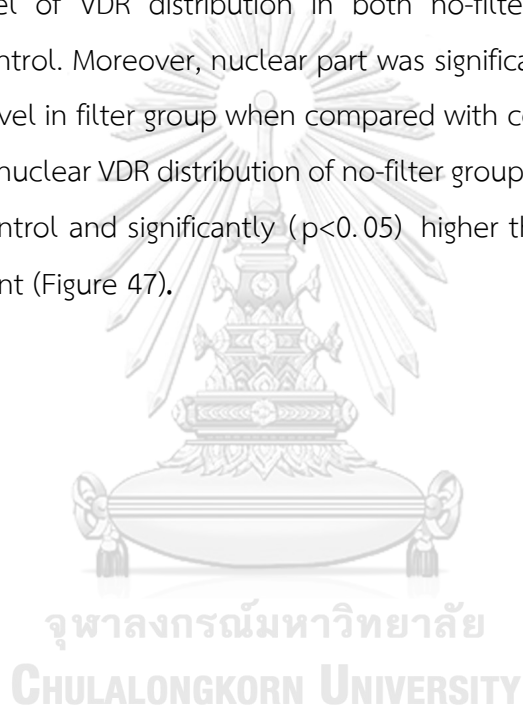
†a,  $p < 0.05$  when compared with no-filter group on 7 days

†b,  $p < 0.05$  when compared with no-filter group and filter groups on 14 days

## 2.2 VDR distribution between cytoplasmic and nuclear compartments in lung tissue after cigarette smoke exposure on 7 and 14 days

After 7 days cigarette smoked exposure, cytoplasmic VDR distribution in rats' lung exhibited the reduction of VDR distribution in both cigarette smoked groups with significantly ( $p < 0.05$ ) decreased in filter group when compared to control. While nuclear compartment showed the similar trended of VDR levels as cytoplasmic compartment in both cigarette smoked groups but higher level than those (Figure 46).

After 14 days cigarette smoked exposure, cytoplasmic part had tended to decrease the level of VDR distribution in both no-filter and filter groups when compared with control. Moreover, nuclear part was significantly ( $p < 0.05$ ) declined of VDR distribution level in filter group when compared with control and no-filter groups. In the other hand, nuclear VDR distribution of no-filter group was slightly reduced when compared with control and significantly ( $p < 0.05$ ) higher than the same group in the cytoplasmic content (Figure 47).



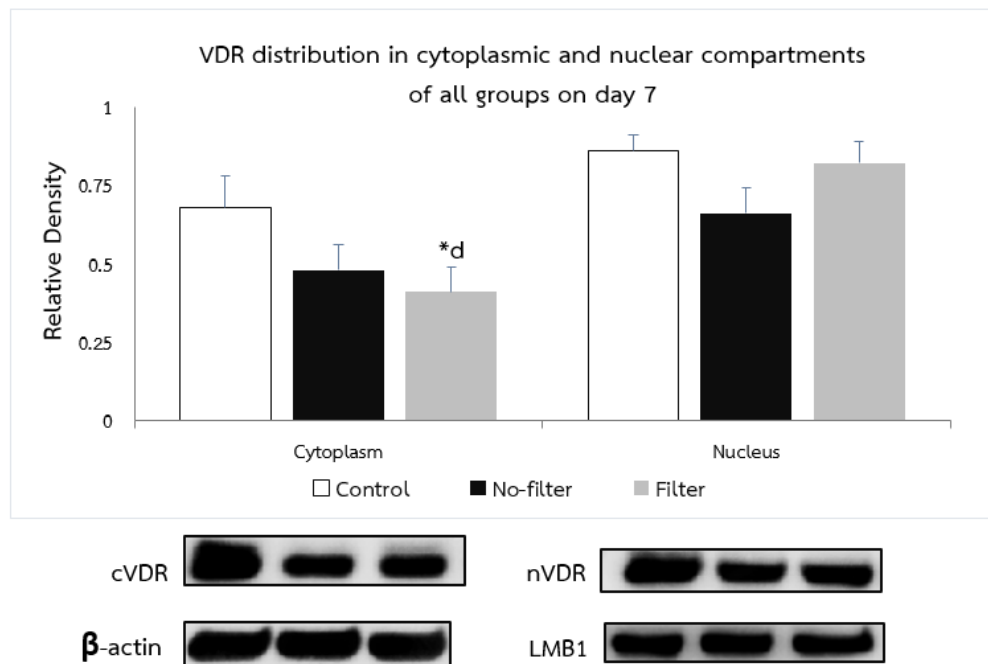


**Figure 46** Effect of cigarette smoke exposure with no-filter and filter to VDR distribution in cytoplasm (cVDR) and nucleus (nVDR) after 7 days exposed of lung rats.

Relative density of cytoplasm represented as ratio of VDR/ $\beta$ -actin

Relative density of nucleus represented as ratio of VDR/Lamin B1

\*d,  $p < 0.05$  compared between filter groups in cytoplasm and nucleus

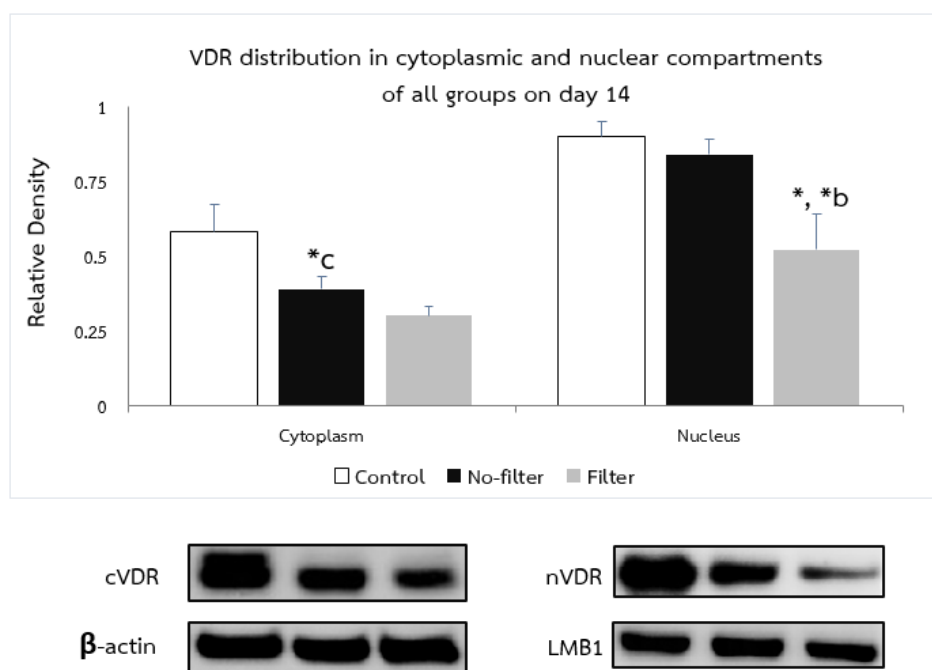


**Figure 47** Effect of cigarette smoke exposure with no-filter and filter to VDR distribution in cytoplasm (cVDR) and nucleus (nVDR) after 14 days exposed of lung rats.

<sup>\*</sup>,  $p < 0.05$  compared with control group

<sup>\*b</sup>,  $p < 0.05$  compared between both CS groups in nucleus

<sup>\*c</sup>,  $p < 0.05$  compared between no-filter groups in cytoplasm and nucleus

### 2.3 p-ERK (p42, sensitive form) between cytoplasmic and nuclear compartments in lung tissue after cigarette smoke exposure on 7 and 14 days

After 7 days of cigarette smoked exposure, cytoplasmic and nuclear p-ERK (p42) expression were highly augmented in no-filter groups whereas filter and control groups in both locations had equally levels of p-ERK (p42) protein expression (Figure 48).

Also, the levels of p-ERK (p42) had similar pattern in cytoplasm and nucleus of all experimental groups on 14 days after smoked exposure. By which both no-filter groups were gradually increased when compared to control and filter groups were higher level than no-filter groups in both sites (Figure 49).

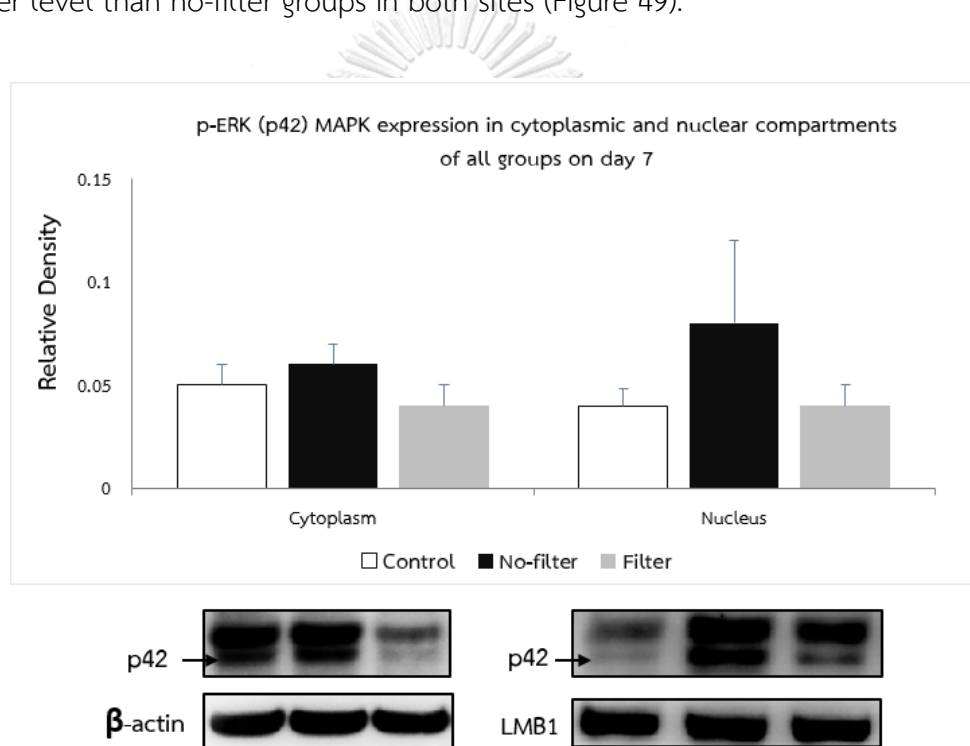


**Figure 48** Cytoplasmic and nuclear p-ERK (p42) protein expression after cigarette smoke exposure with no-filter and filter on 7 days of lung rats.

Relative density of cytoplasm represented as ratio of p-ERK(p42)/ $\beta$ -actin

Relative density of nucleus represented as ratio of p-ERK(p42)/Lamin B1

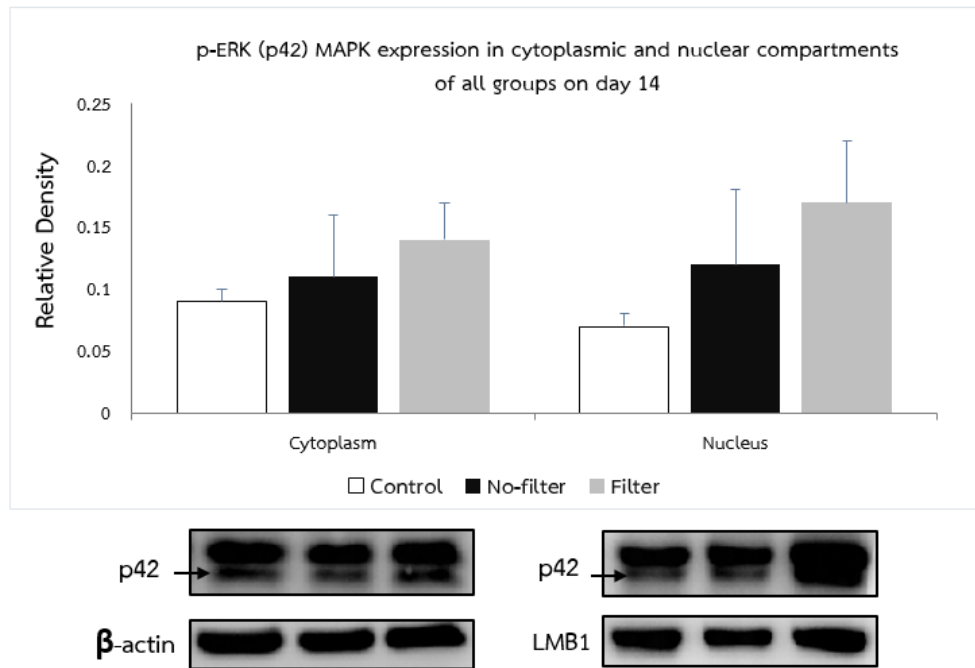


**Figure 49** Cytoplasmic and nuclear p-ERK (p42) protein expression after cigarette smoke exposure with no-filter and filter on 14 days of lung rats.

Relative density of cytoplasm represented as ratio of p-ERK(p42)/ $\beta$ -actin

Relative density of nucleus represented as ratio of p-ERK(p42)/Lamin B1

## 2.4 p-ERK ( p44, less sensitive form) between cytoplasmic and nuclear compartments in lung tissue after cigarette smoke exposure on 7 and 14 days

p-ERK (p44) protein expression after 7 days of cigarette smoked exposure was inactivated in both no-filter and filter groups when compared with controls of cytoplasm and nucleus (Figure 50).

Likewise, p-ERK (p44) protein expression on 14 days, control and no-filter groups were closely levels of p-ERK (p44) protein expression whereas filter group was gradually increased in both cytoplasmic and nuclear compartments (Figure 51).

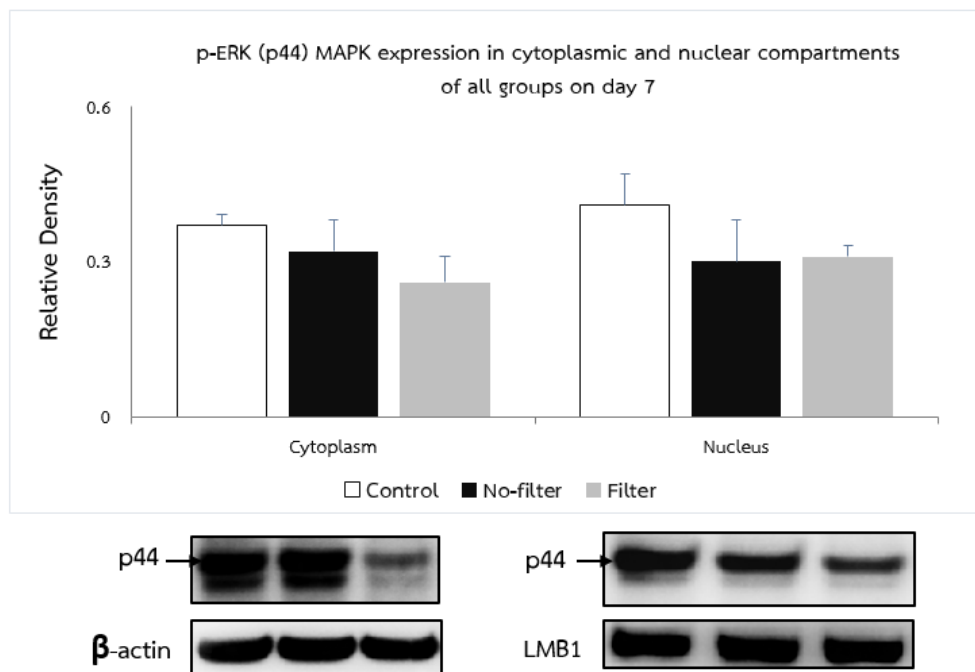


**Figure 50** Cytoplasmic and nuclear p-ERK (p44) protein expression after cigarette smoke exposure with no-filter and filter on 7 days of lung rats.

Relative density of cytoplasm represented as ratio of p-ERK(p44)/ $\beta$ -actin

Relative density of nucleus represented as ratio of p-ERK(p44)/Lamin B1

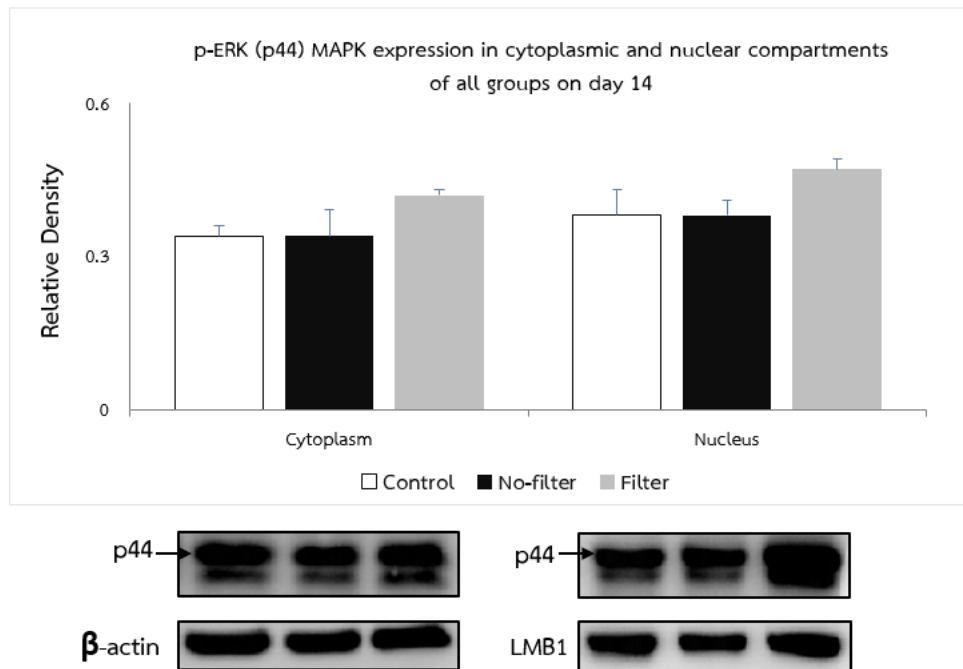


**Figure 51** Cytoplasmic p-ERK (p44) protein expression after cigarette smoke exposure with no-filter and filter on 14 days of lung rats.

Relative density of cytoplasm represented as ratio of p-ERK(p44)/ $\beta$ -actin

Relative density of nucleus represented as ratio of p-ERK(p44)/Lamin B1



## 2.5 p-JNK ( p46, less sensitive form) between cytoplasmic and nuclear compartments in lung tissue after cigarette smoke exposure on 7 and 14 days

After 7 days of cigarette smoked exposure, cytoplasmic and nuclear compartments exhibited slightly increased of p-JNK (p46) protein expression in both filter groups while control and no-filter groups had nearly levels of this expression (Figure 52).

After 14 days of cigarette smoked exposure, cytoplasmic p-JNK (p46) of no-filter group showed higher level than control and filter groups. In contrast, nuclear p-JNK (p46) of both cigarette smoked groups had similar levels when compared with control group (Figure 53).

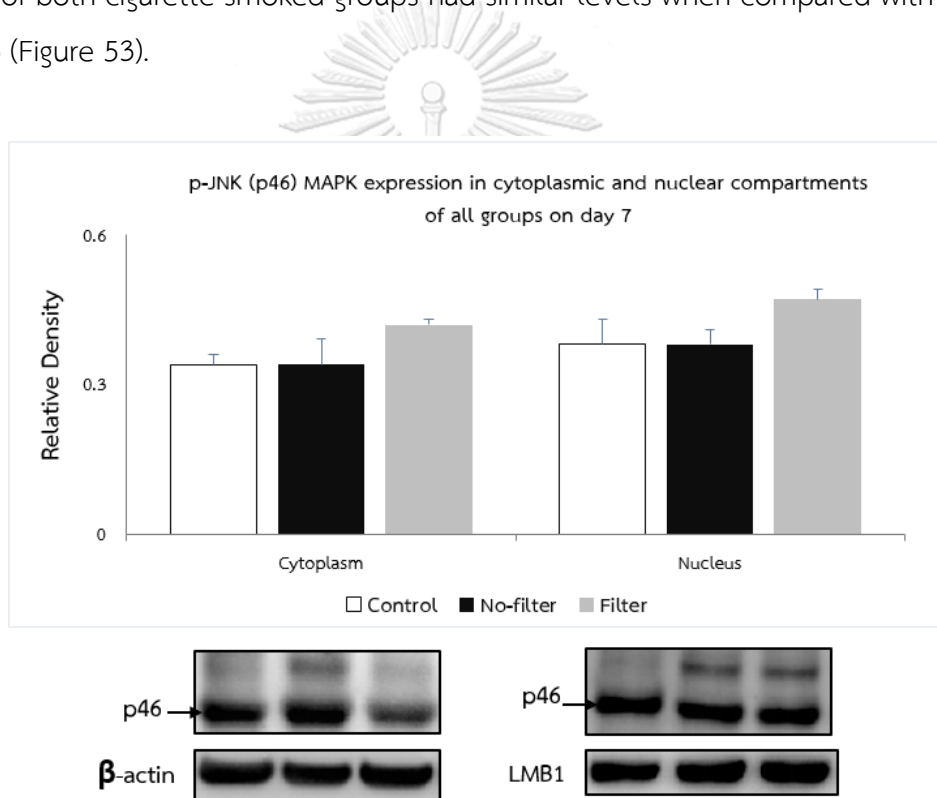


**Figure 52** Cytoplasmic and nuclear p-JNK (p46) protein expression after cigarette smoke exposure with no-filter and filter on 7 days of lung rats.

Relative density of cytoplasm represented as ratio of p-JNK(p46)/ $\beta$ -actin

Relative density of nucleus represented as ratio of p-JNK(p46)/Lamin B1

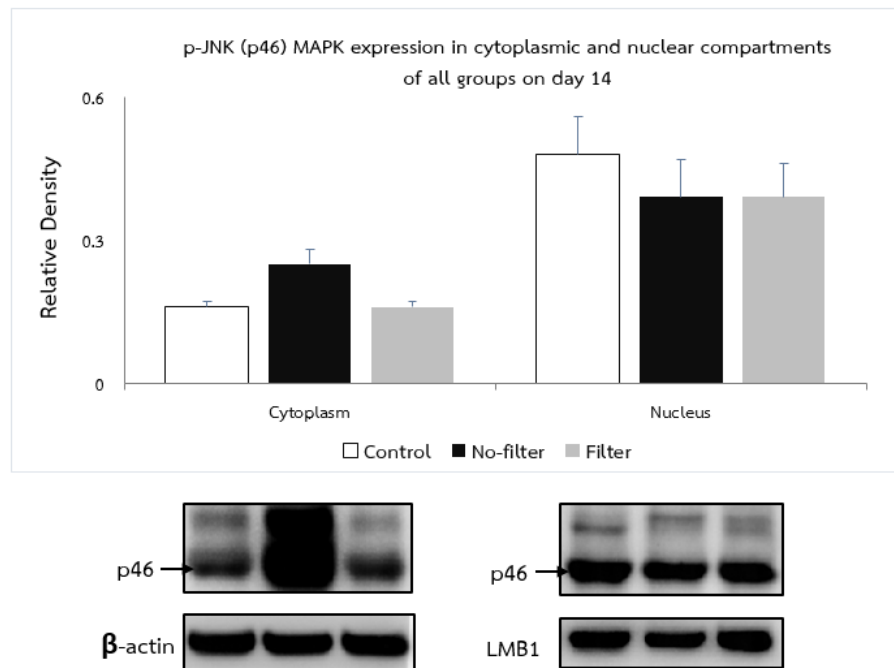


**Figure 53** Cytoplasmic and nuclear p-JNK (p46) protein expression after cigarette smoke exposure with no-filter and filter on 14 days of lung rats.

Relative density of cytoplasm represented as ratio of p-JNK(p46)/ $\beta$ -actin

Relative density of nucleus represented as ratio of p-JNK(p46)/Lamin B1

## 2.6 p-JNK (p54, sensitive form) between cytoplasmic and nuclear compartments in lung tissue after cigarette smoke exposure on 7 and 14 days

p-JNK (p54) protein expression displayed nearly upregulated pattern in cytoplasmic and nuclear compartments after 7 days cigarette smoked exposure. By which no-filter group was highly increased while filter group was gently increased in cytoplasm. For nuclear part, both no-filter and filter groups were slightly increased of p-JNK (p54) protein expression when compared to control (Figure 54).

After 14 days of cigarette smoked exposure, cytoplasmic and nuclear of no-filter and filter groups showed higher levels of p-JNK (p54) protein expression when compared to control which responded similar pattern as 7 days exposure (Figure 55).

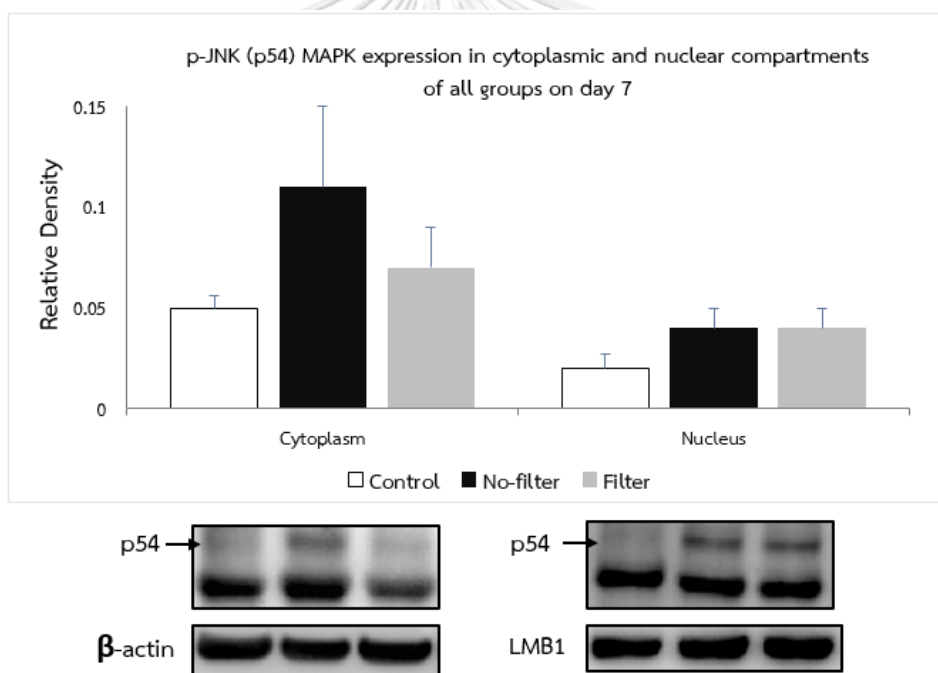


**Figure 54** Cytoplasmic and nuclear p-JNK (p54) protein expression after cigarette smoke exposure with no-filter and filter on 7 days of lung rats.

Relative density of cytoplasm represented as ratio of p-JNK(p54)/ $\beta$ -actin

Relative density of nucleus represented as ratio of p-JNK(p54)/Lamin B1

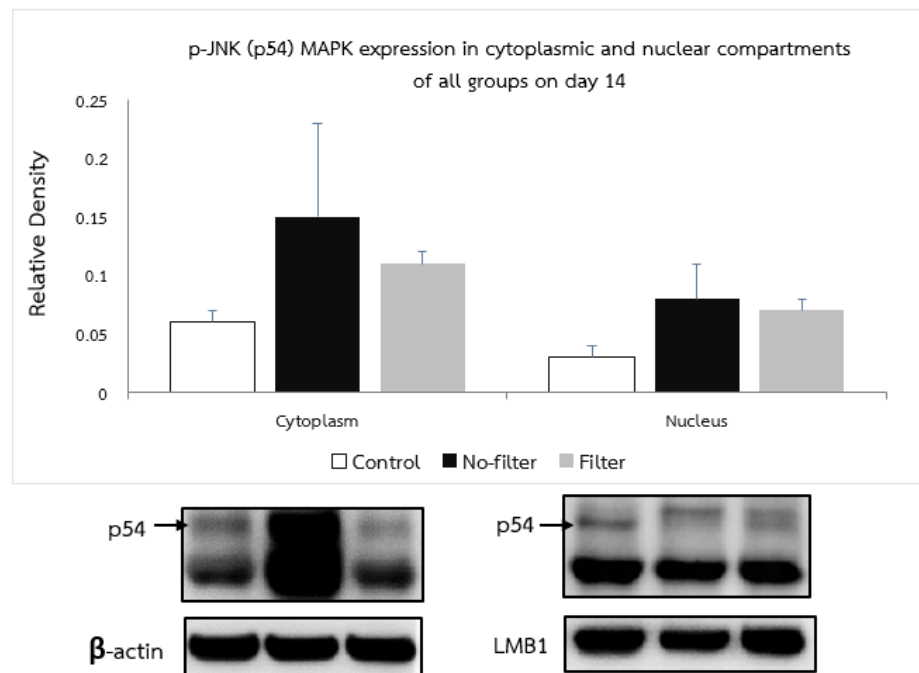


**Figure 55** Cytoplasmic and nuclear p-JNK (p54) protein expression after cigarette smoke exposure with no-filter and filter on 14 days of lung rats.

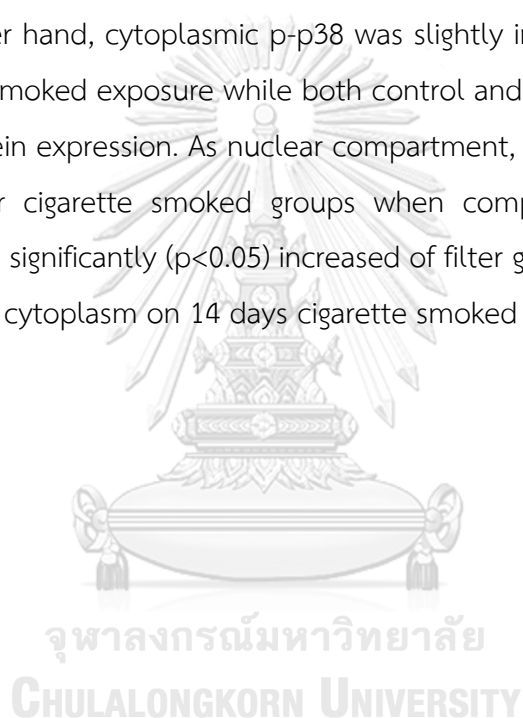
Relative density of cytoplasm represented as ratio of p-JNK(p54)/ $\beta$ -actin

Relative density of nucleus represented as ratio of p-JNK(p54)/Lamin B1

## 2.7 p-p38 between cytoplasmic and nuclear compartments in lung tissue after cigarette smoke exposure on 7 and 14 days

For 7 days cigarette smoked exposure, cytoplasmic p-p38 protein expression was gently escalated in no-filter group whereas control and filter groups had equally levels of this p-p38 protein expression. Furthermore, nuclear part demonstrated significantly ( $p < 0.05$ ) higher of p-p38 in filter group as compared to filter group in cytoplasm but not differed when compared with control and no-filter groups in nucleus (Figure 56).

In the other hand, cytoplasmic p-p38 was slightly inflated in filter group after 14 days cigarette smoked exposure while both control and no-filter groups had lower levels of this protein expression. As nuclear compartment, there had no difference of no-filter and filter cigarette smoked groups when compared with control group whereas there was significantly ( $p < 0.05$ ) increased of filter group when compared with the same group in cytoplasm on 14 days cigarette smoked exposure (Figure 57).



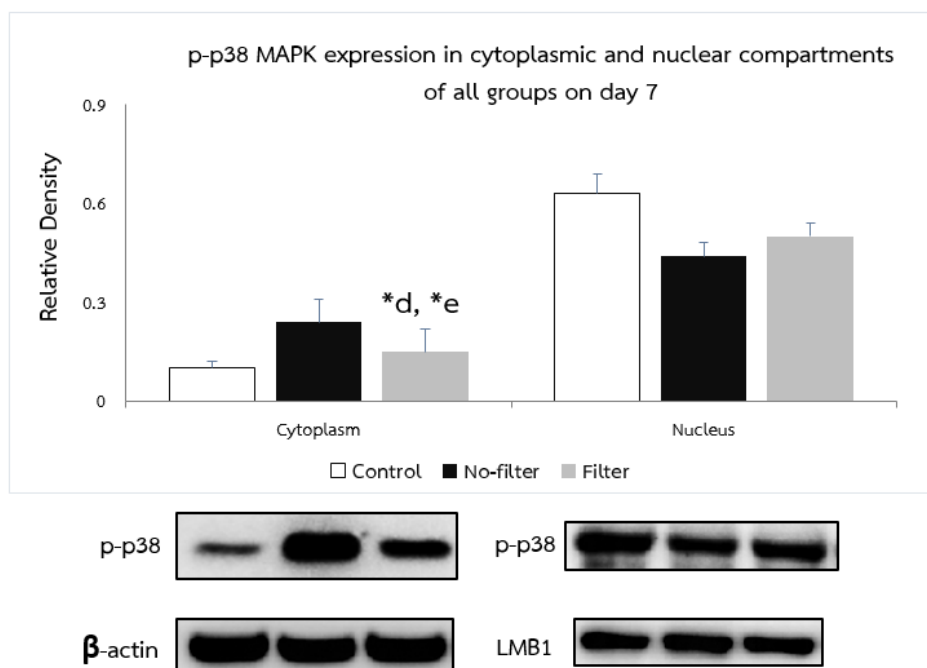


**Figure 56** Cytoplasmic and nuclear p-p38 protein expression after cigarette smoke exposure with no-filter and filter on 7 days of lung rats.

\*d,  $p < 0.05$  compared between filter groups in cytoplasm and nucleus

\*e,  $p < 0.05$  compared between filter and no-filter in cytoplasm and nucleus

Relative density of cytoplasm represented as ratio of p-p38/ $\beta$ -actin

Relative density of nucleus represented as ratio of p-p38/Lamin B1

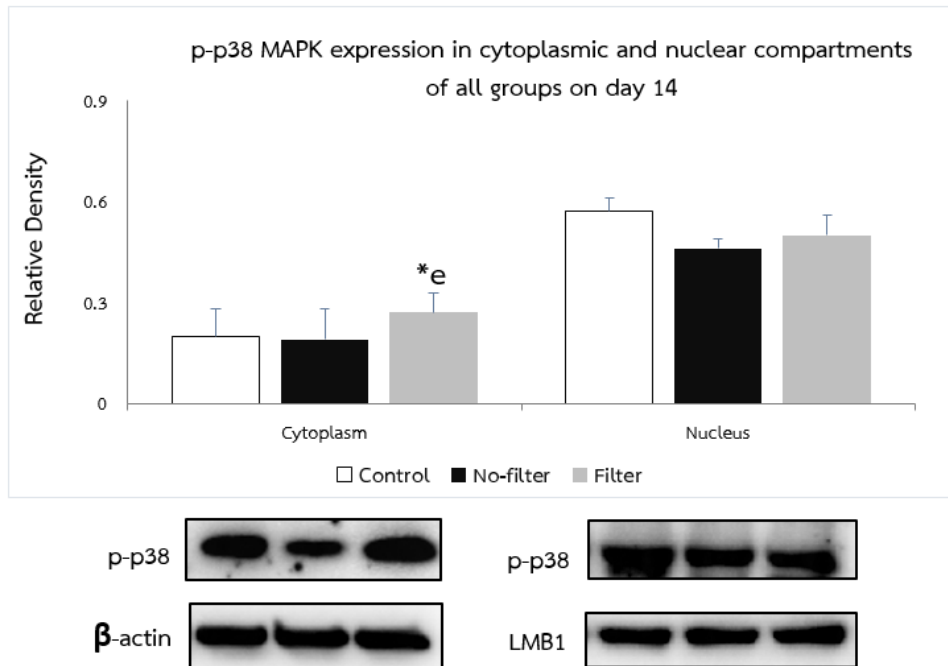


**Figure 57** Cytoplasmic and nuclear p-p38 protein expression after cigarette smoke exposure with no-filter and filter on 7 days of lung rats.

\*e,  $p < 0.05$  compared between filter and no-filter in cytoplasm and nucleus

Relative density of cytoplasm represented as ratio of p-p38/ $\beta$ -actin

Relative density of nucleus represented as ratio of p-p38/Lamin B1

### 3. Immunohistochemistry of lung VDR distribution in early phase after cigarette smoke exposure with no-filter and filter types induced emphysema model

To investigate the localization of VDR in rats' lung, the immunohistochemistry analysis was applied in this study. The results revealed that VDR were also expressed on pneumocytes or alveolar type II (AT II) cells as previously described (55) by which there were highly expressed in both control groups on 7 days and 14 days. After cigarette smoke exposure, VDR had a trend to decrease expression levels on 7 days of no-filter and filter groups but become to increase on 14 days of no-filter group. In contrast, there was significantly ( $p < 0.05$ ) decreased of VDR expression on 14 days of filter group when compared to control group (Figure 58-60).





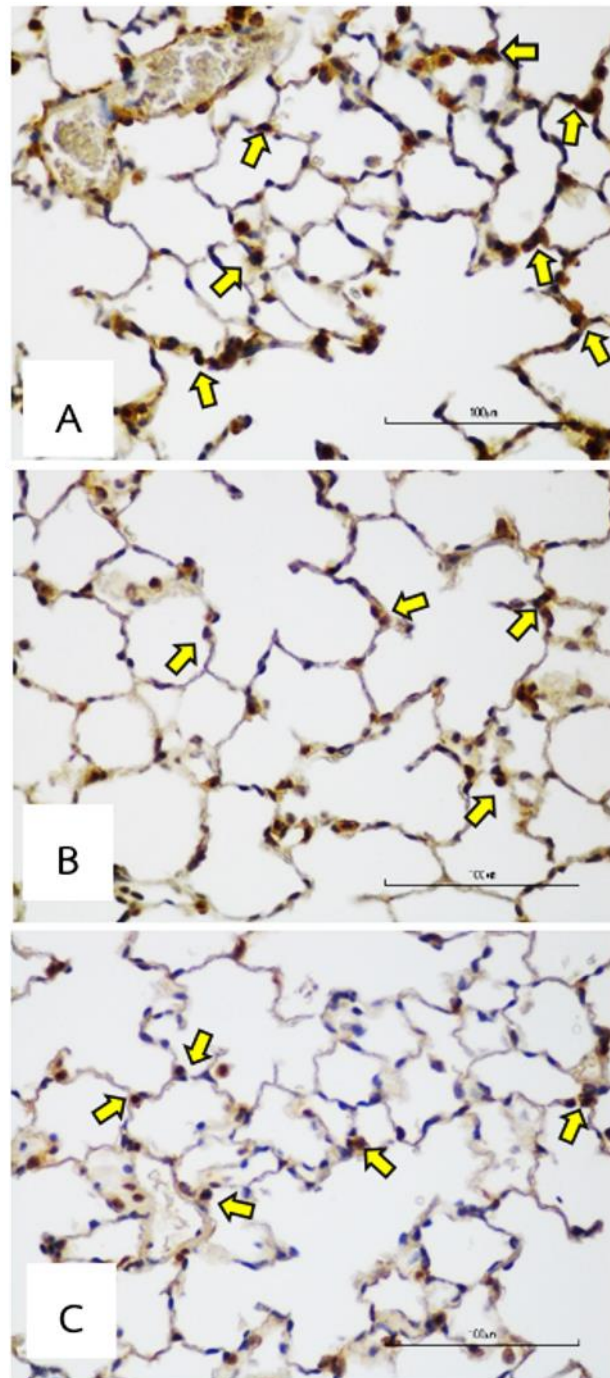


**Figure 58** Immunohistochemistry of VDR expression in alveolar type II cells of control (A), no-filter (B) and filter (C) groups after 7 days of cigarette smoke exposure.

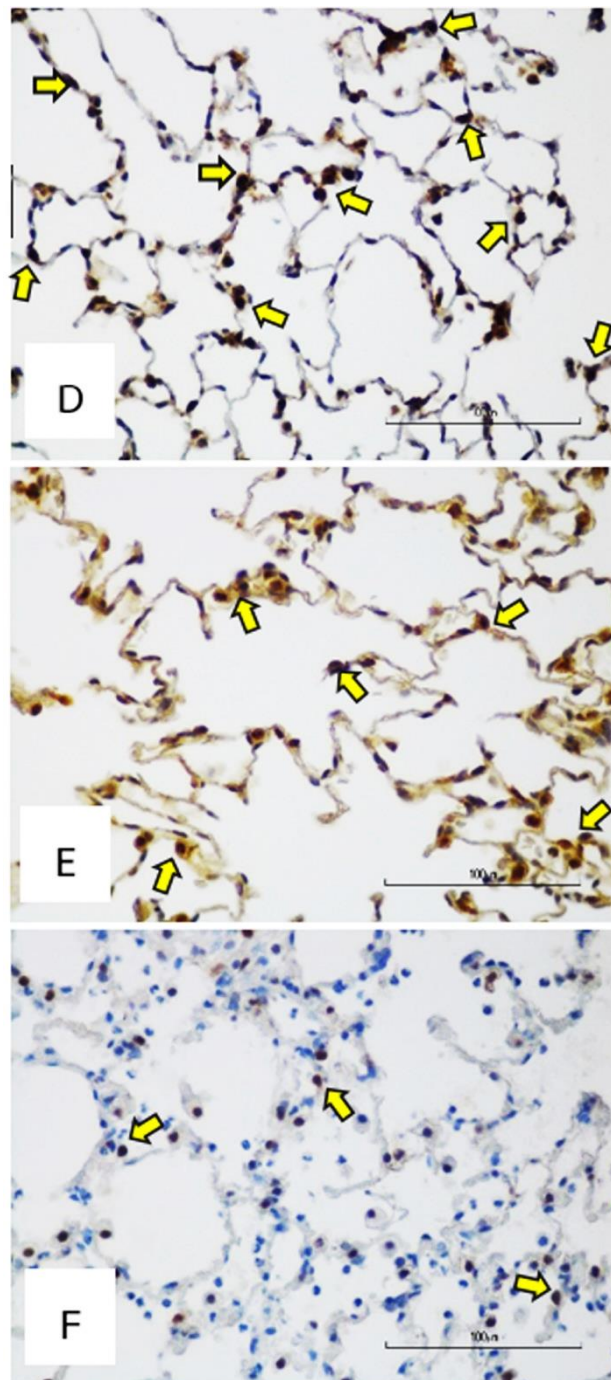


**Figure 59** Immunohistochemistry of VDR expression in alveolar type II cells of control (D), no-filter (E) and filter (F) groups after 14 days of cigarette smoke exposure.

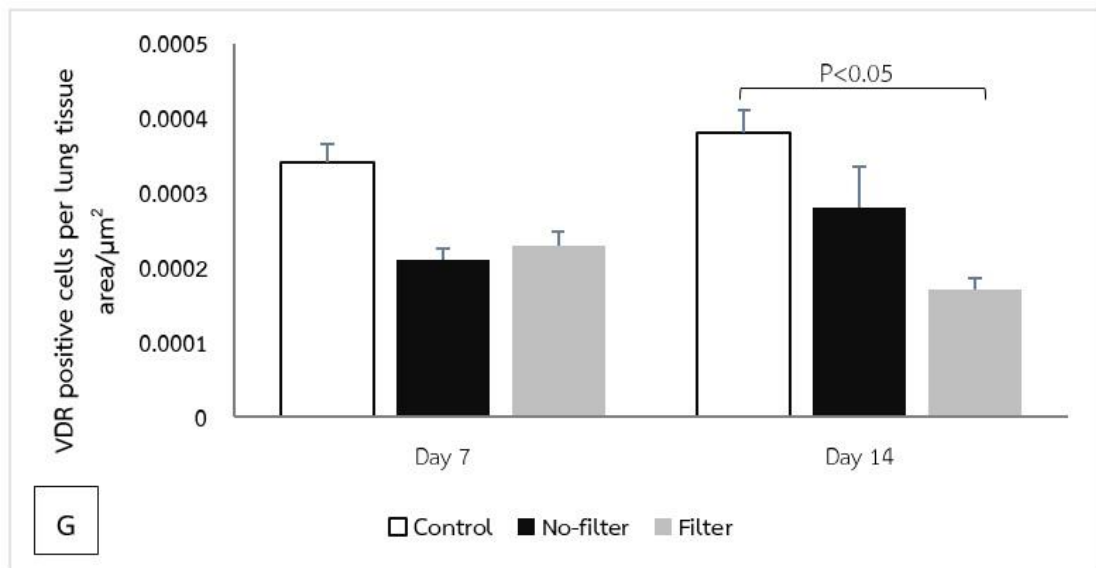


**Figure 60** Quantitative immunohistochemistry of VDR distribution in alveolar type II cells of lung rats after cigarette smoke exposure with no-filter and filter on 7 and 14 days.

p < 0.05, when compared with control group



4.The summary data of histopathological changes, VDR distribution and MAPK protein expression after 7 and 14 days cigarette smoke exposure with no-filter and filter

Parameters	Day 7		Day 14	
	No-filter	Filter	No-filter	Filter
<b><u>1.Histopathology</u></b>				
- Tracheal epithelial cell changes	↑	↑	* ↑	* ↑
- Peribronchiolar epithelial cell proliferation	* ↑	↑	* ↑	↑
- Lung parenchymal infiltration	↑	↑	↑	↑
- Alveolar macrophage count	* ↑	* ↑	* ↑	* ↑
<b><u>2.VDR distribution</u></b>				
- Whole cell	↓	-	-	↓
- Cytoplasm	↓	↓	↓	↓
- Nucleus	↓	-	-	* ↓
- Immunohistochemistry	↓	↓	-	* ↓
<b><u>3.MAPK protein expression</u></b>				
<b>3.1 ERK</b>				
- Whole cell	-	-	↑	↑
- Cytoplasm	↑	-	↑	↑
- Nucleus	↑	-	↑	↑

Parameters	Day 7		Day 14	
	No-filter	Filter	No-filter	Filter
<b>3.2 JNK</b>				
- Whole cell	↑	-	↑	↑
- Cytoplasm	↑	↑	↑	↑
- Nucleus	↑	↑	↑	↑
<b>3.3 p38</b>				
- Whole cell	*↑	↑	-	*↑
- Cytoplasm	↑	↑	-	↑
- Nucleus	-	-	-	-

↑, ↓ indicated the trend of increase or decrease respectively.

\*↑, \*↓ indicated significantly increase or significantly decrease respectively.

## Chapter V DISCUSSION AND CONCLUSION

### **1. Effects of acute and subacute cigarette smoke exposure with no-filter and filter on lung histopathological alterations in rat model**

To explicate the effects of cigarette smoke exposure to the distribution of MAPKs cascades and VDR in the subcellular levels related with the appearances of lung pathogenesis. We demonstrated by designing our experiment into cigarette smoke with no-filter and filter groups for imitating the best human smoking behaviors. After cigarette smoke on acute (7days) and subacute (14days) periods, these two types of cigarette smoke are induced changes of all lung parameters as shown in the table 2.1 and 2.2. According to the previous studies, there were showed similar results that F344 rats displayed bronchial epithelial hyperplasia and slightly increased of inflammatory cells (generally alveolar macrophages and lymphocytes) in short-term cigarette smoke exposure for 5 consecutive days (56). Likewise, for subacute period, there have been found that cigarette smoke extract enhanced epithelial proliferation and bronchiolar epithelial hyperplasia including lung inflammation in vivo (57). Hence, this model can induce moderate configuration of lung histopathology owing to many factors such as duration of exposure, different of cigarette brand, cigarette constituents, and frequency of exposure (47, 58). Consequently, all parameters were reflected as histopathological investigation of lung tissue injuries which corresponded to the early stage of emphysema/COPD.

### **2. The alterations of VDR distribution after 7 and 14 days of cigarette smoke exposure with no-filter and filter in lung rat.**

Vitamin D receptor (VDR) have been distributed between cytoplasm and nucleus through interacting with or without active vitamin D via genomic and non-genomic actions to regulate vitamin d target genes (59). The balance of distribution of cytoplasmic and nuclear VDR are relevant with distinct biological activities such as transcriptional regulation, immune regulatory process, anti-microbial activity and including anti-cancer effects (33). The previous studies reported that cytoplasmic and nuclear VDR act as the indicator of survival outcomes in many types of cancer, the

lack of expression of both VDR locations were correlated with low rate living depended on age, gender, stage and also smoking status (60-63). While the role of subcellular cytoplasmic and nuclear VDR distribution after early cigarette smoke exposure in vivo still has a few information. In the results of current study revealed that cytoplasmic VDR was tended to decreased on 7 and 14 days in both cigarette smoked groups. Moreover, not only nuclear VDR distribution was decreased on 7 days of no-filter group and filter group was significantly ( $p < 0.05$ ) decreased on 14 days, but also nuclear VDR still had higher distribution in nucleus than cytoplasm of all groups at respective time points. However, this is the first time to evaluate subcellular VDR distribution in cigarette smoke exposed with filter group which correlated to the study of Uh et al. They reported that cigarette smoke extracts can interrupt active vitamin d (ligand VDR) to induce VDR translocation from nucleus to cytoplasm which consequent to the reduction of cytoplasmic VDR and accumulation of nuclear VDR in A549 cell (5). Likewise, Ishii et al., reported that cigarette smoke can attenuate VDR mRNA levels in anti-inflammatory action in A549 cells from COPD patients (64). Nevertheless, there was another relating factor in this incidence that is cigarette filter ventilation. In the recent review article suggested that cigarette design change was implicated to reduce cigarette filter ventilation that induced lung adenocarcinoma. The reduction of cigarette filter ventilation causes cigarette slowly burn lead to generate higher puff volumes per cigarette and incomplete combustion resulting in increasing peripheral lung exposure. Thus, cigarette filter ventilation is the supporting character to promotes more toxic substances which expose to the alveolar cells and could be affect to prevent binding of ligand VDR to its receptor in both nucleus and cytoplasm (4, 65, 66).

### **3. Immunohistochemistry of VDR distribution in lung sections after cigarette smoke exposure with two different types on 7 and 14 days.**

Generally, immunohistochemistry analysis of VDR was observed in the alveolar type II (AT II) cells since the gestation stage of fetal lung rats (55). Likewise, in the present study evaluated VDR localization in the lung tissue, our results suggested that VDR distribution had diminished trend after 7 days of both cigarette smoke groups.

However, the discrepancy of VDR distribution in no-filter group between 7 and 14 days was probably due to high ventilation which allowed protein recovery from unextreme noxious stress. Furthermore, VDR distribution in filter group was significantly decreased on 14 days after smoke exposed because there were accumulated more toxicants from incomplete combustion due to low filter ventilation which may disrupted proteins viability (64, 65). Finally, these outcomes indicated that lack of VDR is one of predictable biological marker in the early stage after cigarette smoke exposure which might be related to chronic lung diseases such as emphysema/COPD for long term cigarette smoke exposure.

#### **4. The activation of ERK1/2 MAPK protein expression after early phase cigarette smoke exposure with no-filter and filter in lung rat.**

The activation of ERK1/2 comes up with the general association of cellular proliferation and cell survival which have a variety of external stimuli such growth factors, transforming agents, G protein-coupled receptors and carcinogens base on type of the cells. For the resting state, it's clear that ERK cascades is mainly in cytoplasm, then translocate to the nucleus from activation (67, 68). When ERK 1/2 translocation to nucleus, the transcription factors (TFs) Elk-1, Sap-1a, CYP24 and VDR are phosphorylated to regulate and relate with cell cycle regulatory proteins (33, 69, 70). Moreover, not only cytoplasmic ERK1/2 induce proliferative effects in the nucleus, but also it has stimulating activities in some pro-apoptotic protein in parts of the cytoplasm (71). According to our data, no-filter group showed p-ERK (p42) protein expression was tended to increase in the cytoplasm and nucleus on 7 days whereas both cigarette smoked groups were highly upregulated on 14 days in both locations. From the previous study, acute cigarette smoke had rapid activation of ERK1/2 along with released of TNF- $\alpha$  via macrophages induction and related with proliferative effects in lung cells (72, 73). On the other one, ERK kinase pathway was reactivated by the reduction of the second peak ERK1/2 phosphorylation after prolonged cigarette smoke extract that effected to promote early growth response gene (EGR-1) in lung pathology in vitro (74). Our results showed relatively with earlier in vivo study, the signaling cascade of ERK was stimulated after cigarette smoke induced lung tissue injuries due



to the toxic substances in the smoke passed directly to bronchiolar epithelial cells that led to epithelial hyperplasia (57, 75). Likewise, immunoblotting from lung mice showed the activation of ERK activity after 3 days of cigarette smoked exposure and also correlated with inflammation and cell death mechanism linked to emphysema (14). Clearly, those were involved with cytoplasmic and nuclear ERK1/2 distribution that indicated the activity of ERK1/2 response after smoke exposure. This protein expression was highly activated reside in the nucleus resulting to persuade gene regulation and cytosolic ERK1/2 retention was also incumbent for mitogenic reaction.

#### **5. The activation of JNK MAPK protein expression after early phase cigarette smoke exposure with no-filter and filter in lung rat.**

JNK and p38 cascades are accompanied by oxidative stress and environmental stress which mediated from many cigarette smoke agents. These signals transduction are regulated a variety of cellular process such as apoptosis, inhibit cell growth, cytokines secretion and inflammation (76, 77). After activation of stress kinases, they translocated from cytoplasm to nucleus to regulate downstream target genes, besides it still has dual actions to inactivation and/or downregulation (78, 79). A previous publication suggested that cytoplasmic JNK plays a role in anti-proliferative effect from cytoplasmic protein binding to JNK that lead to cytoplasmic JNK accumulation including inhibition of JNK interacting gene regulated apoptosis activation in the cytoplasm via Fas (80, 81). The present study provides data about JNK protein expression, we found that both exposure types are activated cytoplasmic and nuclear JNK at dual time points. For 7 days after smoked exposure, there were highly increased of cytoplasmic JNK whereas nuclear JNK were gradually escalated in both cigarette smoked groups. While cytoplasmic and nuclear JNK after 14 days smoked exposure, had similar trended of increasing in both cigarette smoked groups as 7 days. Based on previous study, JNK was activated with upregulation of PKC in non-small lung cancer cell with IL-8 stimulation to induce lung inflammation (82, 83). Moreover, animals model also showed the activation of JNK signal after the acute cigarette smoke exposure as in vitro (14). In the other hand, the recent study discovered the involvement of JNK reduction after 1day cigarette smoke exposure by inhibitory effect

of protein phosphatase 2A (PP2A) in acute lung inflammatory mice. This is the one of reasons that the organism had the defense mechanism to release this enzyme against prolong inflammatory state through inactivated JNK signaling (84, 85). From above evidences may apply to our study because our results showed the high level of cytoplasmic JNK of both cigarette smoke types due to no-filter group exposed with directly smoke that emerge JNK expression for an acute period and including filter group had also acute JNK upregulation even there still had filtrated function. These mean JNK cascade has a prominent role in cytoplasm for the inflammatory responses after smoked exposure and might be the cell mechanism to protect tissues or organ damaged.

#### **6. The activation of p38 MAPK protein expression after early phase cigarette smoke exposure with no-filter and filter in lung rat.**

Diversity of p38 responses is provoked by environmental stress stimulation mediated immunological effects, cellular apoptosis, inflammatory cytokines stimulation, altering cell cycle and including cell survival (86-88). The activation of p38 is dependent on phosphorylation of threonine and tyrosine residues which mediated by both specific kinases MKK3 and MKK6 (89, 90). In the resting stage of cells, p38 is located in the cytoplasm and translocated to the nucleus to phosphorylate many related transcription factors for the activation step. Although, there is still uncertainly known about the role of p38 subcellular localization after early cigarette smoke exposure in different no-filter and filter types. From current study on 7 days smoked exposure, our results showed that cytoplasmic p38 was gently upregulated in no-filter and filter groups when compared with control while nuclear p38 had significantly increased in filter group when compared with the same group in cytoplasm. However, nuclear p38 had higher levels than cytoplasmic part and not differed between groups. Notably, for 14 days after smoked exposure, filter group had become to increase the trended of cytoplasmic p38 when compared to control and no-filter groups whereas nuclear p38 had similar pattern as 7 days duration. Like other previous study, there was an occurrence of lung inflammation in acute cigarette smoke induced lung injury through neutrophil infiltration, proteinase expression, apoptosis, oxidative DNA damage

which mediated via p38 MAPK both in vitro and in vivo models (14, 20). Noticeably, there was some study reported that whole body exposed to radiation can increase phosphorylation of cytoplasmic p38 during apoptosis process resulting to support malignant in lymphoma cell line (91, 92). Concomitant with this possibly p38 activated pattern, MAPKAP kinase-2 is nuclear localized signal (NLS) that cooperated with conformational change of p38 to be activated in the nucleus and then relocation into the cytoplasm to phosphorylate their substrates (93). Together these several supporting evidences indicated that, cytoplasmic p38 is the pivotal role in various cell types that integrate extensively cellular responses which might dependent on co-workers for triggering this cascade under stress condition.

In this study found that cigarette smoke with no-filter and filter types can initially originate alveolar macrophage in the alveolar spaces on 7 days (acute) and 14 days (subacute) because the cigarette smoke toxicants are inhaled into the lower respiratory tract which is alveoli. Then the smoke locates in alveoli, where is the area of gas exchanges with slowly flow rate and take more times to expose in this area. Hence, these toxicants are deposited into the alveoli which induce macrophages penetration to those areas (94). In contrast, the characteristic of cigarette smoke that flows through trachea and bronchioles is rapid flow manner and makes these tissues contact with the particles less than alveoli. Thus, alveolar macrophage parameter is vividly expresses among another parameter. Peribronchioles and trachea are the secondary histological changes that apparently elicit on acute period for no-filter group while filter group exhibits on subacute period after cigarette smoked exposure. For lung parenchymal infiltration has prone to induces of neutrophils and leukocytes infiltrate in both cigarette smoke groups due to it is the last barrier before lung parenchymal destruction that requires chronic smoke exposure in generating emphysema pathogenesis. Moreover, various toxic constituents in cigarette smoke influent to VDR distribution by reducing the level of VDR distribution in cytoplasm of both no-filter and filter groups whereas nuclear VDR distribution was only reduced in no-filter group but higher level than cytoplasmic VDR after acute cigarette smoked exposure. Similar to subacute period, cytoplasmic VDR was declined in both cigarette smoked groups while nuclear VDR was became reduce in filter group but the level of

nuclear VDR was still higher than cytoplasmic VDR as well. These circumstances corresponded with previously in vitro study, they demonstrated that cigarette smoke extract effected to decrease cytoplasmic VDR by prohibiting active vitamin D to promotes the translocation of VDR from nucleus to cytoplasm that resulting in accumulation of nuclear VDR (5). Furthermore, there have been found that mRNA level of VDR was lowered for a role in anti-inflammation in lung cells of COPD patients (64). It can be elucidated that both cigarette smoke with no-filter and filter are also affect to cytoplasmic and nuclear VDR distribution in rat lung at different time points.

Of course, this is the first study that investigate the relationship between cigarette smoke with no-filter and filter, subcellular VDR distribution and including three targeted MAPK protein expression. Up to now, there have many earlier publications about the increase of ERK, JNK and p38 that correlated with cigarette smoke but there have no more information about the protein expression of these MAPK inside the cell membrane and nucleus. From our observation, p-ERK and p-JNK of MAPK are classified into two isoforms; p-ERK p42 or ERK1 (sensitive form), p-ERK p44 or ERK2 (less sensitive form), p-JNK p46 or JNK1 (less sensitive form) and p-JNK p54 or JNK2 (sensitive form) respectively unless p-p38.

Generally, the most mammalian tissues have higher level of ERK2 expression than ERK1 (95) but in our condition choses ERK1 as the sensitive isoform because of their higher protein variation like JNK2 isoform in the cigarette smoke groups. After the reduction of cytoplasmic and nuclear VDR distribution on acute period, cellular response of p-ERK p42 was activated in only no-filter cigarette smoked group inside cytoplasm and nucleus whereas p-ERK p44 was no changed the levels of expression in both sites as well. These responses shed light on this p-ERK p44 isoform that mainly related with the proliferative effects as represented in both previous publications and histopathological of tracheal and peribronchiolar epithelium changes from no-filter group. In the line with p-JNK, there was highly activated of p54 isoform in both cigarette smoked groups inner cytoplasmic and nuclear compartments. In contrast, p46 isoform was slightly increased only in filter group when compared to another group of both locations. It can be noted that p-JNK p54 might be the outstanding isoform involved with cell stress responses and inflammatory process from our results. In similar fashion,

cytoplasmic p-p38 was sharply escalated in no-filter group while it was gently increased in filter group which inverse to nuclear p-p38. This confirmed that p-p38 vividly associated with the inflammation in no-filter group after acute cigarette smoke exposure.

In addition, subacute cigarette smoke exposure had additionally influent to reduce cytoplasmic and nuclear VDR distribution particularly in filter group. After that, the cellular responses of p-ERK p42 was also stimulated of both cigarette smoked groups in both subcellular sites, in which filter group were higher level than no-filter group. Because we want to emphasize that the role of proliferation was explicitly react with cellular injury on 14 days after cigarette smoked exposure. Similarly, p-JNK p54 had growing up in no-filter group than filter group as compared with control on both cytoplasm and nucleus. Although, p-JNK p54 was the long isoform that took part in processes of apoptosis incursion but these two isoforms are still partially deal with redundant to most substrates (96, 97). Interestingly, cytoplasmic p-p38 of filter group turned to increase instead of no-filter group whereas the activity of nuclear p-p38 was not differed between groups. Thus, these reports gave data to knowing that p-p38 operated and controlled the activity predominantly in cytoplasm after 14 days cigarette smoked expose with filter type by which it was supposed to be involved with some partner protein such as MAPKAP kinase-2 (93). Moreover, another factor that assume to be involve with sequential reduction of subcellular VDR and MAPK alteration in filter group were low filter ventilation from incomplete combustion (65). Eventually, although cigarette filter can reduce toxicants in the acute phase but our finding indicated that the loss of effectiveness of cigarette filter occurred during subacute phase as a result of increased histological changes, impaired VDR distribution and MAPK upregulation sequentially.

## 7. Conclusion

In summary, this study encourages more supplementary document of emerging literature and provides novel subcellular outcomes after cigarette smoke exposure with filter and no-filter during acute (7days) and subacute (14days) phase in the model of emphysema rat. Based on our results, we present the pathological manifestations after exposed with two types of cigarette smoke exposure which generate nearly severity of lung histopathology. Acute and subacute histopathological outcomes also implicate to the lack of cytoplasmic and nuclear lung VDR especially in cigarette smoke with filter group when expose to smoke for a longer period. Other than, the increment of cytoplasmic and nuclear MAPK activity apparently occurs after subcellular VDR alteration. These consequences indicate the relevant factors as mention above that take part in lung pathogenesis and disclose to the interaction of lung cellular homeostasis to maintain cells and/or tissues viability. Latterly, our research model can infer to the second-hand smoke model which could be beneficial study to point out that cigarette filter has less effects to reduce the severity of lung pathology. These finding are the supportive basis to quit the smoking for the best resolution to prevent chronic respiratory diseases.

## REFERENCES



จุฬาลงกรณ์มหาวิทยาลัย  
**CHULALONGKORN UNIVERSITY**

1. Murray CJ, Lopez AD. Alternative projections of mortality and disability by cause 1990–2020: global burden of disease study. *The Lancet*. 1997;349:1498-504.
2. Bond C. The pros and cons of E-cigarettes: a challenge for public health. *International Journal of Pharmacy Practice*. 2016;24(3):147-8.
3. Yadav UC, Ramana KV, Srivastava SK. Aldose reductase regulates acrolein-induced cytotoxicity in human small airway epithelial cells. *Free Radical Biology and Medicine*. 2013;65:1-22.
4. Hansdottir S, Monick MM, Lovan N, Powers LS, Hunninghake GW. Smoking disrupts vitamin D metabolism in the lungs. *American Journal of Respiratory and Critical Care Medicine*. 2010;181:A1425.
5. Uh ST, Koo SM, Kim YK, Kim KU, Park SW, Jang AS, et al. Inhibition of vitamin D receptor translocation by cigarette smoking extracts. *Tuberculosis and Respiratory Diseases (Seoul)*. 2012;73(5):258-65.
6. Hughes DA, Norton R. Vitamin D and respiratory health. *Clinical and Experimental Immunology*. 2009;158(1):20-5.
7. Yang L, Ma J, Zhang X, Fan Y, Wang L. Protective role of the vitamin D receptor. *Cellular Immunology*. 2012;279(2):160-6.
8. Carlberg C, Seuter S, Heikkinen S. The first genome-wide view of vitamin D receptor locations and their mechanistic implications. *Anticancer Research*. 2012;32:271-82.
9. Isaac KS, Jae-Woong H, Shaoping W, Jun S, Rahman I. Deletion of vitamin D receptor leads to premature emphysema/COPD by increased matrix metalloproteinases and lymphoid aggregates formation. *Biochemical and Biophysical Research Communications*. 2011;406:127-33.
10. Birru RL, Di YP. Pathogenic mechanism of second hand smoke induced inflammation and COPD. *Frontiers in Physiology*. 2012;3:1-8.
11. Goldklang MP, Marks SM, D'Armiento JM. Second hand smoke and COPD: lessons from animal studies. *Frontiers in Physiology*. 2013;4:1-8.
12. Kim EK, Choi EJ. Pathological roles of MAPK signaling pathways in human diseases. *Biochimica et Biophysica Acta (BBA)-Molecular Basis of Disease*. 2010;1802(4):396-405.



13. Gu W, Song L, Li XM, W D, Guo XJ, Xu WG. Mesenchymal stem cells alleviate airway inflammation and emphysema in COPD through down-regulation of cyclooxygenase-2 via p38 and ERK MAPK pathways. *Scientific Reports*. 2015;5:1-11.
14. Marumo S, Hoshino Y, Kiyokawa H, Tanabe N, Sato A, Ogawa E, et al. p38 mitogen-activated protein kinase determines the susceptibility to cigarette smoke-induced emphysema in mice. *BMC Pulmonary Medicine*. 2014;14(1):1-14.
15. Holick MF, Chen TC. Vitamin D deficiency: a worldwide problem with health consequences. *The American Journal of Clinical Nutrition*. 2008;87(4):1080-6.
16. Centers for Disease Control and Prevention (US), National Center for Chronic Disease Prevention and Health Promotion (US). How tobacco smoke causes disease: the biology and behavioral basis for smoking-attributable disease: a report of the surgeon general. 3. Atlanta (GA): Centers for Disease Control and Prevention (US): Chemistry and Toxicology of Cigarette Smoke and Biomarkers of Exposure and Harm; 2010. p. 487-94.
17. Yoshida T, Tuder RM. Pathobiology of cigarette smoke-induced chronic obstructive pulmonary disease. *Physiological Reviews*. 2007;87(3):1047-82.
18. Lee J, Taneja V, Vassallo R. Cigarette smoking and inflammation: cellular and molecular mechanisms. *Journal of Dental Research*. 2012;91(2):142-9.
19. Kern JC, Kehrer JP. Acrolein-induced cell death: a caspase-influenced decision between apoptosis and oncosis/necrosis. *Chemico-Biological Interactions*. 2002;139(1):79-95.
20. Moretto N, Bertolini S, Iadicicco C, Marchini G, Kaur M, Volpi G, et al. Cigarette smoke and its component acrolein augment IL-8/CXCL8 mRNA stability via p38 MAPK/MK2 signaling in human pulmonary cells. *American Journal of Physiology-Lung Cellular and Molecular Physiology*. 2012;303(10):929-38.
21. Shin HJ, Sohn HO, Han JH, Park CH, Lee HS, Lee DW, et al. Effect of cigarette filters on the chemical composition and in vitro biological activity of cigarette mainstream smoke. *Food and Chemical Toxicology*. 2009;47(1):192-7.

22. Cavallo D, Ursini CL, Fresegna AM, Maiello R, Ciervo A, Ferrante R, et al. Cytogenotoxic effects of smoke from commercial filter and non-filter cigarettes on human bronchial and pulmonary cells. *Mutation Research/Genetic Toxicology and Environmental Mutagenesis*. 2013;750(1-2):1-11.
23. Adams JD, O'Mara-Adams KJ, Hoffmann D. Toxic and carcinogenic agents in undiluted mainstream smoke and sidestream smoke of different types of cigarettes. *Carcinogenesis*. 1987;8(5):729-31.
24. Clifford RJ, John AS, Daniel BD, Dennis BM, Marie DB, JoAnn ME, et al. The nonskeletal effects of vitamin D: an endocrine society scientific statement. *Endocrine Reviews*. 2012;33(3):456-92.
25. Moore DD, Kato S, Xie W, Mangelsdorf DJ, Schmidt DR, Xiao R, et al. International Union of Pharmacology. LXII. The NR1H and NR1I receptors: constitutive androstane receptor, pregnene X receptor, farnesoid X receptor alpha, farnesoid X receptor beta, liver X receptor alpha, liver X receptor beta, and vitamin D receptor. *Pharmacological Reviews*. 2006;58(4):742-59.
26. Makowski A, Brzostek S, Cohen RN, Hollenberg AN. Determination of nuclear receptor corepressor interactions with the thyroid hormone receptor. *Molecular Endocrinology*. 2003;17(2):273-86.
27. Li YC, Pirro AE, Amling M, Delling G, Baron R, Bronson R, et al. Targeted ablation of the vitamin D receptor: an animal model of vitamin D-dependent rickets type II with alopecia. *Proceedings of the National Academy of Sciences of the United States of America*. 1997;94(18):9831-5.
28. Barsony J, Marx SJ. Immunocytology on microwave-fixed cells reveals rapid and agonist-specific changes in subcellular accumulation patterns for cAMP or cGMP. *Proceedings of the National Academy of Sciences of the United States of America*. 1990;87(3):1188-92.
29. Freedman LP. Increasing the complexity of coactivation in nuclear receptor signaling. *Cell*. 1999;97(1):5-8.
30. York B, O'Malley BW. Steroid receptor coactivator (SRC) family: masters of systems biology. *Journal of Biological Chemistry*. 2010;285(50):38743-50.

31. Christophe R, Leonard FP. Mechanisms of gene regulation by vitamin D3 receptor: a network of coactivator interactions. *Gene*. 2000;246:9-21.
32. Janos Z, John SW, Jesse GF, Patrick SJ. Handbook of vitamins, fifth edition. CRC Press; 2013. p. 60-2.
33. Hii CS, Ferrante A. The non-genomic actions of vitamin D. *Nutrients*. 2016;8(3):1-14.
34. Buitrago C, Pardo VG, Boland R. Role of VDR in 1 $\alpha$ ,25-dihydroxyvitamin D3-dependent non-genomic activation of MAPKs, Src and Akt in skeletal muscle cells. *The Journal of Steroid Biochemistry and Molecular Biology*. 2013;136:125-30.
35. Holick MF. Vitamin D deficiency. *The New England Journal of Medicine*. 2007;357:266-81.
36. DeLuca HF. Overview of general physiologic features and functions of vitamin D. *The American Journal of Clinical Nutrition*. 2004;80:1689S-96S.
37. García de Tena J, El Hachem Debek A, Hernández Gutiérrez C, Izquierdo Alonso JL. The role of vitamin D in chronic obstructive pulmonary disease, asthma and other respiratory diseases. *Archivos de Bronconeumología (English Edition)*. 2014;50(5):179-84.
38. Christakos S, Dhawan P, Liu Y, Peng X, Porta A. New insights into the mechanisms of vitamin D action. *Journal of Cellular Biochemistry*. 2003;88(4):695-705.
39. Heaney RP, Dowell SM, Hale CA, Bendich A. Calcium absorption varies within the reference range for serum 25-hydroxyvitamin D. *Journal of the American College of Nutrition*. 2003;22(2):142-6.
40. Wim J, An L, Claudia C, Roger B, Chantal M, Marc D. Vitamin D beyond bones in chronic obstructive pulmonary disease. *American Journal of Respiratory and Critical Care Medicine*. 2009;179:630-6.
41. Carlberg C, Seuter S. A genomic perspective on vitamin D signaling. *Anticancer Research*. 2009;29(9):3485-93.
42. Mercer BA, D'Armiento JM. Emerging role of MAP kinase pathways as therapeutic targets in COPD. *International Journal of COPD*. 2006;1(2):137-50.

43. Ronda AC, Buitrago C, Colicheo A, Boland AR, Roldàn E, Boland R. Activation of MAPKs by 1 $\alpha$ ,25(OH)<sub>2</sub>-vitamin D<sub>3</sub> and 17 $\beta$ -estradiol in skeletal muscle cells leads to phosphorylation of Elk-1 and CREB transcription factors. *Journal of Steroid Biochemistry and Molecular Biology*. 2007;103:462–6.
44. Lee JC, Kumar S, Griswold DE, Underwood DC, Votta BJ, Adams JL. Inhibition of p38 MAP kinase as a therapeutic strategy. *Immunopharmacology*. 2000;47(2–3):185-201.
45. Mercer BA, Kolesnikova N, Sonett J, D'Armiento J. Extracellular regulated kinase/mitogen activated protein kinase is up-regulated in pulmonary emphysema and mediates matrix metalloproteinase-1 induction by cigarette smoke. *The Journal of Biological Chemistry*. 2004;279:17690–6.
46. Mochida-Nishimura K, Surewicz K, Cross JV, Hejal R, Templeton D, Rich EA, et al. Differential activation of MAP kinase signaling pathways and nuclear factor-kappaB in bronchoalveolar cells of smokers and nonsmokers. *Molecular Medicine*. 2001;7(3):177-85.
47. Brito MV, Yasojima EY, Silveira EL, Yamaki VN, Teixeira RK, Feijó DH, et al. New experimental model of exposure to environmental tobacco smoke. *Acta Cirurgica Brasileira*. 2013;28(12):815-9.
48. Chang A. StatsToDo 2014 [updated March 2014. Available from: [https://www.statstodo.com/SSizAOV\\_Pgm.php](https://www.statstodo.com/SSizAOV_Pgm.php).
49. Buckingham KW, Wyder WE. Rapid tracheal infusion method for routine lung fixation using rat and guinea pig. *Toxicologic Pathology*. 1981;9(1):17-20.
50. Carson FL, Cappellano CH. *Histotechnology*. Chicago: ASCP Press; 2009. 319 p.
51. Dogan OT, Elagoz S, Ozsahin SL, Epozturk K, Tuncer E, Akkurt I. Pulmonary toxicity of chronic exposure to tobacco and biomass smoke in rats. *Clinics (Sao Paulo)*. 2011;66(6):1081-7.
52. Kerr KM. Pulmonary preinvasive neoplasia. *Journal of Clinical Pathology*. 2001;54(4):257.
53. Ramos-Vara JA, Miller MA. When tissue antigens and antibodies get along: revisiting the technical aspects of immunohistochemistry-the red, brown, and blue technique. *Veterinary Pathology*. 2013;51(1):42-87.

54. Smith PK, Krohn RI, Hermanson GT, Mallia AK, Gartne F, Provenzano MD, et al. Measurement of protein using bicinchoninic acid. *Analytical Biochemistry*. 1985;150(1):76-85.
55. Lykkedegn S, Sorensen GL, Beck-Nielsen SS, Pilecki B, Duelund L, Marcussen N, et al. Vitamin D Depletion in Pregnancy Decreases Survival Time, Oxygen Saturation, Lung Weight and Body Weight in Preterm Rat Offspring. *PLOS ONE*. 2016;11(8):e0155203.
56. Carter CA, Misra M. Effects of Short-Term Cigarette Smoke Exposure on Fischer 344 Rats and on Selected Lung Proteins. *Toxicologic Pathology*. 2010;38(3):402-15.
57. Lee H, Jung KH, Park S, Kil YS, Chung EY, Jang YP, et al. Inhibitory effects of *Stemona tuberosa* on lung inflammation in a subacute cigarette smoke-induced mouse model. *BMC Complementary and Alternative Medicine*. 2014;14:513.
58. Murray LA, Dunmore R, Camelo A, Da Silva CA, Gustavsson MJ, Habel DM, et al. Acute cigarette smoke exposure activates apoptotic and inflammatory programs but a second stimulus is required to induce epithelial to mesenchymal transition in COPD epithelium. *Respiratory Research*. 2017;18(1):82.
59. Maguire O, Campbell MJ. *Nuclear Receptors: Current Concepts and Future Challenges*. Netherland: Springer 2010. p. 203-36.
60. Srinivasan M, Parwani AV, Hershberger PA, Lenzner DE, Weissfeld JL. Nuclear Vitamin D Receptor Expression is Associated with Improved Survival in Non-Small Cell Lung Cancer. *The Journal of Steroid Biochemistry and Molecular Biology*. 2011;123(1-2):30-6.
61. Brożyna AA, Jozwicki W, Janjetovic Z, Slominski AT. Expression of vitamin D receptor (VDR) decreases during progression of pigmented skin lesions. *Human Pathology*. 2011;42(5):618-31.
62. Brożyna AA, Jóźwicki W, Slominski AT. Decreased VDR expression in cutaneous melanomas as marker of tumor progression: new data and analyses. *Anticancer Research*. 2014;34(6):2735-43.

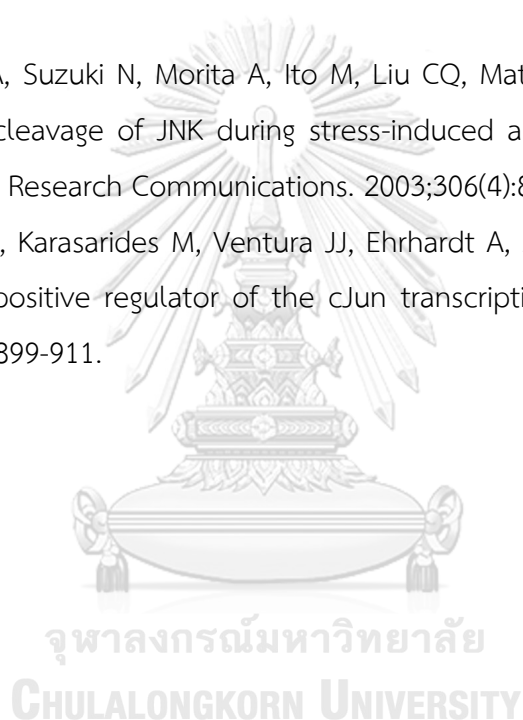
63. Varshney S, Bhadada SK, Saikia UN, Sachdeva N, Beher Arunanshu, Arya AK, et al. Simultaneous expression analysis of vitamin D receptor, calcium-sensing receptor, cyclin D1, and PTH in symptomatic primary hyperparathyroidism in Asian Indians. *European Journal of Endocrinology*. 2013;169(1):109-16.
64. Ishii M, Yamaguchi Y, Nakamura T, Akishita M. The vitamin D receptors may function as antiinflammatory effects in patients with COPD. *Chest*. 2015;148:690A.
65. Song MA, Benowitz NL, Berman M, Brasky TM, Cummings MK, Hatsukami DK, et al. Cigarette filter ventilation and its relationship to increasing rates of lung adenocarcinoma. *JNCI: Journal of the National Cancer Institute*. 2017;109(12):djj075-djj.
66. Barsony J, Renyi I, McKoy W. Subcellular distribution of normal and mutant vitamin D receptors in living cells. *The Journal of Biological Chemistry*. 1997;272:5774-82.
67. Chen RH, Sarnecki C, Blenis J. Nuclear localization and regulation of erk- and rsk-encoded protein kinases. *Molecular and Cellular Biology*. 1992;12(3):915-27.
68. Traverse S, Gomez N, Paterson H, Marshall C, Cohen P. Sustained activation of the mitogen-activated protein (MAP) kinase cascade may be required for differentiation of PC12 cells. Comparison of the effects of nerve growth factor and epidermal growth factor. *Biochemical Journal*. 1992;288(2):351-5.
69. Lenormand P, Sardet C, Pagès G, Allemain G, Brunet A, Pouyssegur J. Growth factors induce nuclear translocation of MAP kinases (p42mapk and p44mapk) but not of their activator MAP kinase kinase (p45mapkk) in fibroblasts. *The Journal of Cell Biology*. 1993;122(5):1079.
70. Zhao J, Yuan X, Frödin M, Grummt I. ERK-dependent phosphorylation of the transcription initiation factor TIF-IA is required for RNA polymerase I transcription and cell growth. *Molecular Cell*. 11(2):405-13.
71. Yohannes M, Yohannes T. How ERK1/2 activation controls cell proliferation and cell death is subcellular localization the answer? *Cell Cycle* 2009;8(8):1168-75.
72. Demirjian L, Abboud RT, Li H, Duronio V. Acute effect of cigarette smoke on TNF- $\alpha$  release by macrophages mediated through the erk1/2 pathway.

- Biochimica et Biophysica Acta (BBA)-Molecular Basis of Disease. 2006;1762(6):592-7.
73. Dey N, Chattopadhyay DJ, Chatterjee IB. Molecular mechanisms of cigarette smoke-induced proliferation of lung cells and prevention by vitamin C. *Journal of Oncology*. 2011:16.
  74. Shen N, Shao Y, Lai SS, Qiao L, Yang RL, Xue B, et al. GGPPS, a new EGR-1 target gene, reactivates ERK 1/2 signaling through increasing Ras prenylation. *The American Journal of Pathology*. 2011;179(6):2740-50.
  75. Kuo WH, Chen JK, Lin HH, Chen BC, Hsu JD, Wang CJ. Induction of apoptosis in the lung tissue from rats exposed to cigarette smoke involves p38/JNK MAPK pathway. *Chemico-Biological Interactions*. 2005;155(1):31-42.
  76. Mossman BT, Lounsbury KM, Reddy SP. Oxidants and signaling by mitogen-activated protein kinases in lung epithelium. *American Journal of Respiratory Cell and Molecular Biology*. 2006;34(6):666-9.
  77. Plotnikov A, Zehorai E, Procaccia S, Seger R. The MAPK cascades: signaling components, nuclear roles and mechanisms of nuclear translocation. *Biochimica et Biophysica Acta (BBA)-Molecular Cell Research*. 2011;1813(9):1619-33.
  78. Dhanasekaran DN, Reddy PE. JNK signaling in apoptosis. *Oncogene*. 2008;27(48):6245-51.
  79. Rincón M, Davis RJ. Regulation of the immune response by stress-activated protein kinases. *Immunological Reviews*. 2009;228(1):212-24.
  80. Moriguchi T, Toyoshima F, Masuyama N, Hanafusa H, Gotoh Y, Nishida E. A novel SAPK/JNK kinase, MKK7, stimulated by TNF $\alpha$  and cellular stresses. *The EMBO Journal*. 1997;16(23):7045-53.
  81. Dickens M, Rogers JS, Cavanagh J, Raitano A, Xia Z, Halpern JR, et al. A cytoplasmic inhibitor of the JNK signal transduction pathway. *Science*. 1997;277(5326):693.
  82. Lang W, Wang H, Ding L, Xiao L. Cooperation between PKC- $\alpha$  and PKC- $\epsilon$  in the regulation of JNK activation in human lung cancer cells. *Cellular Signalling*. 2004;16(4):457-67.

83. Liu MH, Lin AH, Lee HF, Ko HK, Lee TS, Kou YR. Paeonol attenuates cigarette smoke-induced lung inflammation by inhibiting ROS-sensitive inflammatory signaling. *Mediators of Inflammation*. 2014;2014:13.
84. Wallace AM, Hardigan A, Geraghty P, Salim S, Gaffney A, Thankachen J, et al. Protein phosphatase 2A regulates innate immune and proteolytic responses to cigarette smoke exposure in the lung. *Toxicological Sciences*. 2012;126(2):589-99.
85. Lee JS, Favre B, Hemmings BA, Kiefer B, Nagamine Y. Okadaic acid-dependent induction of the urokinase-type plasminogen activator gene associated with stabilization and autoregulation of c-Jun. *Journal of Biological Chemistry*. 1994;269(4):2887-94.
86. Huang G, Shi LZ, Chi H. Regulation of JNK and p38 MAPK in the immune system: Signal integration, propagation and termination. *Cytokine*. 2009;48(3):161-9.
87. Sohn SJ, Thompson J, Winoto A. Apoptosis during negative selection of autoreactive thymocytes. *Current Opinion in Immunology*. 2007;19(5):510-5.
88. Thornton TM, Rincon M. Non-classical P38 Map kinase functions: cell cycle checkpoints and survival. *International Journal of Biological Sciences*. 2009;5(1):44-52.
89. Derijard B, Raingeaud J, Barrett T, Wu IH, Han J, Ulevitch RJ, et al. Independent human MAP-kinase signal transduction pathways defined by MEK and MKK isoforms. *Science*. 1995;267(5198):682.
90. Han J, Lee JD, Jiang Y, Li Z, Feng L, Ulevitch RJ. Characterization of the structure and function of a novel MAP Kinase Kinase (MKK6). *Journal of Biological Chemistry*. 1996;271(6):2886-91.
91. Segreto HRC, Oshima CTF, Franco MF, Silva MRR, Egami MI, Teixeira VPC, et al. Phosphorylation and cytoplasmic localization of MAPK p38 during apoptosis signaling in bone marrow granulocytes of mice irradiated in vivo and the role of amifostine in reducing these effects. *Acta Histochemica*. 2011;113(3):300-7.
92. Horie K, Ohashi M, Satoh Y, Sairenji T. The role of p38 mitogen-activated protein kinase in regulating interleukin-10 gene expression in Burkitt's lymphoma cell lines. *Microbiology and Immunology*. 2013;51(1):149-61.



93. Ben-Levy R, Hooper S, Wilson R, Paterson HF, Marshall CJ. Nuclear export of the stress-activated protein kinase p38 mediated by its substrate MAPKAP kinase-2. *Current Biology*. 1998;8(19):1049-57.
94. Sahu SK, Tiwari M, Bhangare RC, Pandit GG. Particle size distribution of mainstream and exhaled cigarette smoke and predictive deposition in human respiratory tract. *Aerosol and Air Quality Research*. 2013;13:324-32.
95. Buscà R, Pouysségur J, Lenormand P. ERK1 and ERK2 Map Kinases: specific roles or functional redundancy? *Frontiers in Cell and Developmental Biology*. 2016;4:53.
96. Enomoto A, Suzuki N, Morita A, Ito M, Liu CQ, Matsumoto Y, et al. Caspase-mediated cleavage of JNK during stress-induced apoptosis. *Biochemical and Biophysical Research Communications*. 2003;306(4):837-42.
97. Jaeschke A, Karasarides M, Ventura JJ, Ehrhardt A, Zhang C, Flavell RA, et al. JNK2 is a positive regulator of the cJun transcription factor. *Molecular Cell*. 2006;23(6):899-911.





APPENDIX

จุฬาลงกรณ์มหาวิทยาลัย  
**CHULALONGKORN UNIVERSITY**

## Appendix 1 Research tools

1. Analytical balance, Ohaus: model AR2140
2. Autoclave, Selecta: model presoclave 75
3. Biomedical freezer, Panasonic: model MDF-U537D
4. Centrifuge, Thermo scientific: model Thermo legend X1R
5. Electrophoresis tank, Bio-Rad: model Mini-protein tetra system
6. Fume hood, Captair: model filtair 824
7. Heat block, Tehne: model DB-2D
8. Hot air oven, Memmert
9. Light microscope, Olympus: model BX41
10. Magnetic stirrer, HL instruments: model MS 115
11. Microplate *spectrophotometer*, Thermo scientific: model Multiskan GO
12. Microtome, Shandon Finesse
13. Microwave, Elextrolux
14. Orbital shaker, Biosan Sthart: model OS-10
15. Oven, Binder: model B28
16. pH meter, Fisher scientific: model AB15
17. PowerPac basic power supply, Bio-rad
18. Refrigerator, Sanyo
19. *Refrigerate centrifuge*, Boeco: model U-32R
20. Spin-down centrifuge, LabTech: model GMC 260
21. Tissue embedding, Leica biosystems: model EG1150H
22. Tissue grinder, Pyrex
23. Tissue processor, Leica biosystems: model TP1020
24. Ultrasonic processor, BECThai: model VC 750
25. Vortex mixer, Vision scientific: model KMC-1300V

## Appendix 2 Materials and equipment

1. Auto pipettes 2,20, 200 and 1000  $\mu$ l (Gilson)
2. Automated semi-enclosed benchtop tissue processor (TP1020, Leica biosystem)
3. Beakers 50, 250, 500, 1,000 and 2,000 ml (Pyrex)
4. Bottles size 100, 250, 500, 1,000 and 2,000 ml (Pyrex)
5. Centrifuge tubes 1.5 ml (Axygen)
6. Cigarette filter (Marlboro)
7. Cigarette lighter
8. Clot blood tubes
9. Commercial cigarettes (Marlboro red)
10. Conduction pipe 1 m
11. Conical tubes 15 and 50 ml (NUNC)
12. Coplin jars
13. Cover glass 22x22 mm, thick 0.13-0.17 mm (HAD)
14. Cylinders 50,500 and 1,000 ml (Pyrex)
15. Filter paper No.1 (Whatman)
16. Glass microscope slides 25.4x76.2 mm, thick 1-1.2 mm
17. Inhalation chamber 23x31.5x19 cm
18. Micro air pump 12V
19. Needle gauge 18G, 20G and 26G (Nipro)
20. Petri dish
21. Pipette tips 10,200 and 1000 $\mu$ l (Gilson)
22. Smoke storage box
23. Staining jars
24. Sterile gauze pads 4"x4" (Traichon limited)
25. Surgical equipment e.g. forceps, scissors, scalpel, clamp etc.
26. Syringe 10 ml (Nipro)
27. Tissue cassettes (Thermo Scientific)
28. Weighting paper (Whatman)
29. 96 wells microplates flat bottom (Corning)

### Appendix 3 Chemicals and reagents

1. Ammonium persulfate (SIGMA-ALDRICH, product number A3678)
2. Anti-Lamin B1 antibody (Abcam, cat. no.ab133741)
3.  $\beta$ -actin antibody (Cell signaling, cat. no.4970)
4. Bovine serum Cohn Analog<sup>TM</sup>,  $\geq 98\%$  (agarose gel electrophoresis), powder, cell culture tested (SIGMA-ALDRICH, product number A1470)
5. Eosin (ready to use) (C.V. laboratories co., ltd)
6. Ethanol absolute for analysis EMSURE® ACS, ISO,Reag. Ph Eur (Merck, cat. no.100983)
7. Ethanol 95% (Zenith science)
8. ExcelBand<sup>TM</sup> Enhanced 3-color regular range protein marker (SMOBIO, PM 2510/PM2511)
9. Formaldehyde solution, min. 37% (Merck, cat. no. 1.03003.2500)
10. Glycerol (SIGMA-ALDRICH, product number G5516)
11. Glycine GR for analysis (Merck, cat. no. 104201)
12. Halt protease and phosphatase inhibitor cocktail and EDTA (Thermo scientific, cat. no.78440)
13. Liquid nitrogen (ready to use)
14. Methanol for analysis EMSURE® ACS, ISO,Reag. Ph Eur (Merck, cat. no.106009)
15. Mayer's haematoxylin (ready to use) (C.V. laboratories co., ltd)
16. NE-PER nuclear and cytoplasmic extraction reagents (Thermo scientific, cat. no.78835)
17. Paraplast<sup>TM</sup> (Leica Biosystem, code.39601006)
18. Phospho-ERK1/2 MAPK antibody (Cell signaling, cat. no.4376)
19. Phospho-p38 MAPK antibody (Cell signaling, cat. no.4511)
20. Phospho-SAPK/JNK antibody (Cell signaling, cat. no.4668)
21. Pierce BCA protein assay kit (Thermo scientific, cat. no.23227)
22. Potassium chloride, SigmaUltra,  $\geq 99.0\%$  (KCl) (SIGMA-ALDRICH, product number P9333)
23. Potassium phosphate monobasic, powder,  $\geq 99.0\%$  ( $\text{KH}_2\text{PO}_4$ ) (SIGMA-ALDRICH, product number P5655)

24. Immobilon-P PVDF membrane 0.45  $\mu\text{m}$  pore size (Merck Millipore, IPVH00010)
25. Restore plus western blot stripping buffer (Thermo scientific, cat. no.46430)
26. SAPK/JNK antibody (Cell signaling, cat. no.9252)
27. Secondary anti-rabbit IgG, HRP link antibody (Cell signaling, cat. no.7074)
28. Sodium chloride, 95% (NaCl) (Merck, cat. no. 1.06404.1000)
29. Sodium Dodecyl Sulfate (SIGMA-ALDRICH, product number 862010)
30. Sodium pentobarbital 5.47% (CEVA SANTE ANIMALE)
31. Sodium phosphate dibasic, SigmaUltra,  $\geq 99\%$  ( $\text{Na}_2\text{HPO}_4$ ) (SIGMA-ALDRICH, product number S9638)
32. Sodium phosphate monobasic monohydrate, ACS reagent, 98.0- 102.0% ( $\text{NaH}_2\text{PO}_4 \cdot \text{H}_2\text{O}$ ) (SIGMA-ALDRICH, product number S9638)
33. Sterile water (ready to use)
34. Supersignal west femto maximum sensitivity substrate (Thermo scientific, cat. no.34095)
35. Surgipath paraplast tissue embedding medium (Leica biosystems, code.39601006)
36. T-PER tissue protein extraction reagent (Thermo scientific, cat. no.78510)
37. Tris base  $\geq 99.8\%$  pure (Bio-rad, product number 1610719)
38. Tween20 for molecular biology, viscous liquid (SIGMA-ALDRICH, product number P9416)
39. Ultrapure TEMED (Invitrogen, cat. no.15524010)
40. Vitamin D receptor antibody (R&D systems, cat. no.NBP1-51322)
41. Xylene purified solvents (Leica Biosystems, code.3803665)
42. 40% Acrylamide /Bis, 37.5:1 (Bio-rad, product number 1610148)
43. 2-Mercaptoethanol (SIGMA-ALDRICH, product number M6250)

#### Appendix 4 Whole cell, cytoplasmic and nuclear protein extraction protocol

##### Whole cell proteins extraction

Frozen lung tissues were washed by ice cold PBS.

↓  
Cut the tissue into small pieces and weight the tissue samples with a ratio of 1 g of tissue to 20 ml T-PER reagent.

↓  
Add protease, phosphatase inhibitors and EDTA in T-PER reagent with a ratio of 1 g of tissue to 10  $\mu$ l of individual reagent before use.

↓  
Place the tissues into Dounce tissue grinder pestle and add T-PER in proper volume for homogenization on ice.

↓  
Then sonicate the samples with setting 30% amplitude, run 15 second and pause 10 second for 1.30 minutes by ultrasonic processor.

↓  
After that centrifuge the tube at 10,000 $\times$ g (4°C) for 5 minutes to pellet cell/tissue detritus.

↓  
Transfer the supernatant (whole cell proteins compartment) in clean centrifuge tube and collect at -80°C to the further analysis.

Note: The samples were performed on ice in all procedures.

### Cytoplasmic and nuclear proteins extraction

Frozen lung tissue is washed by ice cold PBS.



Cut the tissue into small pieces and weight the tissue samples for the appropriate ratio of cytoplasmic and nuclear extraction reagents following the table below.

Tissue weight (mg)	CER I ( $\mu$ l)	CER II ( $\mu$ l)	NER ( $\mu$ l)
20	200	11	100
40	400	22	200
80	800	44	400
100	1000	55	500



Add protease, phosphatase inhibitors and EDTA in CER I and NER reagent (unnecessary to add in CER II) before use as the same ratio in whole cell extraction protocol.



Homogenize tissue by using Dounce tissue grinder pestle in the appropriate volume of CER I following the table.



Vortex the tube on the highest for 5 seconds to completely suspend the cell pellet and incubate the tube on ice for 10 minutes.



Then add ice cold CER II in the tube and vortex the tube at the highest speed for 5 seconds. Incubate the tube on ice 1 minute.



Vortex the tube at highest speed 5 seconds and centrifuge the tube about 16,000xg



for 5 minutes to separate the cytosolic component.



Accumulate the supernatant (cytoplasmic proteins) to the sterile pre-chilled tube for measure protein concentration and storage at  $-80^{\circ}\text{C}$  until used.



Suspend the pellet in the appropriate ice cold NER volume and use the pipette tip to disperse the insoluble fraction as much as possible.



Sonicate the tube on ice at setting 30% amplitude, run 15 seconds and pause 15 seconds for 2 minutes to break the nuclear membrane.



After that, vortex the tube at highest speed for 15 seconds and incubate the tube on ice for 10 minutes, repeat these two steps until 60 minutes.



Centrifuge the tube at  $16,000\times g$  ( $4^{\circ}\text{C}$ ) for 15 minutes.



Rapidly transfer the supernatant (nuclear proteins) to the sterile pre-chilled tube for measure protein concentration and storage at  $-80^{\circ}\text{C}$  until used.

Appendix 5 The formula for gel preparation (gel size 1.5 mm)

Gel compositions	5% Stacking gel (2 plates)	10% Separating gel (2 plates)
-Distilled water	3,688 $\mu$ l	6,990 $\mu$ l
-100% glycerol	150 $\mu$ l	360 $\mu$ l
-1.5M Tris-HCl pH8.8 (4°C)	1,562 $\mu$ l	3,750 $\mu$ l
-40% Acrylamide (4°C)	788 $\mu$ l	3,750 $\mu$ l
-20% SDS	31.2 $\mu$ l	75 $\mu$ l
-10% APS	23.5 $\mu$ l	56.25 $\mu$ l
-TEMED(4°C)	7.8 $\mu$ l	18.75 $\mu$ l
Total volume	6,250.5 $\mu$ l (6.25 ml)	15,000 $\mu$ l (15 ml)

## Appendix 6 Buffer and reagents preparation for the western blot analysis

### Stock solutions preparation

#### **1.5 M Tris-HCl pH 8.8**

Tris base 27.23 g

Distilled water 80 ml

#### **0.5 M Tris-HCl pH 6.8**

Tris base 6 g

Distilled water 60 ml

#### **10% SDS 20 ml**

SDS 2 g

Distilled water 20 ml

#### **0.5% bromophenol blue 20 ml**

Bromophenol blue 0.1 g

Distilled water 20 ml

#### **Sample buffer 9.5 ml (loading dye)**

Distilled water 3.55 ml

0.5 M Tris-HCl (pH 6.8) 1.25 ml

Glycerol 2.5 ml

10% (w/v) SDS 2 ml

0.5% (w/v) bromophenol blue 0.2 ml

#### **10X Phosphate buffer saline (PBS) pH 7.3 1L**

Sodium chloride (NaCl) 80 g

Potassium Chloride (KCl) 2 g

Sodium phosphate dibasic ( $\text{Na}_2\text{HPO}_4$ ) 6.1 g

Potassium phosphate monobasic ( $\text{KH}_2\text{PO}_4$ ) 2 g

Dissolve the reagents in 950 ml distilled water

Adjust pH to 7.3 and then add distilled water to 1 L

#### **10X Running buffer (SDS electrophoresis buffer) 1L**

Tris-base (MW 121.1) 30.3 g

Glycine (MW 75.07) 144g

SDS (MW 288.38) 10g

Add distilled water to 1L

**10X Western transfer buffer 1L**

Tris-Base 30.28 g

Glycine 144.2 g

Add distilled water to 1L

**Ready to used solutions preparation****1X Running buffer 1L**

10X running buffer 100 ml

Add distilled water 900 ml

**1X transfer buffer 1L**

10X western transfer buffer 100 ml

Add Distilled water 700 ml

Methanol 200 ml

\* Do not add transfer buffer close to methanol because it will make the turbid solution.

**1X PBS 0.1% Tween (PBST)**

10X PBS 100 ml

Distilled water 900 ml

0.1% Tween-20 1 ml

**1% Bovine serum albumin (BSA) 10 ml blocking buffer**

0.1 g BSA

10 ml PBST

**VITA**

Name: Mr.Fatist Okrit

Date of birth: January 17, 1991

Place of birth: Nakhon Si Thammarat, Thailand

Home address: 776/7 Soi Ratdej, Sriprad Road, Tambon Khlang, Amphoe Muang, Nakhon Si Thammarat, 80000

Education: 2013: Bachelor of Science (Physical Therapy) with the second class honor, The Faculty of Allied Health Science, Chulalongkorn University.

Research grants: The Graduate Scholarship from the 72th Anniversary of His Majesty King Bhumibol Adulyadej Scholarship, Thailand, the 90th Anniversary Fund of Chulalongkorn University (Ratchadaphiseksomphot Endowment Fund), Thailand, Ratchadapiseksompotch Fund, Faculty of Medicine, Chulalongkorn University, Thailand .



จุฬาลงกรณ์มหาวิทยาลัย  
**CHULALONGKORN UNIVERSITY**